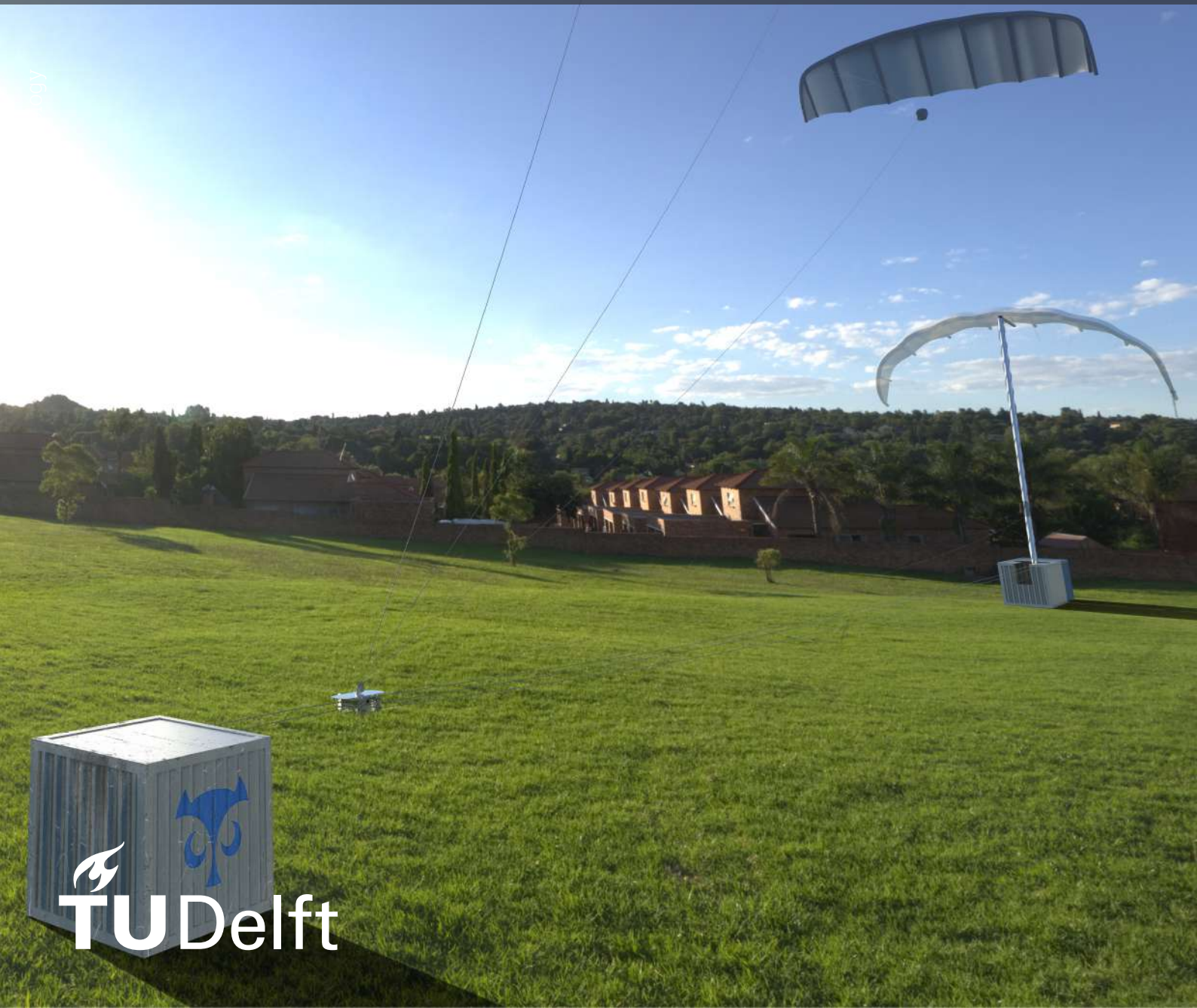


Design Synthesis Exercise: Final Report

Autonomous landing, storage and re-launching of a
kite power system

AE3200

Group 20



1999

Design Synthesis Exercise: Final Report

Autonomous landing, storage and re-launching
of a kite power system

by

Group 20

Student Name	Student Number
van Breukelen García, Alejandro	5293030
Cerbino, Filippo	5222486
Dubois, Justin	5217091
Esser, Timo	5225108
Gün, Kerem	5222664
Jerez, Eduardo	4841115
Lacal, Daniel	5319927
van Leeuwen, Roel	5257069
Olimid, Dominic	5260957
Smit, Adriaan	4471741
Stevens, Sebastien	4833414

Tutor: Dr. - Ing. Roland Schmehl
Coaches: Ir. Sam van Elsloo
Ir. Rashika Jain
Project Duration: April 2023 - June 2023
Faculty: Faculty of Aerospace Engineering, Delft

Preface

This is the final and complete report of the work of 11 Aerospace Engineering students, spanning 10 weeks. As a Design Synthesis Exercise, it is rigorous training in designing a system from an idea to developing a final design and a road map towards its possible production. As such it is a worthy end project of the Bachelor's programme, as it encompasses all the material part of the academic curriculum. In addition to this, careful planning is needed to deliver a final and coherent design. The importance of project management is made obvious; the time that is spent on this at the start will pay off greatly in the weeks after.

And what better start is there than visiting the company we worked with closely, on the very first day? Thanks to Kitepower and the glowing enthusiasm of its employees, the welcome was as inspiring as it was motivating. This inspiration was enduring throughout the whole duration of the project, in no small part due to the unwavering help and interest of our tutor dr.-ing. Roland Schmehl. It is hard to overestimate his knowledge of the field and his willingness to share this with us, with selfless goals of the progress of the field always in mind.

What is a temple without its pillars? We would be nowhere without the practical knowledge and guidance of our coaches Ir. Sam van Elsloo and Ir. Rashika Jain. They have shown time and time again their passionate personal involvement and engagement with our project - answering our last-minute questions, the extensive and very elaborate feedback, the constructive criticism; they are the pillars of the wealth of knowledge on which we have built this endeavour.

We would like to express our sincerest gratitude to everyone who has made this extraordinary project possible; our aforementioned tutor and coaches, the experts currently or formerly involved with Kitepower, Dromec and all other companies that were kind enough to assist us in this journey. Paying special attention to Ir. Jelle Poland, Ir. Oriol Cayón Domingo, Ir. Joep Breuer, Bryan van Ostheim, Ir. Eduard Ijsselmuiden, Ir. Jonas Kampermann, Ir. Geerart de Vree and Walter Hueber, who have provided us with a wealth of technical knowledge. And we would like to thank the teaching assistants, the DSE organising committee, and last but not least the faculty of Aerospace Engineering for providing the opportunity to gain such practical knowledge.

Lastly, let us turn to you, dear reader: we hope that you find reading this report as interesting as we found making it. We have certainly learned a lot and we hope that you may do the same.

*Group 20
Delft, June 2023*

Executive Overview

The aim of this executive overview is to summarise the content of this extensive report regarding the design of an Landing, Launching and Storage (LLS) system for a soft kite Airborne Wind Energy (AWE) system.

An innovative idea does not translate automatically to financial gain. With new technologies, such as AWEs it is crucial to assess the potential market for a product and the associated economic performance. Four market segments exist for energy generation: on-shore on-grid, on-shore off-grid, off-shore on-grid and off-shore off-grid. AWE performs best in on-shore off-grid applications due to its high mobility, higher capacity factor compared to wind and relatively lower land usage. AWE soft kites are currently targeting 100 kW to 500 kW range, which is currently dominated by medium-power diesel generators.

Financial Overview

This target market is distributed across the world, with a higher concentration in developing countries. The regions close to the equator are disregarded due to the low wind zone surrounding the intertropical convergence zone. The value decided upon was 140 GW with an annual compound growth of 5.5 % from 2023 to 2030. The LLS is integrated with the kite and ground station and will be sold as a package to the customer. Three companies have been identified as potential clients for the LLS and the product has been discussed with one of them, namely Kitepower BV.

Once the system is ready for commercialisation, the sales profile is expected to follow a trend as indicated in Figure 1. This forecast would need to be updated once actual data is gathered, as it relies mostly on predictions that do not have historical backing.

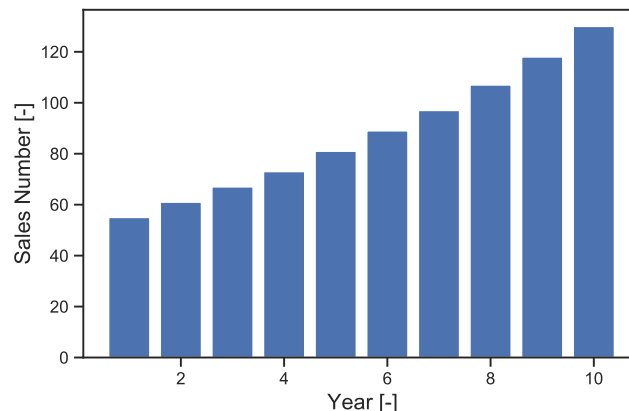


Figure 1: Airborne Wind Energy system sales forecast

The financial prediction of the project is visualised in Figure 2a and Figure 2b. The product will be sold over a period of 10 years, accounting for a significant portion of the gross revenue. However, the bulk of the profit is skewed towards the maintenance, service, and replacement accounting for over 80 % of the total profit. The net revenue over 20 years amounts to 193 million euro. The net present value is heavily discounted (30 %) giving 8.5 million euro and the internal rate of return of the investment is 45.65 %.

Although the performance is encouraging, a more refined analysis is needed to increase the confidence in the results. This includes using more sophisticated company valuation methods,

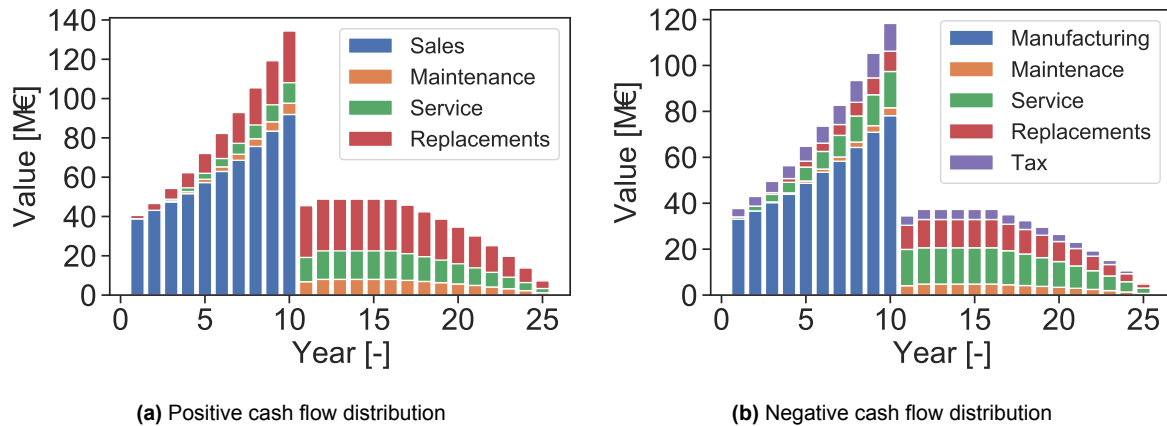


Figure 2: Annual cash flow throughout the lifetime of the project

using real-based sales data and maintenance costs.

Sustainability

Several sustainability goals were set for the present project. Amongst them, those related to greenhouse emissions payback period and recyclability stand most pressing. Several strategies, such as minimising the use of steel, using the least polluting Lithium-Ion batteries available, and logistically opting for the most efficient means of transport allow for the design to minimise greenhouse emissions so the emissions payback period is shortened.

In Table 1, the emissions and payback period can be observed per subsystem and for the total system including the AWE and LLS systems.

The system's emissions payback period of 1754 hours, roughly equivalent to 72 days or almost 2 and a half months, is well within the 1.8 to 22.5-month range typical for wind turbines in Northern Europe.

Regarding recyclability, the mass of recyclable materials in the system is around 71 % of the total mass of the system.

Table 1: Emissions and payback times per subsystem

Subsystem	Emissions [kgCO ₂ e]	Payback Period [h]
Tower	137	5
Guiding Cable	179	7
Cable Cart	267	10
Anchoring Mechanism	420	16
Electrical System	37780	1445
Ground Station	4560	174
Kite & KCU	646	25
Transport	1886	72
Total	45876	1754

Conceptual Design

Now that the requirement and functions of the system have been identified, a brainstorm of possible designs has to be done. Lots of different concepts were developed, but only four were considered as the final possible options. These are: Offset Winch Launch (OWL), Winch with Rover Assisted Positioning (WRAP), Horizontal Axis Spinning Launch (HASL), and Rail

Assisted Winch (RAW). Some initial estimations for each concept were done like the energy required, masses, costs, carbon equivalent, and emissions. A trade-off process is required in order to select the most appropriate design. The selected criteria are launch performance, environmental adaptability, scalability, costs, technical feasibility, and sustainability. In the following figures, the grading scale is illustrated. One is the worst and four is the best. Analysing a series of customer needs, it was possible to find the weight for the different criteria.

Table 2: Trade-off table with weights

Relative Weight	Concept				
	Criteria	OWL	WRAP	HASL	RAW
0.141	Performance	3	4	2	1
0.123	Scalability	3	4	1	1
0.131	Environment Adaptability	3	2	4	4
0.222	Costs	4	2	2	3
0.245	Technical Feasibility	3	3	1	2
0.139	Sustainability	2	1	4	4
TOTAL		3.086	2.636	2.174	2.5

Table 2 shows the trade-off table. In the bottom-most row, the final score for each concept is shown. The offset winch launch design obtained the best grade, and some initial parameter estimations are:

Table 3: Initial estimations of the OWL

Parameters	Value Estimated
Height of pole	15 meters
Reel in speed	12 m/s
Energy per launch cycle	0.54 kWh
Minimum costs	12800 €
Maximum costs	16700 €
Carbon equivalent emissions	4000 kg



Figure 3: Offset winch launch

Now that the final design has been chosen it is possible to identify the subsystems which are the landing tower, anchoring, guiding cables, cable cart, electrical system, ground station and kite.

Final Configuration and Layout

The final configuration of the OWL consists of a main container and an offset container connected by the guiding cable. The main container houses the tower with RSS and the winch with LLS, the offset container is empty and functions as storage for equipment belonging to the AWE. The cable cart drives over the guiding cable, allowing the swivel access point to move to an offset position. All these parts can be identified in Figure 4, depicting the system midway in the winch launching process.

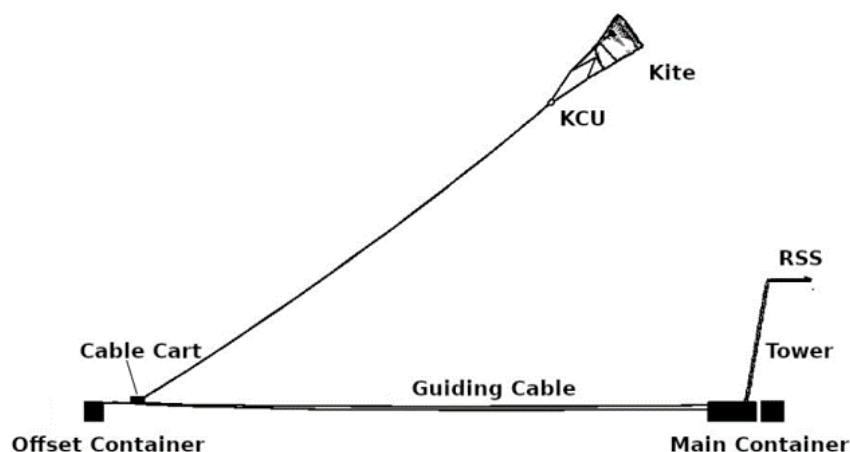


Figure 4: Complete system side view

Operations

The OWL system can launch in two different ways, depending on the wind conditions. For high wind conditions (above 6 m s^{-1} at 10 m), the tower orientates itself into the direction of the wind and, since the cut-in speed is exceeded, the kite can simply take off from the tower. In the case when the wind speed is below the tower launch wind speed, the tower is aligned in the direction of the offset container and a Stepped Tow Launch (STL) is performed

For the STL, a cable cart with a swivel access point drives over a guiding cable that is tensioned between the main container and an offset container. This allows the kite to be towed towards the offset container, exactly the same as how sailplanes are tow launched. Since the height obtained this way is not sufficient, a step tow procedure is performed after the initial tow. By gliding the kite downwind, another tow can be done to a higher altitude.

This process is repeated until the wind velocity at the kite's altitude exceeds the parking speed of the kite and operations can begin. By simulating this STL, it was found that 3 steps on average would suffice to reach a cut-in wind speed for the kite.

Notice that the initial towing in the low wind case is not necessarily aligned with the direction of the wind. This is not an issue since the winch can tow at a velocity that can overcome these low wind speeds, evidently, it is still recommended to orient the system such that it is aligned with the dominant wind direction of the site.

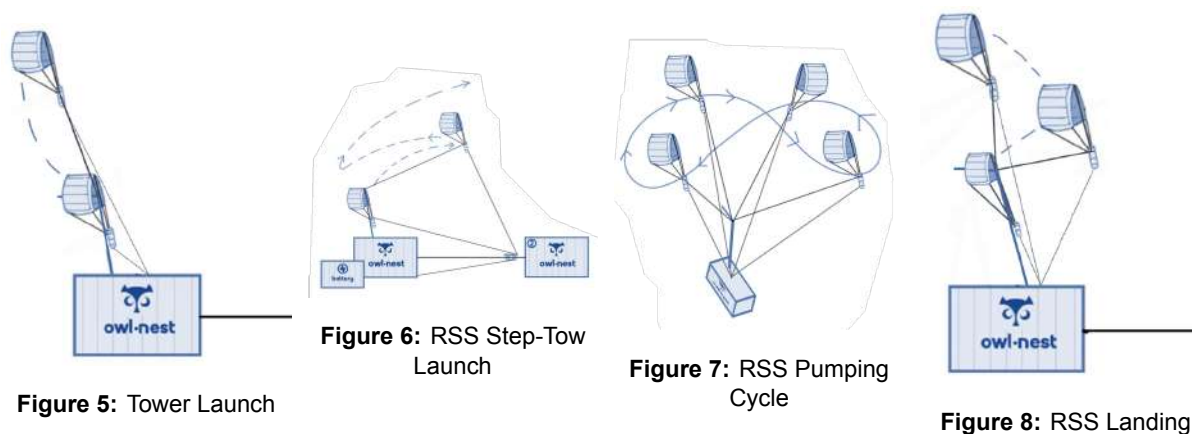
When the wind dies down or a storm breaks out, the kite needs to be landed. The landing procedure consists of first descending the kite from operational height to a lower height above the tower by steering the kite to the edge of the power zone. The last part of the descent is done with the kite at the zenith, this allows for better control and a more beneficial position with respect to the tower.

While the kite is performing this descent manoeuvre, the tower on the ground station will rotate to align with the direction of the approaching kite, approximately in the direction of the wind.

When the kite is close to the tower, the Leading Edge Tether (LET) is released from the KCU to allow for more control of the final descent. This LET is reeled into the top of the tower, directing the kite onto the RSS. The main tether is reeled into the main container, keeping tension on the bridle lines.

The LET is only released for the landing phase, it is kept attached to the KCU during all other phases of operation.

The step-by-step operational procedures have been illustrated in Figure 5, 6, 7 and 8.



Tower

The tower is positioned inside the main container and consists of three hollow cylindrical aluminium 6061-T6 sections. The first is inside the container and is positioned on a beam which is positioned on a 2.3 m rotating bearing inside the container. The second section is 16 m tall, equipped with helical strakes, and angled at 10° .

The Rolling Storage System (RSS) has a solenoid and a lever clamp to respectively latch to the LE and TE. A UV coating protects the stored kite from the sun.

Guiding Cables

There are two 85 m long guiding cables on which the cable cart moves from the main container to the offset container. These are designed for a rated tension of 50 kN each. Furthermore, there are breaker pieces which will snap if the tension exceeds 150 kN. These cables are made out of 14 mm thick Dyneema®.

Cable Cart

The cable cart is one of the key components involved in the launching of the kite in low-wind conditions. It is connected to the guiding cables on which it drives through 8 wheels pressed on the cable with the aid of a clamping mechanism consisting of 8 springs, 2 per wheel-set to avoid any slipping from occurring. It contains also a swivel access point, to allow the tether to be redirected from the ground station towards the kite. The cart is fully autonomous, with the two electric motors powered by a battery which is recharged at the main container. Lastly, the cart also presents a simple clamping mechanism consisting of an extruded metal sheet plate with a hole in the middle allowing it to be pinned to either container.

Anchoring

Both containers experience large loads from the guiding cable and the tower. Therefore it was found that they will need to be anchored down. This is done by ten anchors in total, six for

the main container and four for the offset container. The anchors are positioned away from the container and connected with guy lines to the corner castings of the container. For the main container, two extra connection points and reinforcement were added.

Electrical Subsystem

The electrical subsystem remains mostly identical compared to the original AWE system. The system needs to be expanded to provide power to the additional actuators and the cable cart.

Ground Station

The ground station consists of the main and offset container and is responsible for interfacing all the individual subsystems. A preliminary mock-up of an internal frame accomplishing these tasks has been designed but no sizing has been done.

Finalised Design

With the final design done, it is now possible to check whether the stakeholder requirements imposed by the stakeholders have been dealt with. The best way to illustrate this is by using a compliance matrix. Most requirements have been complied with except three of them: there shall be no financial impact of the LLS system on the other subsystems (STK-OEM-08), the LLS shall be upgradeable to allow for the use of larger kite systems (STK-OEM-17) and the LLS system shall be able to sustain common transportation loads without damage (STK-OEM-13). The LLS does affect other subsystems that conform to the AWE for example, the kite and KCU have to suffer some modification that would lead to higher costs. If the kite were to be scaled up, there is a limit for this type of system. At some point, for example, the tower's height would be too large to comply with the requirement of storing in a 20ft container. Regarding the loads suffered during transportation, it is difficult to calculate this without any testing involved. That is why that requirement is still TBD.

Resource allocation will serve as a comparison between the initial estimations and the final values obtained after the final design. These estimations consist of the tower height, the winch reel speed, energy consumed per cycle and costs. The tower height has been increased to accommodate the bridle system, the final height of the landing tower is 18 m. The reel speed of the winch was the same as the estimated (12 m s^{-1}) but Dromec will have to develop a new winch that can roll at those speeds while being loaded with very high forces. The estimated energy consumed is 0.34 kWh, which is an insignificant amount of energy from the battery. This was already the case when doing the estimated energy consumed, and the final energy consumed is 63 % of the initially estimated (0.54 kWh). To quantify the costs, a breakdown has been done. The maintenance and operation costs will not be considered for this quantification. Summing up all the different components that conform to the subsystems yields a final price of $\simeq N35,700$. Having said price would meet the stakeholder requirement of not going over €40,000. Lastly, the time taken to complete a cycle was also calculated. This period takes into account the launching sequence (from the moment the winch starts reeling in, until the end of 3 step-tows), landing from a height of 400 metres and the fold/unfolding of the kite with the RSS. The total time taken to complete all these phases is around 6.5 minutes.

Logistics

The logistics that are involved in this project take place in multiple stages. Due to costs, all the components will be outsourced rather than manufactured in-house. Multiple European companies have been considered as possible suppliers of different parts. All these companies are inside the EU which reduces the customs tariffs and the distances are not as large as if the suppliers were from different continents. Apart from reducing costs, this project aims to have the lowest carbon footprint. This is another reason why the suppliers must be relatively close so

the transportation's CO₂ emissions are as lowest as possible. Now, the location for assembly of the LLS will take place in Lithuania. The selected country has tax benefits and low labour wages that will improve considerably improve the profit, making the investors more content. Once all the components have been assembled in Lithuania, they will be ready to be shipped to the designated location. For inter-continental transport, sea freight has been chosen over air because of the lower costs and lower carbon footprint. Within the nation, when sea freight is not possible, rail freighting will always be chosen. Road transport will be left as a last resort.

Conclusion

This system was designed to allow the autonomous launch, land and storage of a soft kite AWE system. This report aims to explain the development process of how the final design was obtained. The team has tried to meet as many of the stakeholder's requirements as possible. To produce an even more detailed design a few recommendations have been written if a further investigation were to be done for this OWL: more accurate financial data, improving the modelling of the STL, finding a solution for scaling up the tower, replacing the cable cart by a tether retraction link between the offset point/main tether and have more accurate data on the electric loads of the microgrid that the AWE should be connected to.

Contents

Preface	i
Executive Overview	ii
Acronyms	xii
Nomenclature	xiii
1 Introduction	1
2 Financial Overview	2
2.1 Industry Overview	2
2.2 Target Market	2
2.3 Competitive Field	4
2.4 Product Profitability Assessment	5
2.5 Recommendations	8
3 Functional Analysis	9
4 Requirements	13
4.1 Stakeholder Requirements	13
4.2 System Requirements	14
4.3 Sustainability Requirements	15
5 Conceptual Design	16
5.1 Initial Concepts	16
5.2 Trade-off	17
5.3 Final Design	20
6 Operations	21
6.1 Launching and Landing Determination	21
6.2 Launch Phase	21
6.3 Land Kite	24
6.4 Store the kite	25
6.5 Recommendations	25
7 Tower	26
7.1 Functional Analysis	26
7.2 Requirement Analysis	26
7.3 Design	28
7.4 Costs	38
7.5 Verification and Validation	39
7.6 RAMS Characteristics	40
7.7 Sustainability	41
7.8 Recommendations	41
8 Guiding Cables	42
8.1 Functional Analysis	42
8.2 Requirement Analysis	42
8.3 Design	43
8.4 Costs	46
8.5 Verification and Validation	46

8.6	RAMS Characteristics	47
8.7	Sustainability	48
8.8	Recommendations	48
9	Cable Cart	49
9.1	Functional analysis	49
9.2	Requirements Analysis	49
9.3	Design of the Cable Cart	50
9.4	Costs	60
9.5	Verification and Validation	61
9.6	RAMS Characteristics	62
9.7	Sustainability	63
9.8	Recommendations	63
10	Anchoring Mechanism	65
10.1	Functional Analysis	65
10.2	Requirements Analysis	65
10.3	Design	66
10.4	Costs	72
10.5	Verification & Validation	72
10.6	RAMS Characteristics	73
10.7	Sustainability	73
10.8	Recommendations	74
11	Electrical System	75
11.1	Functional Analysis	75
11.2	Requirements Analysis	75
11.3	Design	76
11.4	Costs	78
11.5	Verification & Validation	79
11.6	RAMS Characteristics	79
11.7	Sustainability	80
11.8	Recommendations	80
12	Ground Station	81
12.1	Functional Analysis	81
12.2	Requirements Analysis	81
12.3	Design	82
12.4	Costs	85
12.5	Verification and Validation	86
12.6	RAMS Characteristics	86
12.7	Sustainability	87
12.8	Recommendation	87
13	Kite and KCU	88
13.1	Functional Analysis	88
13.2	Requirements Analysis	88
13.3	Design	89
13.4	Cost	93
13.5	Verification & Validation	93
13.6	RAMS Characteristics	93
13.7	Sustainability	95
13.8	Recommendations	95

14 Communication and Data Handling	96
14.1 Data Streams	96
14.2 Requirements on Communications	96
14.3 Design	97
14.4 RAMS Characteristics	98
14.5 Recommendation	98
15 Final Design	99
15.1 Configuration and Layout	99
15.2 Compliance Matrix	99
15.3 Resource Budget	102
16 RAMS	105
16.1 Reliability	105
16.2 Availability	105
16.3 Maintainability	105
16.4 Safety	105
17 Design Development Overview	106
18 Logistics	109
18.1 Production Logistics	109
18.2 Transportation of System	110
18.3 Setup System	111
18.4 Maintenance	111
18.5 End of life	112
18.6 Costs	112
18.7 Sustainability	112
19 Sustainability	113
19.1 Greenhouse Emissions Payback Period	113
19.2 Manufacturing	113
19.3 Transport	115
19.4 End-of-life	118
19.5 Payback Period	118
19.6 Recyclability	118
19.7 Observations	119
19.8 Recommendations	119
20 Conclusion	120
A Risk Register	124
B Financial Overview Model	129
B.1 Access to the Model	129
B.2 Model Interface	129
B.3 Analytical Approach	131
B.4 Glossary for Financial Overview Model	133

Acronyms

2D Two-Dimensional.	KT Kite.
AC Alternating Current.	LCA Life Cycle Assessment.
ASTM American Society for Testing and Materials.	LCOE Levelised Cost Of Energy.
AWE Airborne Wind Energy.	LE Leading Edge.
BRDL Bridles.	LET Leading Edge Tether.
CAD Computer-Aided Design.	LETRS Leading Edge Retraction System.
CAGR Compound Annual Growth Rate.	LLS Landing, Launching and Storage.
CDH Communication and Data Handling.	NPV Net Present Value.
CE Chief engineer.	OEM Original Equipment Manufacturer.
CME Chief Mechanical engineer.	OWL Offset Winch Launch.
CSC Chief Stability and Control.	PE Poly-Ethylene.
DC Direct Current.	PET Polyethylene Terephthalate.
DO Design Office.	PGO Power Grid Operator.
DoD Depth of Discharge.	PVS People in Vicinity of the System.
DSE Design Synthesis Exercise.	RAMS Reliability, Availability, Maintainability and Safety.
Dyneema [®] Trademark for UHMWPE (Ultra high molecular weight poly-ethylene) fibre.	RAW Rail Assisted Winch.
EBITDA Earnings Before Interest, Tax, Depreciation and Amortisation.	ROI Return on Investment.
ECC External Control Centre.	RSK Risk.
EM Electrical Machine.	RSS Rolling Storage System.
EU European Union.	SAM Service Addressable Market.
FBD Free Body Diagram.	SOM Service Obtainable Market.
FEM Finite Element Method.	SPT Standard Penetration Testing.
FFD Functional Flow Diagram.	STK Stakeholder.
GCU Ground Control Unit.	STL Stepped Tow Launch.
GHG Green House Gasses.	SWOT Strengths Weaknesses Opportunities Threats.
GOV Government.	TAM Total Available Market.
HASL Horizontal Axis Spinning Launch.	TBD To Be Determined.
HMWPE High Molecular Weight Poly-Ethylene.	TCH Technical.
IRR Internal Rate of Return.	TE Trailing Edge.
KCU Kite Control Unit.	US United States.
	UV Ultra-Violet.
	V&V Verification and Validation.
	WRAP Winch with Rover Assisted Positioning.

Nomenclature

Symbol	Definition	Unit
a	Acceleration	$[m/s^2]$
A	Area	$[m^2]$
c	Damping coefficient	$[Ns/m]$
C	Capacity	$[Ah]$
C_D	Drag coefficient	$[-]$
C_L	Lift coefficient	$[-]$
C_R	Resultant force coefficient	$[-]$
C_τ	Tangential drag coefficient	$[-]$
d	Moment arm	$[m]$
d_t	Tether diameter	$[m]$
D	Diameter	$[m]$
D	Drag force	$[N]$
E	Energy	$[J \text{ or } Wh]$
E	Lift to drag ratio	$[-]$
E	Young's modulus	$[Pa]$
f	Frequency	$[Hz]$
f	Reeling factor	$[-]$
f_{nat}	Natural frequency	$[Hz]$
f_{opt}	Optimal reeling factor	$[-]$
F	Force	$[N]$
F_t	Tether force	$[N]$
g	Gravitational acceleration	$[m/s^2]$
h_{blend}	Blending height	$[m]$
h_{ref}	Reference height	$[m]$
I	Moment of inertia	$[m^4]$
I_{xx}	Moment of inertia around the x-axis	$[m^4]$
I_{xy}	Product of inertia around the z-axis	$[m^4]$
I_{yy}	Moment of inertia around the y-axis	$[m^4]$
l	Length	$[m]$
l_u	Undeformed length	$[W]$
L	Length	$[m]$
L	Lift force	$[N]$
m	Mass	$[kg]$
M	Moment	$[Nm]$
M_I	Mass matrix	$[m]$
M_x	Moment around the x-axis	$[Nm]$
M_y	Moment around the y-axis	$[Nm]$
n	Mode number	$[-]$
n	Amount of ...	$[-]$
N	Normal force	$[N]$
p	Bearing stress	$[Pa]$
p	Pitch	$[m]$
P	Power	$[W]$
$P_{bearing}$	Bearing stress	$[Pa]$
P_w	Wind power density	$[kg/s^3]$

Symbol	Definition	Unit
r	Radius	[m]
Re	Reynolds number	[-]
R_{turn}	Turn radius	[m]
S	Area	[m ²]
St	Strouhal number	[-]
t	Time	[s]
t	Thickness	[m]
t_{Al}	Tons of aluminium	[tons]
t_{CO_2}	Tons of CO_2	[tons]
t_{Nylon}	Tons of nylon	[tons]
t_{PE}	Tons of Poly-Ethylene	[tons]
t_{PET}	Tons of Polyethylene Terephthalate	[tons]
t_{Steel}	Tons of steel	[tons]
T	Temperature	[K]
T	Tension	[N]
T	Torque	[Nm]
u	Free-stream velocity	[m/s]
v	Velocity	[m/s]
v_{glide}	Glide speed	[m/s]
v_t	Reel-in speed	[m/s]
v_w	Wind speed at mean height	[m/s]
C_τ	Tangential apparent velocity	[m/s]
V	Voltage	[V]
V_{glide}	Glide velocity	[m/s]
V_{turn}	Turn velocity	[m/s]
V_z	Velocity in vertical direction	[m/s]
W	Weight	[N]
x	Distance from the y-axis	[m]
y	Distance from the x-axis	[m]
z_0	Landscape roughness parameter	[-]
α	Elevation Angle	[degrees]
α	Landscape roughness parameter	[-]
α_t	Thermal coefficient	[1/K]
β	Descent angle	[degrees]
γ	Glide slope	[degrees]
Δ	Change in ...	[-]
η	Efficiency coefficient	[-]
μ_s	Static friction coefficient	[-]
ν	Kinematic viscosity	[-]
ρ	Density	[kg/m ³]
σ	Stress	[Pa]
$\sigma_{bending}$	Bending stress	[Pa]
σ_y	Yield stress	[Pa]
σ_z	Bending stress in the z-direction	[Pa]
ϕ	Bank angle	[degrees]
ω	Radial velocity	[degrees/s]

Introduction

Growth is inevitable. The world is facing an ever-expanding global population boom, necessitating the construction of new communities and infrastructure in previously undeveloped regions. This drastic growth brings the urge for renewable energy in off-grid areas, where mobile and scalable energy systems are in heavy demand for supplying such operations. Airborne wind energy (AWE) systems stand to be the key player in this industry and be the transformative force that alleviates the energy burden from these applications.

One of the key challenges standing before the commercialisation of the AWE is the inability to operate in full autonomy continuously. The absence of a fully autonomous system, able to provide all non-production operational phases, launch, landing, and storage, is the key factor limiting the competitiveness of this technology. In the aim of providing a design solution that would eliminate the relative under-performance compared to conventional systems and make soft-body kite based AWE products a lucrative option in the energy market, *OWL NEST* was found. *OWL NEST* is the name of this project. DSE Group 20 has proposed the following Mission Need Statement and Project Objective Statement.

Mission Need Statement

Provide a system that fully automates the landing, storage and re-launching process of an airborne wind energy system utilising soft kites.

Project Objective Statement

Design of an airborne wind energy system utilising soft kites with reliable, autonomous landing and re-launching capabilities, including safe and compact storage of the kite and tether to be commercially available by 2030, by 11 students in 10 weeks.

This is the final of the four reports written to achieve these goals. These have been the Project Plan, Baseline Report, Midterm Report, and this Final Report. The design of the product has evolved throughout each report, and this final paper gives an exhaustive description. Firstly, the target market is identified, and a financial analysis is conducted to assess the investment-worthiness of the project in Chapter 2. Secondly, an expanded view of the functional analysis is provided in Chapter 3. Following from the identified functions, the design requirements are detailed in Chapter 4. With this limited design space, the conceptual designs were investigated and presented in Chapter 5. After the operations are discussed in Chapter 6, each subsystem is further detailed in the following order. Chapter 7 considers the landing tower, Chapter 8 the guiding cable, Chapter 9 the cable cart, Chapter 10 the anchoring mechanism, Chapter 11 the electrical system, Chapter 12 the ground station, and finally Chapter 13 the kite and KCU. After every subsystem is discussed, Chapter 14 introduces the communication and data handling structure, which is the final system feature to be discussed before the final design is presented in Chapter 15. This is followed by the discussion of the design development overview in Chapter 17. With the design finalised, the logistics and manufacturing aspects are discussed in Chapter 18. Finally, the design is assessed in terms of sustainability in Chapter 19.



Financial Overview

Any business venture is doomed to fail without the backing of a sound financial plan. This chapter aims to demonstrate that a AWE product can be viable given a set of assumptions. Section 2.1 gives a brief overview of the AWE industry and is followed by Section 2.2 which gives a comprehensive view of the target market. A competitive analysis is performed in Section 2.3 to identify the strengths and weaknesses of the product. Lastly, profitability is assessed in Section 2.4 and the chapter ends with recommendations for further study in Section 2.5.

2.1. Industry Overview

The potential of AWE has been explored for more than 40 years, with the first developments of this technology starting in the 1980s [1]. Currently, it is estimated that the market size is around \$132 million, with a Compound Annual Growth Rate (CAGR) of 9.7%¹. The forecast is that this industry will be valued in the realm of \$210 million by 2027. This is around the time when the LLS is planned to be commercialised (see footnote 1). This growth is driven by the demand for renewable electricity around the world. This transition is incentivised by governments worldwide, who financially support businesses and individuals to transition to clean energy. In this regard, Shell, one of the largest energy companies around the world, invested \$288m in solar and wind energy in order to comply with their 2030 objective of cutting down their CO_2 emissions by 50% (see footnote 1). Developments by key players in the energy business accelerate the growth of the industry, opening new doors for novel technologies.

There are multiple types of AWE technologies: kites, lifting balloons or drones among others. One of the most promising categories is that of soft-body kites; the technology may be ancient, yet it is highly versatile. With increased mobility and low investment costs, it can outperform current wind turbines in capacity factor and height of harvested wind². The approximate soft body market CAGR for the period between 2022 and 2027 is estimated to be 7.1% (see footnote 1).

2.2. Target Market

AWE systems have the potential to compete in the global energy market as well as in niche sectors. In the United States, who accounts for 15.48% of the world energy consumption³, i.e. 5383 TWh, the revenue related to selling energy amounted to \$432.476 billion (FY2021)⁴. By extrapolation, the overall revenue from energy can be estimated as high as \$2.9 trillion. These figures are for an estimated 7.173 billion people, as there are an estimated 715 million people without access to electricity. Since energy is a fundamental need for all people in the world and a key driver for economic prosperity and well-being, the Total Available Market (TAM) is the worldwide energy market servicing a total of 7.8 billion people in 2021.

It is unlikely that one company can address the entirety of the TAM, especially when the market is large and segmented. Therefore, the market is reduced to the Service Addressable Market

¹<https://www.industryarc.com/Report/19385/airborne-wind-energy-market.html>, accessed on 01-06-2023

²<https://www.wind-energy-the-facts.org/the-cost-of-energy-generated-by-wind-power.html>, accessed on 01-06-2023

³<https://www.bp.com/content/dam/bp/business-sites/en/global/corporate/pdfs/energy-economics/statistical-review/bp-stats-review-2022-full-report.pdf>, accessed on 01-06-2023

⁴https://www.eia.gov/electricity/monthly/epm_table_grapher.php?t=epmt_5_02, accessed on 02-06-2023

(SAM) which is a subset of the TAM that can be reached by the LLS company. Additionally, the product design specifically targets soft kite power plants, which typically have lower power ratings than rigid winged systems. In a first approach, the SAM can be subdivided into four different markets: on-shore off-grid, on-shore on-grid, off-shore on-grid and off-shore off-grid.

Service Available Market (SAM)

The first segment regroups remote and temporary applications of low-power systems. The customers for such temporary systems include the military, disaster relief organisations and mining companies. For remote locations, AWE could be used for isolated micro-grids or in extreme climate areas. In comparison to diesel power, the initial investment costs are higher, but the running costs are much lower, which means that they can be operated cheaply. According to current projections, the market for diesel generators is expected to grow with a CAGR of 5.5 % in the period 2023 to 2030⁵. Within this market, plants less than 0.5 MW will be investigated further as it readily corresponds to the available technology of soft kites. The installed capacity amounts to 200 GW in developing countries [2]. It is expected that AWE and solar energy will be able to capture a significant portion of this market over the next decades [3]. However, wind is not available in zones close to the equator. Regardless, Southeast Asia, Central America, the northern part of South America the Caribbean, Central Africa and a part of Eastern Africa leaves roughly around 140 GW of installed diesel generators [2].

The on-shore on-grid part of the market consists of common grid electricity generation. The main obstacle for AWE to compete with other sources on a well-connected grid is the current-estimated price of AWE systems. At the moment, the Levelised Cost Of Energy (LCOE) for AWE is estimated at 120 N/MWh for a 100 kW system and 33 N/MWh to 59 N/MWh for a 1.2 MW [4]. On the other hand, renewable energies have as of 2021 a LCOE of 33 N/MWh to 75 N/MWh [5]. Therefore AWE could be competitive with traditional renewable energies at a larger scale, however, AWE are not yet mature enough and hence not yet competitive in this market segment. A path towards large-scale deployment is proposed [3]. The strategy is to use small-scale systems as technology demonstrators to fund and provide operational experience for megawatt-scale power plants. Therefore, the on-shore on-grid will not be addressed in this analysis.

Next, the off-shore on-grid application is considered. The business case for AWE would be to either re-purpose decommissioned off-shore wind turbine farms or implant new farms specifically made for AWE [3]. As with the on-shore on-grid sector, this would only be applicable to large-scale AWE farms and lies outside of the scope of this report.

The last segment considered is off-shore off-grid applications which would target remote oil and gas platforms and perhaps be used in ship propulsion as attempted by Skysails⁶. For the former, very large AWE systems would be needed, which is not the target market. For the latter, it is unclear whether there is significant demand.

Service Obtainable Market

The Service Obtainable Market (SOM) is the portion of the SAM that can be reasonably expected to be gained by the product, i.e. LLS for soft kites. In this case, the primary target market is the on-shore off-grid energy for power plants less than 0.5 MW. As stated previously, the installed capacity of diesel generators potentially useful for AWE accounted for 140 GW which could translate to an equivalent of 1,400,000 100 kW systems. Even with the drive towards renewable energy, the diesel generator market is expected to increase with a CAGR of 5.5 % from 2023 to 2030 likely signifying that the renewable energy growth will not be able to fully satisfy the

⁵<https://www.bloomberg.com/press-releases/2023-03-02/global-generator-sales-market-size-and-analysis-predicted-growth-to-reach-usd-32-8-billion-by-2030-with-a-cagr-of-5-5-report>, accessed on 16-06-2023

⁶<https://skysails-marine.com/>, accessed on 06-06-2023

demand for on-shore off-grid power plants⁷.

The LLS system is not a standalone product and must be integrated with a soft kite AWE system. As of 2023, there are no independent companies that provide an LLS system, as it is usually part of the AWE provider itself. In this view, the market obtainable is limited by the market share of soft kite systems providers. In the case of power plants with a size less than 0.5 MW it is assessed that the SOM previously calculated is realistic for soft kites. Four companies have been identified as potential clients of the LLS, namely: Kitepower, SkySails, Kitenergy and X-Wind^{8 9} [6]. Out of these, SkySails has already an automated LLS system and hence will not be considered. The development costs for AWE are significant [3], and there is still a considerable amount of support needed before achieving a viable product [7]. Relieving the burden of the LLS for AWE companies by outsourcing it could help them achieve commercial viability earlier, but also provides an investment opportunity. After discussion with an expert in the field, the market share for a LLS system is estimated to be 40 % of the total soft kite AWE market. Due to time constraints, this value will not be investigated further and will be used as it is.

2.3. Competitive Field

The analysis can be expanded by performing a Strengths Weaknesses Opportunities Threats (SWOT) and deriving associated requirements to build upon the strengths and opportunities associated with the product while reducing the impact of weaknesses and external threats.

S.1: Because AWE systems operate at a higher altitude than conventional wind, these systems can harvest more reliable and powerful wind currents, expanding the geographic areas that are commercially viable for wind. Furthermore, some of these new areas such as remote island communities can experience more extreme weather conditions, which leads to STK-OEM-14.

S.2: AWE is easier to transport, mount and install than conventional wind energy, making it favourable for temporary applications and remote regions. The associated requirements are STK-OEM-11, STK-OEM-12 and STK-OEM-15.

S.3: AWE can deliver more energy per km^2 than other renewable energies sources [7]. In consequence, to keep the advantage, the LLS should not affect the overall cost per energy performance of the existing system. This aspect is covered in STK-OEM-05 and STK-OEM-06.

S.4: AWE has a smaller environmental impact than conventional wind due to fewer materials used in production and the lack of deep ground foundations. This can be further reinforced by compliance with a sustainability policy (STK-OEM-10) and prohibiting the emission of toxic compounds (STK-PVS-02).

W.1: Currently, only one soft wing AWE company possesses the capability to launch, land and store autonomously. This is a weakness of existing systems, as it is very important for customers to have an autonomous system. As such this driving requirement is translated in STK-OEM-01, STK-OEM-02, STK-OEM-03 and STK-OEM-04.

O.1: The world demand for on-shore off-grid energy is expected to increase, as shown by the forecasted increase in sales of diesel generators (see SOM). This opportunity is used to increase the market share of AWE systems by capturing a fraction of the new generator sales.

O.2: With more than €8.7 billion (FY2022) investments in renewable energy from public funds

⁷<https://www.bloomberg.com/press-releases/2023-03-02/global-generator-sales-market-size-and-analysis-predicted-growth-to-reach-usd-32-8-billion-by-2030-with-a-cagr-of-5-5-report>, accessed on 16-06-2023

⁸<https://ore.catapult.org.uk/wp-content/uploads/2019/02/An-Introduction-to-Airborne-Wind-Stephanie-Mann-AP0020.pdf>, accessed on 06-06-2023

⁹<https://x-wind.de/>, accessed on 06-06-2023

in Europe alone [8, 9], there is a large opportunity to acquire the funds necessary for the development of AWE. This is taken into account in the business strategy.

T.1: For unproven technologies, sourcing capital can be challenging. To limit the initial capital needs, the manufacturing of LLS components will be outsourced to commercial partners. This is a business decision and will be used in the pricing model.

T.2: Electrical systems used in the renewable energy transitions often make use of rare earth materials, which are only found in a few countries across the world¹⁰. Even if AWE requires less of these materials, an increase in price could affect the viability of the product. To mitigate this effect, an analysis of the increase in production cost is performed to quantify the impact.

T.3: The regulatory framework for AWE below 500 m is not yet developed [7]. This can pose significant challenges for the deployment of the systems. Requirement STK-GOV-01 enforces the incorporation of the safety regulations when these are released.

T.4: In new technologies, the market is often rapidly evolving and one can fall behind if not adapting to the change in demand and competition. To mitigate this effect, the LLS design should allow for upgradability (STK-OEM-17).

2.4. Product Profitability Assessment

The economical viability of the LLS is intricately connected to that of the AWE as a whole. As such, the profitability of the LLS is calculated based on the viability of the AWE itself. Throughout this section, a financial analysis is performed for first the AWE system and then translated to the LLS. All quantities are expressed in FY 2023 (unless said otherwise) and all the future prices are indexed for inflation. In consequence, all costs and prices discussed are real. All calculations have been conducted using the in-house Financial Overview Model. The working principle, assumptions, and a link to access the tool are provided in Appendix B.

Sales forecast

The first step to assess the viability of a product is to estimate the number of sales for a given period. In this case, a long-range forecast is considered most appropriate, as the aim is to investigate the long-term viability of the product. As such, a reference period of 10 years is chosen. The target market growth is assessed to be 5.5 % as identified in Section 2.2. The other parameters that are of interest are the initial market share of AWE taken to be 0.25 % giving a number of first-year sales estimated at 55 units. These have been found by iteration to achieve commercial viability and with discussion with experts in the field (personal communication, 16-06-2022). This would correspond to a roll-out in 2025 according to the latest predictions [7]. The resulting yearly sales profile is shown in Figure 2.1.

Although exponential growth is assumed, the sales are not expected to slow down during the reference period due to an abundance in the supply of AWE systems as over the selling period the market share expected to be captured is only 0.6 %, i.e. a cumulative sale of 878 out of a potential of 150,000 forecast. The main limiting factor is expected to come from upscaling the production processes if a competitive price can be proposed.

Expected Costs

The cost of the system can be split into two origins. The first is the research and development costs of the system before commercial roll-out at the technology readiness level (TRL) of 9. Initially, these costs were estimated at €90 million, according to [3]. After discussion with Kitepower B.V. (personal communication, 08-06-2022) a more optimistic target is set to €15

¹⁰<https://www.iea.org/reports/the-role-of-critical-minerals-in-clean-energy-transitions/executive-summary>, accessed on 15-06-2023

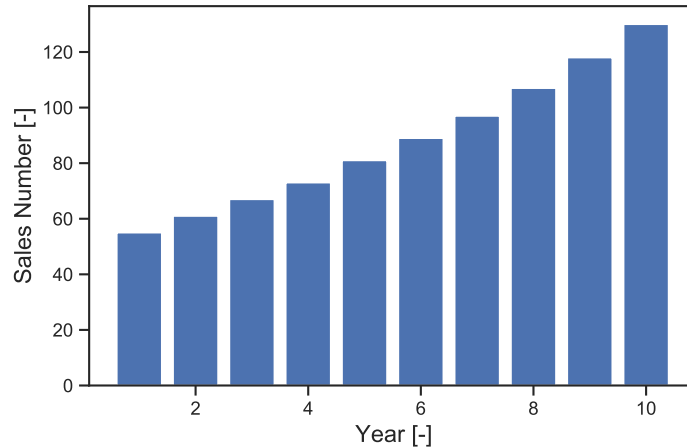


Figure 2.1: Airborne Wind Energy system sales forecast

million including an assumption of a €5 million governmental grant leading the effective capital investment of €10 million. This large difference can be explained by the off-sourcing of the manufacturing, leading to smaller required investment costs. The sum would need to be recovered over the lifetime of the product. Out of this capital, €7.5 million are allocated to the LLS, and €2.5 million to the remaining subsystems of the AWE system.

The second source of cost relates to the individual cost of each product. These include manufacturing, operation, maintenance, logistical and decommissioning costs. As a first approach, the 4 latter costs are estimated from literature [10]. The estimated manufacturing cost is estimated from a discussion with experts in the field. Table 2.1 regroups the values taken for the cost estimation for a single product. After the detailed design is performed, these values are updated to reflect more accurate estimates of the costs.

Table 2.1: Initial cost estimate (per unit)

Category	Estimated Cost [€]
Manufacturing	636000
Operation and Maintenance	25275
Consumables	17000
Manpower	6525
Insurance	1750
Logistics	8920
Transport and Installation	4000
Civil Works	4920
Decommissioning	4920

Pricing Approach

As discussed previously, the target market is currently largely dominated by high-cost diesel generators. Renewable technologies such as solar panels and small wind turbines are significantly cheaper and have started to invade the market [11]. However, the current level of technological maturity of AWE renders it competitive for niche applications against fossil fuel alternatives. As a consequence, the pricing approach will focus on guaranteeing a profit margin rather than selling the product to compete with wind or solar.

The underlying business approach used here is consistent with what is being used in AWE start-ups. It consists of selling the product with a small profit and generating the bulk of the net

revenue from maintenance and repairs to the system as seen from Figure 2.2a and Figure 2.2b. Due to the nature of startups, the future revenue is heavily discounted, e.g. 30 %, to account for the uncertainty in performance¹¹. Suitable real profit margins are found to be 6 % for the initial sales and replacements, and 30 % for the servicing and maintenance operations leading to a Net Present Value (NPV) of €8.5 million, expected net revenue of €193 million corresponding to Return on Investment (ROI) of 1926 % and an Internal Rate of Return (IRR) of 45.65 %.

These values are found over extended periods of time and are subject to significant variations due to uncertainties. Furthermore, the advantageous Dutch tax system for innovative businesses is used which reduces the corporate income tax from 25.8 % to 9 %¹².

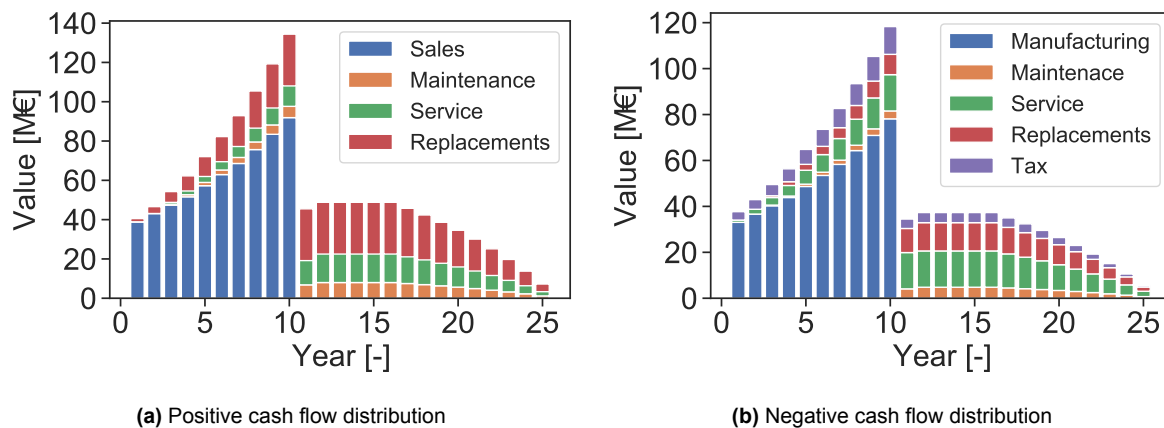


Figure 2.2: Annual cash flow throughout the lifetime of the project

Sensitivity Analysis

Courtesy of the discussion above, the sale price for financial viability is dependent on many parameters. The aim of this sensitivity analysis is to discuss some of the most critical parameters and hence have an estimate of the profit margin allowed by the model. The financial performance is quantified using the ROI, NPV, IRR and the Earnings Before Interest, Tax, Depreciation and Amortisation (EBITDA).

Figure 2.3a and Figure 2.3b express the model's sensitivity to the sales forecast parameters, the initial market share and the growth rate of the market share. As expected, the starting share has a larger influence on the outcome compared to the growth rate. Within a 30 % margin on both parameters, the product is still viable, although there is a significant difference in return. One possible strategy to mitigate this effect would be batch production. In this approach, the systems would not be manufactured before a certain amount of initial orders have been reached.

On the other hand, the model is highly sensitive to an increase in costs and tax, as shown in Figure 2.3c and Figure 2.3d. This is due to small profit margins on the initial sale, which represents the bulk of the revenue. In consequence, the selling price will need to be adjusted to reflect an increase in costs. This will likely happen over the lifetime of the product as the taxation regime will change from innovative to standard raising significantly the costs. However, it is expected that by that time the company will overcome its initial struggles and be able to survive a higher taxation regime.

For further exploration a scenario analysis would be insightful as it allows evaluating the compounding effect of varying multiple parameters. Investigating favourable and less favourable scenarios would provide a more complete perspective on the sensitivity of the returns.

¹¹<https://eqvista.com/company-valuation/discount-rate/>, accessed on 20-06-2023

¹²<https://business.gov.nl/running-your-business/business-taxes/filing-your-tax-returns/how-t>

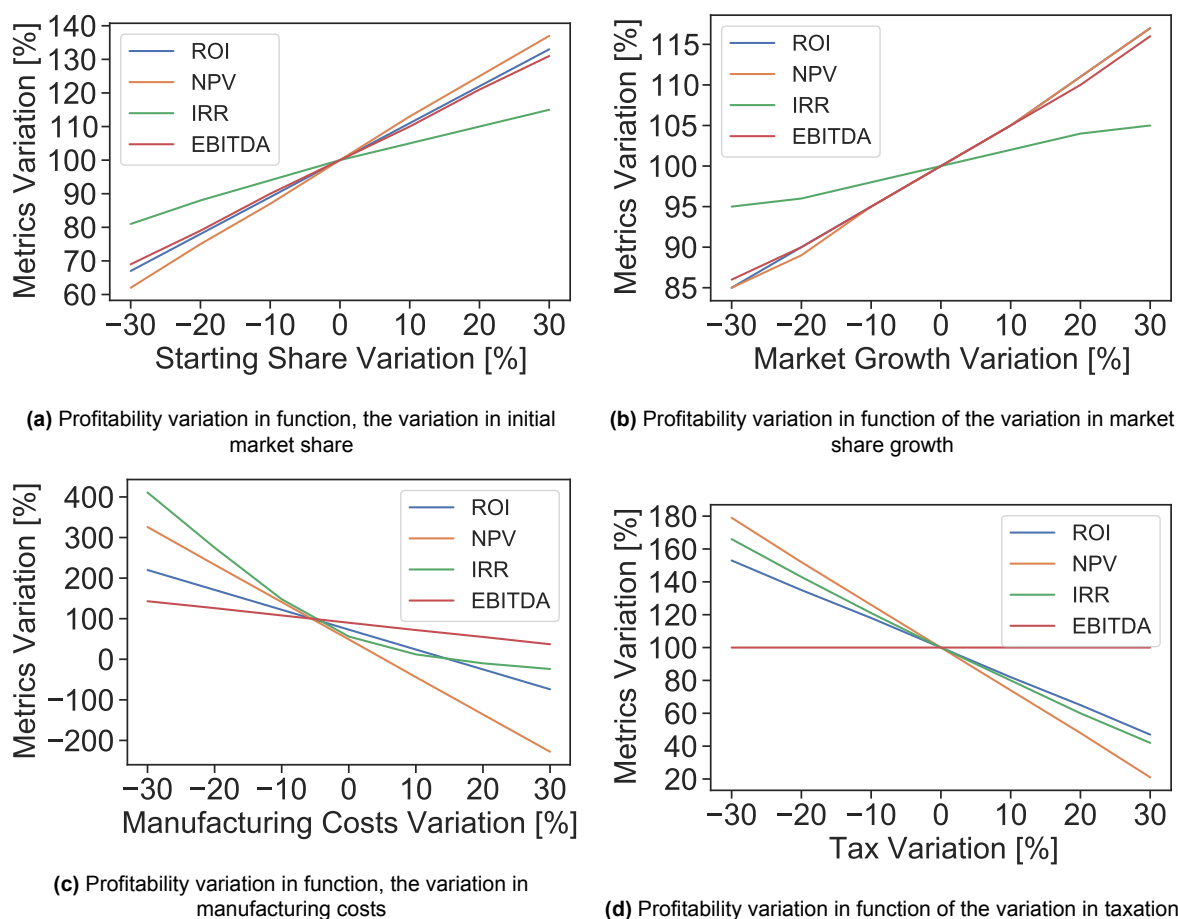


Figure 2.3: Sensitivity analysis on the influence of the variation of some model assumptions on economic performance

2.5. Recommendations

The approach discussed up to now is a first assessment of the financial performance of the product, and improvements can be made in several areas. The first aspect would be an improved sales estimation based on sales intent data. The novelty of the AWE industry does leave the possibility of using historical data. Access to yearly revenue and sales from multiple companies in this industry would aid in generating more accurate predictions for future projects.

Another improvement to the existing model would be the integration of several valuation methods in order to determine the enterprise value. In general, it is recommended to average multiple industry-standard start-up valuation methods as a preliminary estimate. Such methods are namely; scorecard method¹³, checklist method¹⁴, and venture capital method¹⁵. The results can be combined with the discounted cash flow method to obtain a better estimation.

Some final suggestions are to integrate component reliability to identify failures throughout a system's lifetime, a revised target market analysis accounting for key mobility needs and an overview that allows comparison between different selling strategies and forecasts.

o-use-the-innovation-box/, accessed on 20-06-2023

¹³<https://eqvista.com/scorecard-valuation-method-explained/>, accessed on 19-06-2023

¹⁴<https://matters2.com/the-checklist-valuation-method/>, accessed on 19-06-2023

¹⁵https://thebusinessprofessor.com/en_US/business-personal-finance-valuation/venture-capital-method, accessed on 19-06-2023

Functional Analysis

The functional analysis identifies the functions the system needs to perform in order to successfully complete its mission of landing, storing and relaunching the kite of an AWE system. And then the functional flow diagram is shown followed by the functional breakdown diagram.

Functional Flow Diagram and Breakdown Structure

The functions that have been used in the functional flow diagram and the functional breakdown structure are the most prevalent and top-level functions of the system. These functions include:

- FUN.0 Produce System
- FUN.1 Transport System
- FUN.2 Setup System
- FUN.3 Wait for Take-Off
- FUN.4 Deploy Kite
- FUN.5 Launch Kite
- FUN.6 Operate Kite
- FUN.7 Land Kite
- FUN.8 Store Kite
- FUN.9 Maintenance
- FUN.10 Prepare for Transport
- FUN.11 Execute End of Life
- FUN.12 Deliver Power

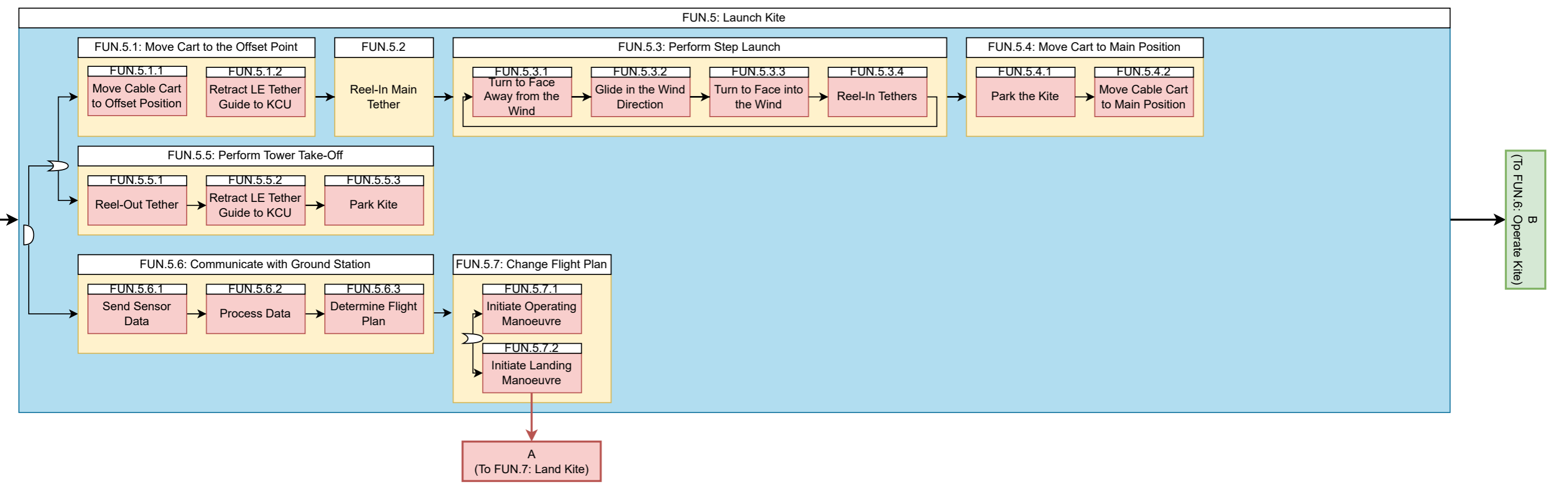
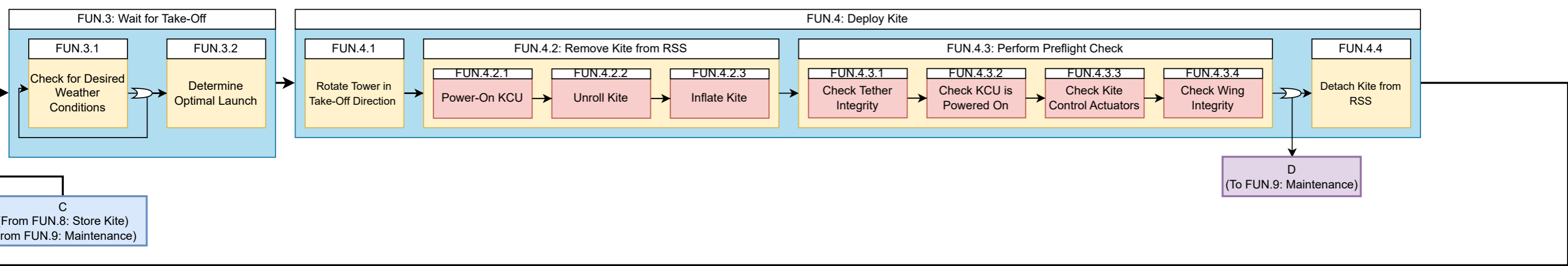
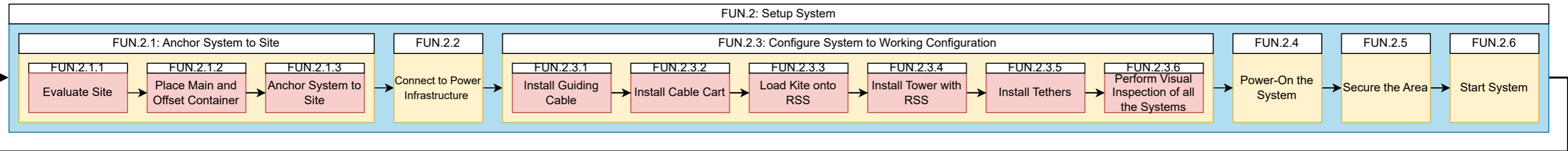
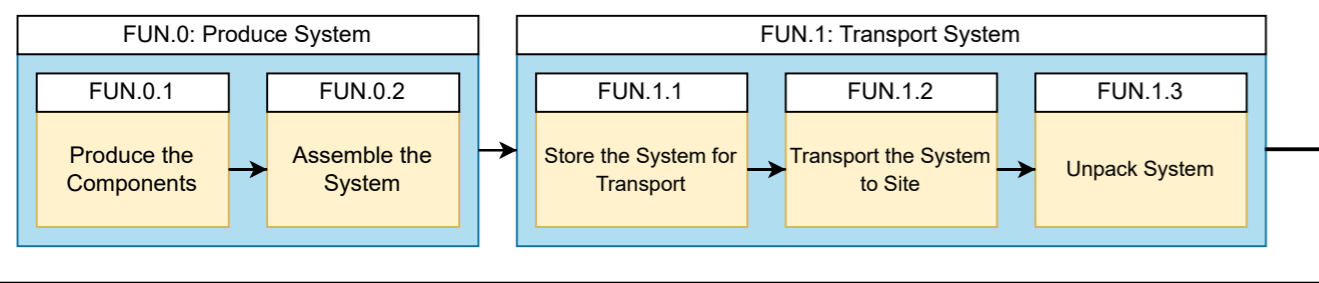
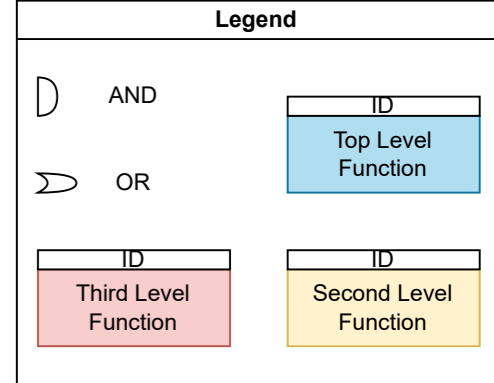
FUN.0 follows from the full design of the system. The assembly is carried out in Lithuania and delivered internationally (FUN.1). At the destination, the dominant wind direction is assessed and the containers are placed and anchored correspondingly. The other components are unpacked and installed. The system is inspected and activated. The operational mode starts and the system autonomously finds an economical time to launch, as explained in Section 6.1.

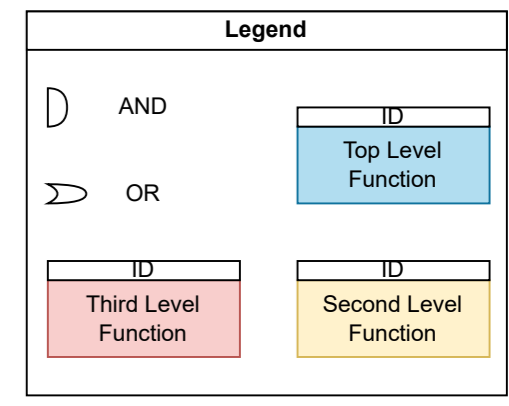
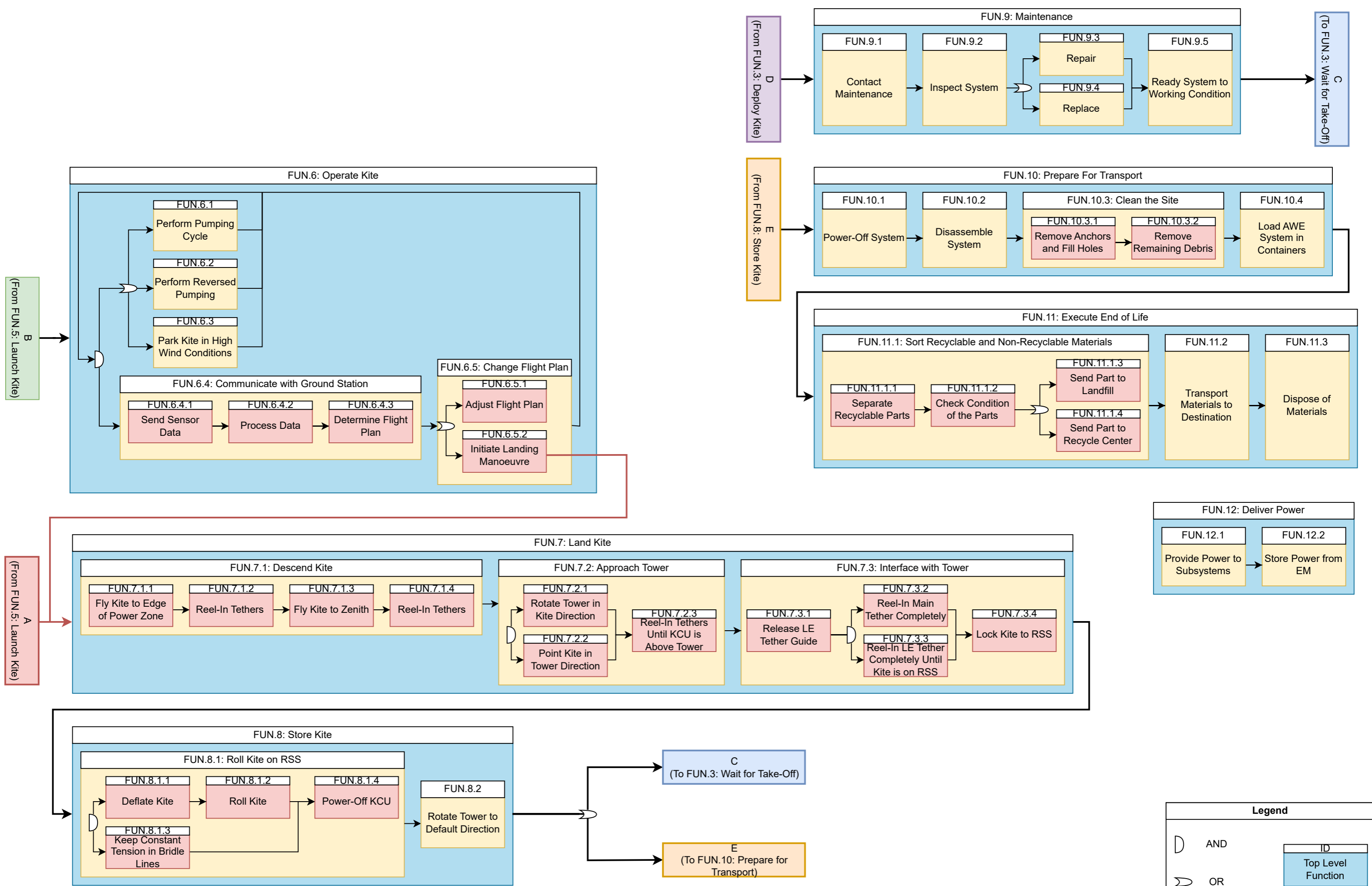
When the decision to launch has been made, the kite can either use the cable cart in low wind or just be released from the tower in stronger wind. In the former the cart is at the ground station, as it drives to the offset station it takes the tether with it over the swivel access point, it arrives at the offset station and attaches to it. The tether is then reeled in quickly, causing the kite to take flight. After towing and if the kite is not high enough a step-tow launch will be performed, which is explained in Section 6.2.2. This is done as many times as necessary till an altitude with sufficient wind speed is obtained to climb normally to operational altitude. With strong winds, the kite will be able to take flight directly from the tower. The tether is reeled out and the kite rises while making crosswind manoeuvres, after which it goes into operational mode.

The operational mode of FUN.6 consists of alternating pumping and reversing. When the winds are too strong the kite can be set into a safe parking mode. During this mode, it is continually assessed whether it is still economical to keep flying. With low winds, it will cost energy to remain in flight, so landing may be favourable. During landing the kite flies towards the tower while the leading edge bridle and the main tether are reeled in. The LE bridle is then used to guide the kite towards the tower, on which it subsequently lands.

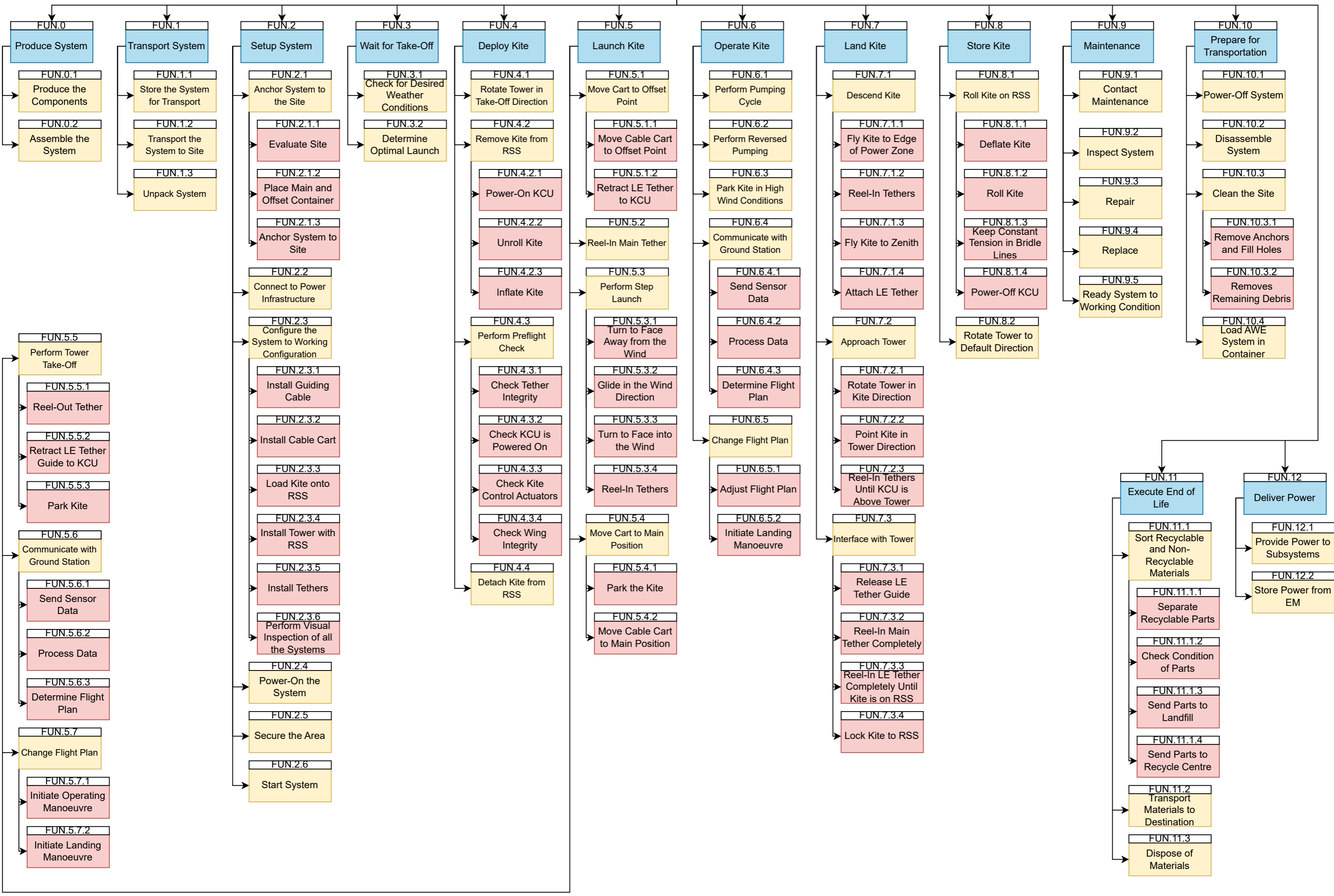
Once the kite is secured, FUN.8 begins storing the kite by deflating it and rolling it up into the Rolling Storage System, while tension is kept in the bridle lines, as explained in Section 13.3.5. Then either the cycle is continued, maintenance is performed, or the system is prepared for transport. For the latter, the system is disassembled and removed, leaving no mark on the environment as required by the unwritten laws of common decency. The system could be made ready for re-deployment and be stationed elsewhere, or, as any object in this cruel world, it will meet its ultimate fate at the pearly gates.

FUN.12 is the function related to the power usage and generation of the system. These functions happen in parallel during the operational life of the system. Following the functional flow diagram, the functions are ordered hierarchically in the functional breakdown structure.





Automatic Landing, Storage and Re-Launching of a Soft Kite Power System



In this chapter, the more global requirements are going to be addressed. Firstly, the stakeholder requirements are shown in Section 4.1, since the team's main priority is to comply with the stakeholder's necessities. This is followed by the parent requirements in Section 4.2, which will drive the design of the concept. Finally, in order to comply with the sustainability regulations some environmental requirements are stated in Section 4.3.

4.1. Stakeholder Requirements

There are five main stakeholders which are affected by the design of an LLS system. STK indicates that the requirement is a Stakeholder requirement. The second part of the identifier indicates the origin of the requirement.

- **OEM:** Original Equipment Manufacturer
- **DO:** Design Office
- **GOV:** Government
- **PGO:** Power Grid Operator
- **PVS:** People in Vicinity of the System

The stakeholder requirements are presented in Table 4.1.

Table 4.1: Stakeholder requirements

ID	Stakeholder Requirement
STK-OEM-01	The LLS system shall operate autonomously for 6 months.
STK-OEM-02	The LLS system shall enable the autonomous deployment of a soft kite AWE system to nominal operating conditions.
STK-OEM-03	The LLS System shall enable the autonomous retrieval of a soft kite AWE system from nominal operating conditions.
STK-OEM-04	The LLS System shall enable the autonomous storage of a soft kite AWE system.
STK-OEM-05	The LLS System shall be able to function within the operating window of the AWE system.
STK-OEM-06	The LLS System shall not hinder the performance of the AWE system.
STK-OEM-07	The additional costs of the LLS System for the 100 kW variant shall be at maximum €40,000 per system.
STK-OEM-08	There shall be no financial impact of the LLS System on the other subsystems.
STK-OEM-09	The LLS System shall allow for the replacement of its individual components in case of failure.
STK-OEM-10	The LLS System shall comply with the company sustainability goals.
STK-OEM-11	The LLS System shall be contained within a standard 20-foot shipping container.
STK-OEM-12	The LLS System shall not negatively affect the mobility of the AWE System
STK-OEM-13	The LLS System shall be able to sustain common transportation loads without damage
STK-OEM-14	The LLS System shall be able to operate in harsh environments.
STK-OEM-15	The LLS System shall not lengthen the installation time of the AWE system over 24h.

STK-OEM-16	The LLS shall be able to operate on batteries when no energy is generated.
STK-OEM-17	The LLS shall be upgradeable to allow for the use of larger kite systems.
STK-PGO-01	The LLS System shall not cause damage to the power grid connected to the AWE system.
STK-PGO-02	The LLS System shall not hamper the interface with the power grid.
STK-GOV-01	The LLS System shall comply with the safety standards applicable to AWE systems.
STK-DO-01	The design of the LLS System shall be completed in 10 weeks.
STK-DO-02	The LLS System shall be designed by 11 aerospace engineering students.
STK-DO-03	The LLS System design office shall have the freedom to redesign the other subsystems.
STK-PVS-01	The LLS System shall keep noise generation within the bounds of the regulations applicable to AWE system.
STK-PVS-02	The LLS System shall not produce toxic products harmful to the environment.

Many of the stakeholder requirements, trickled down to the parent of system requirements, or system constraints. The stakeholder requirements focused mainly on the working of the LLS system, however, the design of this system will ultimately affect the rest of the AWE System, so system requirements were added for the operation of the AWE system as a whole. Finally, the Design Office requirements are not reflected in the system requirements, as they do not affect the operation of the system, but only constrain how the product is developed.

4.2. System Requirements

As previously said, the requirements stated in this section will cover the parent requirements that are driving and are regarding the LLS itself. Driving requirements can be defined as requirements that are user-defined or derived. These have quite an important role when designing the product and are stated in Table 4.2.

Table 4.2: Driving Parent Requirements

Identifier	Requirement
LLS-GEN-OP-01	The system shall perform its functions without human intervention.
LLS-GEN-OP-02	The system shall be able to function in winds up to level 8 in the Beaufort scale.
LLS-GEN-OP-03	The setup of the system shall not take longer than 24 hours.
LLS-GEN-OP-04	The system shall be compatible with current AWE systems.
LLS-GEN-OP-15	The size of the folded soft kite in the 100kW system shall not exceed 5x1x1 meters.
LLS-GEN-OP-16	The AWE system shall be able to survive in remote harsh environments.
LLS-GEN-STRUC-01	The system shall not exceed its mass budget.
LLS-GEN-STRUC-02	The structure shall be able to support limit loads without permanent deformations.
LLS-GEN-STRUCT-03	The system shall be able to sustain wind velocities up to 30 m/s without failure.
LLS-GS-OP-01	The ground station shall facilitate the nominal operation of the system.
LLS-GS-OP-02	The ground station shall measure the wind speed accurately.
LLS-GS-ELEC-01	The ground station shall provide electrical energy as output.
LLS-GS-ELEC-02	The ground station shall not be reliant on the external power supply.
LLS-GS-STRUC-01	The ground station shall not exceed its mass budget.

LLS-GS-STRUC-04	The ground station shall be able to support limit loads without permanent deform
LLS-TETH-STRUC-01	The tether shall be able to support limit loads without permanent deformation.
LLS-GS-ELEC-02	The ground station shall not be reliant on an external power supply.

4.3. Sustainability Requirements

In recent years, sustainability has had a major influence on the design of any new product that wants to be introduced to the market. For this reason, a set of requirements regarding sustainability will now be stated. The parent requirement's identifier for sustainability is CON-LLS-GEN-03: The LLS system development and operation shall be conducted in an environmentally sustainable manner.

Table 4.3: Child requirements of CON-LLS-GEN-03

Identifier	Requirement
CON-LLS-GEN-03-01	The entire system shall be carbon neutral during its operation
CON-LLS-GEN-03-02	The entire system shall be 30% recyclable.
CON-LLS-GEN-03-03	The system shall have a lifetime of 20 years.
CON-LLS-GEN-03-04	The greenhouse emissions payback time of the system shall be lower than 22.5 months.
CON-LLS-GEN-03-05	Any aluminium used for the production of parts shall have a GWP footprint lower than $0.6 t_{CO_2e}/t_{Al}$
CON-LLS-GEN-03-06	Any carbon steel used for the production of parts shall have a GWP footprint lower than $2.0 t_{CO_2e}/t_{Steel}$
CON-LLS-GEN-03-07	Bio-Based Trademark for UHMWPE (Ultra high molecular weight polyethylene) fibre (Dyneema®) shall be used for the tether.
CON-LLS-GEN-03-08	The batteries used in the system shall have a GWP footprint lower than $76 g_{CO_2e}/kWh$.

Before jumping into the final design of the product, it is worth mentioning the trade-off procedure that led to the choice of the final concept. Firstly the considered concepts will be outlined in Section 5.1, then the trade-off process with the criteria and relative weights used will be treated in Section 5.2 and lastly the budgets of the final concepts will be treated in Section 5.3.

5.1. Initial Concepts

Four concepts were considered for the final design: Offset Winch Launch (OWL), Winch with Rover Assisted Positioning (WRAP), Horizontal Axis Spinning Launch (HASL), and Rail Assisted Winch (RAW).

Offset Winch Launch (OWL)

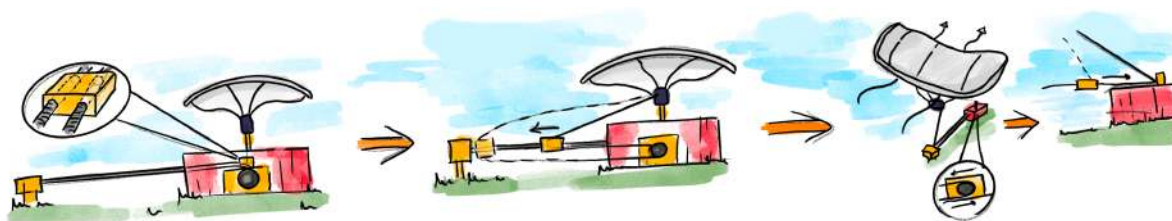


Figure 5.1: Offset Winch Launch (OWL)

The system comprises a movable cart containing a swivel access point used as an offset winch point and able to move between the ground station and an offset container on two cable guides. The kite would be landed on a rotating tower placed on top of the ground station and rolled up around a tilted rotating mast where it would be stored. In low wind conditions, the kite would be launched by reeling in the tether connected to the cart offset from the ground station. In high wind conditions (above 6 m s^{-1}), the kite would be launched directly from the tower, oriented in the downwind direction. In both situations, before launching, the kite needs to be inflated while still laying on the tower.

Winch with Rover Assisted Positioning (WRAP)

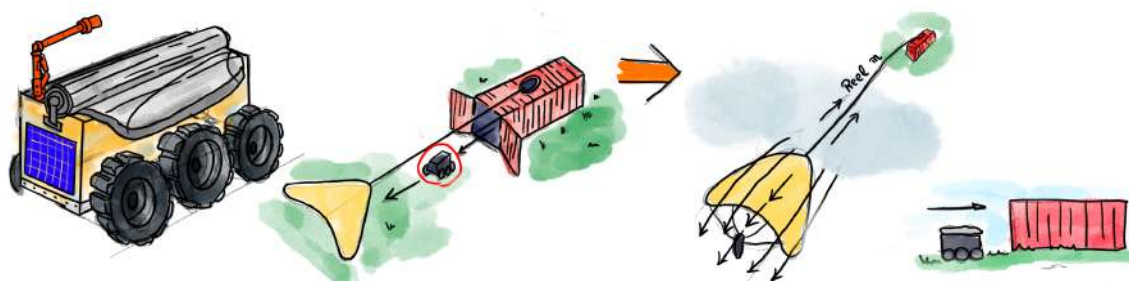


Figure 5.2: Winch with Rover Assisted Positioning (WRAP)

In this concept, a winch and a rover are involved to carry out the launching, landing and storing procedures. The soft wing would be free to land out in the field, and it is the task of the rover to approach it and roll it around a rotating pole, with the aid of a robotic arm. The rover is used to

move the kite out in the field in the desired downwind position, from where it can then be inflated and winched in towards the ground station at the required take-off speed and hence launched.

Horizontal Axis Spinning Launch (HASL)

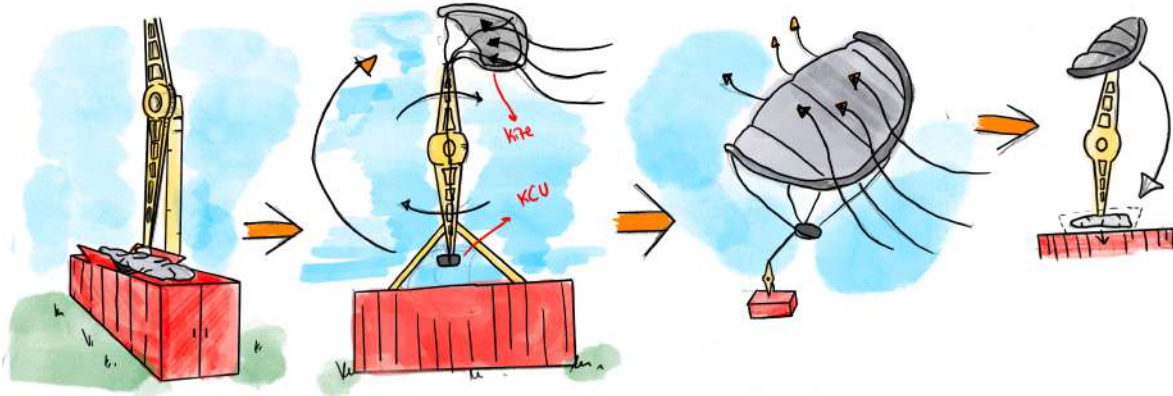


Figure 5.3: Horizontal Axis Spinning Launch (HASL)

This system involves a spinning arm, on which the kite lands and is stored. The kite approaches the tower firstly with the KCU, which is secured to the arm, and then the kite is landed on a rolling axis mounted on the edge of the tower and used eventually to wrap the kite around it. It is then stored by bringing it close to the ground and placed inside a container. The launching is achieved by spinning the tower and disconnecting the kite previously inflated and the KCU from the arm.

Rail Assisted Winch (RAW)



Figure 5.4: Rail Assisted Winch (RAW)

Here a rail mounted on a rotating tower is used to perform the landing, storing and launching operations. The ground station is rotated to align the kite downwind for the launching phase. The soft wing is accelerated along the rail by reeling in the tether, allowing the kite to take off. The kite is landed by reeling it in such that an attachment point on the trailing edge interfaces with the rail, securely locking the kite on the structure. The tower is able to rotate around its longitudinal axis, letting the kite wrap around it, hence storing it.

5.2. Trade-off

In order to select the final design, a trade-off was performed. Six different criteria were chosen to properly quantify the overall performance of each concept, namely the performance, environment adaptability, scalability, costs, technical feasibility and sustainability.

5.2.1. Trade-off Criteria

In order to select the most relevant criteria for the system, the customers' needs were carefully derived from the stakeholder requirements for the system. The needs and relative requirement ID are shown in Table 5.1.

Table 5.1: Requirements and customer needs

REQUIREMENT ID	CUSTOMER NEEDS
CON-LLS-GEN-01-13	Autonomy
CON-LLS-GEN-01-04	Low Maintenance
CON-LLS-GEN-02	Low Maintenance
CON-LLS-GEN-04	Safety
CON-LLS-GEN-05	Safety
CON-LLS-GEN-03	Environmentally Friendly
CON-LLS-GEN-01-05	Easy Installation
CON-LLS-GEN-01-07	Easy Installation
CON-LLS-GEN-01-08	Easy Installation
CON-LLS-GEN-01-01	Economical
CON-LLS-GEN-01-02	Economical
CON-LLS-GEN-01-03	Compact Sizing
CON-LLS-GEN-01-08	Compact Sizing
CON-LLS-GEN-01-12	High Upgradability
CON-LLS-GEN-01-14	High Altitude Reach

After reviewing the customer's needs, six criteria for the trade-off were selected:

- **Performance:** it is related to the initial altitude that can be reached by the kite immediately after being launched. It is a very important parameter, as this is the starting altitude from where the step tow launch procedure brings the kite to the operational altitude. Based on it, the number of steps and energy involved in the step launch process varies.
- **Environment Adaptability:** it is related to the environmental conditions in which the LLS is located. Since the system may be deployed in remote locations, it is important to assess the different terrains and weather conditions this system may work in.
- **Scalability:** it represents the possibility for the LLS of upgrading to higher-rated power systems. This factor has a large impact on the attractiveness to the customer.
- **Costs:** this is a driving factor that influences the design. Having a cheap design makes the system more appealing to the customers. A hard requirement on the total price of the LLS for the 100 kW system of €40000 was set by the stakeholders (STK-AEP-07), which makes this criterion of utmost importance.
- **Technical feasibility:** it is related to the possible market applicability of the system. Reliability and complexity have been considered as part of this criterion. The first one is linked to the probability of an unrecoverable failure to occur, while the latter is related to the amount and type of components involved in each concept
- **Sustainability:** it is a very important and driving requirement for the LLS design, as well as a stakeholder requirement (STK-PVS-02). It is assessed by estimating the total amount of equivalent carbon emissions and energy utilised by each concept.

5.2.2. Criteria Weighting

Every criterion has also been given a relative weight, based on its importance, derived from the stakeholders' needs shown in Table 5.1. Table 5.2 shows the outcome of the weighting analysis. The grading scheme chosen was 0,1,3,6 or 9, 9 being the best and 0 being the worst grade.

Table 5.2: Trade-off criteria weights (zero, one, three, six, or nine) determination

Customer Importance Rating	Customer Needs	PERFORMANCE	SCALABILITY	ENVIROMENTAL ADAPATABILITY	COSTS	TECHNICAL FEASIBILITY	SUSTAINABILITY
5	Autonomy	3	1	3	3	9	1
4	Low Maintenance	-	1	9	6	9	1
2	Safety	-	3	1	-	6	1
4	Environmentally Friendly	-	1	-	1	0	9
1	Easy Installation	1	9	-	3	1	-
4	Economical	3	3	1	9	3	1
3	Compact Sizing	-	1	-	9	3	3
2	High Upgradability	9	9	1	3	6	6
3	High Altitude Reached	9	1	3	-	-	-
SUM		73	64	68	115	127	72
WEIGHTS		14.1%	12.3%	13.1%	22.2%	24.5%	13.9%

5.2.3. Trade-off Matrix

Each concept was evaluated for the criteria shown in Section 5.2.1 using a grading scheme from 1 to 4. The results are shown in Table 5.3, where a short reasoning for every given grade is included.

Combining these grades with the relative weights for each criterion calculated in Table 5.2 allows finalising the trade-off leading to the choice of the final design. The weighted trade-off table is shown in Table 5.4.

Table 5.4: Trade-off table with weights

Relative Weight	Concept				
	Criteria	OWL	WRAP	HASL	RAW
0.141	Performance	3	4	2	1
0.123	Scalability	3	4	1	1
0.131	Environment Adaptability	3	2	4	4
0.222	Costs	4	2	2	3
0.245	Technical Feasibility	3	3	1	2
0.139	Sustainability	2	1	4	4
TOTAL		3.086	2.636	2.174	2.5

After the trade-off was completed, the best concept resulted in being the OWL, with a weighted average of 3.086.

Table 5.3: Trade-off table reasoning

Concept Criteria	OWL	WRAP	HASL	RAW
Performance	60 m max. launch altitude [3]	200 m max. launch altitude [4]	20 m max. launch altitude [2]	10 m max. launch altitude [1]
Scalability	Low-medium complications up-scaling [3]	Low complications in scaling up [3]	High complications in scaling up [1]	High complications in scaling up [1]
Environment Adaptability	Rocky terrain with large weather variations [3]	Uneven terrain with medium weather variations [2]	All types of terrain (incl. unpassable) and extreme weather conditions [4]	All types of terrain (incl. unpassable) and extreme weather conditions [4]
Costs	€15,000 [4]	€31,000 [2]	€35,000 [2]	€28,000 [3]
Technical Feasibility	Low complexity and medium to low incident recovery capability [3]	Low complexity and medium to low incident recovery capability [3]	High complexity and low incident recovery capability [1]	Medium complexity and low incident recovery capability [2]
Sustainability	4000 kg carbon equivalent emissions and 0.54 kWh per cycle [2]	3400 kg carbon equivalent emissions and 5.5 kWh per cycle [1]	1500 kg carbon equivalent emissions and 0.22 kWh per cycle [4]	1900 kg carbon equivalent emissions and 0.29 kWh per cycle [4]

5.3. Final Design

The final chosen design was carried out in more detail, in order to have a more accurate preliminary estimation of the key parameters of the system, such as cost, structural dimensions, energy required per launch and carbon equivalent emissions involved in its production.

At this preliminary stage, it was decided to have a stationary cable with the cart moving over it, for cost and sustainability reasons, as a moving cable would have introduced numerous extra components in the system. It was also decided to use the battery already present in the original system as an anchoring point, instead of having a driving pole in the ground, which would have been difficult to set up and remove from the site. The relevant initial estimations carried out for the OWL system are summarised in Table 5.5.

Table 5.5: Initial Estimations of the OWL

Parameters	Value Estimated
Height of pole	15 <i>m</i>
Reel in speed	12 <i>m/s</i>
Energy per launch cycle	0.54 <i>kWh</i>
Minimum costs	12800 €
Maximum costs	16700 €
Carbon equivalent emissions	4000 <i>kg</i>

The design team recommends that in the future, all the concepts are studied in detail, as well as novel versions of the final concept, such as the use of a pulley system (like currently used by Kitepower in their tower launch) to pull the tether to the offset point, instead of a cable cart.

The OWL launch, landing and storage concept is a new type of operating an AWE system. Therefore it is important to be clear about how the system works. First Section 6.1 explains when the kite will be launched and landed based on the economics of the system. Secondly, Section 6.2 explains how the kite will be brought to its operational altitude. Then, in Section 6.3 the landing of the kite is discussed, followed by storage in Section 6.4, and finally recommendations in Section 6.5.

6.1. Launching and Landing Determination

For the system to be economically viable, it should be determined what the optimal time to launch is based on a wind forecast, and when flying, what the optimal time to land will be. The profitability of the launch depends on the wind forecast. If you can launch just before the wind is enough to produce energy at operational height, launching might be the correct decision. On the other hand, the kite can fly in no wind by means of reversed pumping. Though, when the wind forecast is low for a long period it is more beneficial to land the kite, otherwise it can be useful to bridge this time until the wind picks up again because launching and landing might cost more energy.

For this strategy, an anemometer will be used for instantaneous wind measurements and several wind forecasts for long-term strategy development. Wind forecasts are taken from multiple sources; The Global Forecasting System from the US and the European Centre for Medium-Range Weather Forecasts being the most detailed and reliable. To have a low variation in wind forecasts only wind data for six hours ahead will be used. It should be noted however that there are other factors that might necessitate a sooner launch or landing, such as a thunderstorm that is approaching.

6.2. Launch Phase

As a part of the operations, the kite has to be launched. This will be realised in two ways, depending on the wind speed. For wind speeds above 6 m s^{-1} , the lift-to-weight ratio of the kite is 1, meaning that the OWL system can launch the soft wing from the mast on top of the container, as explained in Section 6.2.3. On the other hand, for low wind conditions, an alternative way of launching is required since the lift-to-weight ratio is below one. To allow for launch, a Stepped Tow Launch (STL) will be used, which is explained in Section 6.2.2. Based on the performance during the STL the winching system will be sized. For this, it is essential to understand the wind shear that allows for identification of the parking altitude of the kite. The wind shear is based on a theoretic model, as explained in Section 6.2.1.

6.2.1. Wind Shear

The wind shear is the variation of wind with increasing height due to friction with the ground. The resulting curve has an increasing trend with altitude. This trend is composed of a bottom layer curve (Equation 6.1) and a top layer curve (Equation 6.2)[12]. In these equations V_{ref} is the reference speed at reference altitude h_{ref} . h_{blend} is the blending height, which is the transition from the bottom to the top layer. z_0 and α are parameters describing the roughness of the landscape with 0.01 and 0.143 respectively for an open land area which is the type of land where the AWE system will operate.

$$V(h) = V(h_{ref}) \frac{\ln(\frac{h}{z_0})}{\ln(\frac{h_{ref}}{z_0})} \quad (6.1)$$

$$V(h) = V(h_{blend}) \left(\frac{h}{h_{blend}} \right)^\alpha \quad (6.2)$$

6.2.2. Stepped Tow Launch

It is crucial that the OWL system allows the kite to reach the operational height where the pumping cycle for the production of energy can begin. The target altitude of 155 m, for the lowest wind condition of 4 m/s at 10 m height (requirement LLS-GEN-OP-02-01), must be reached in the shortest time possible using as little energy as possible. For low velocities, this goal will be reached by performing an initial winching take-off followed by a STL. This operation can be split into the following functions from the FFD in Chapter 3.

- FUN.5.1: Move Cart to Offset Winching Point
- FUN.5.2: Reel-In Tether
- FUN.5.3: Perform Step Launch
- FUN.5.4: Move Cart to Main Position

The take-off can only be done when the kite is positioned at a distance from the winching point. This is achieved by routing the main tether away from the main container to the offset container by means of a cable cart that drives over a guiding cable tensioned between both containers. The leading edge tether (which is required for landing) needs to be attached to the KCU before launch to prevent it from tangling with the bridle lines during the next parts of the launching manoeuvre.

The next step is to start the STL procedure. This is a take-off technique for para-gliders and is useful when a kite requires taking off from a flat location. The procedure consists of four phases; towing, turning after the tow, gliding and turning after the glide.

Towing The towing phase is centred around reeling in the tether to accelerate the kite to the apparent velocity required to gain a certain altitude. More generally, the radial velocity (given by reeling in the tether) results in a tangential velocity of the kite, therefore allowing it to take off. In Equation 6.3 the resulting tangential velocity is calculated due to the radial velocity[13].

$$a = \cos(\theta)\cos(\phi)\cos(\chi) - \sin(\phi)\sin(\chi)$$

$$b = \sin(\theta)\cos(\phi)$$

$$\frac{v_{\tau,k}}{v_w} = a + \sqrt{a^2 + b^2 - 1 + E^2(b - f)^2} \quad (6.3)$$

Where θ , ϕ and χ are the spherical orientation parameters of the kite shown in Figure 6.1. E is the lift-to-drag ratio of the kite. Lastly, f equals the normalised reeling velocity compared to the wind speed.

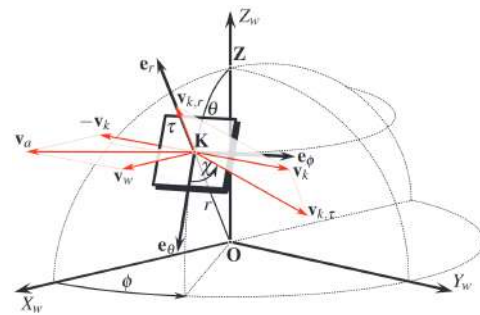


Figure 6.1: Wind oriented coordinate system showing the location of the kite with the θ , ϕ and r . Too, the heading of the kite is indicated with χ [13]

The towing reaches at some point a more horizontal trajectory, which is a less effective part of the launch. To limit this part, a limit will be set on the elevation angle of the kite. Apart from this, there is the reeling velocity, which is of importance to the towing performance. Analysis shows that the higher the velocity, the faster the kite reaches the destination altitude, though it requires more energy during the tow itself.

During this towing, the apparent velocity of the kite should be above 6 m s^{-1} to ensure enough

lift is produced. With a tailwind launch (worst case scenario) this means that the reeling speed should be the sum of the reeling speed of the best case scenario and the wind speed. This adds up to a winch speed of 12 m s^{-1} .

The limiting factor of the launch is mainly the load in the tether. This can maximally be 25 kN [14]. To comply with this, the reeling speed and lift setting should be varied over the tow. Varying the lift changes the drag too. Therefore, the drag polar is modelled with the operational and landing lift-drag settings which are $(1.05; 0.13)$ and $(0.2; 0.1)$, respectively.

These values are used to find the coefficients in Equation 6.4.

$$C_D = a + bC_L^2 \quad (6.4)$$

The towing theory used for the performed analysis has one foremost downside, namely the fact that it is not validated for extreme cases like towing faster than the wind or towing with a tailwind.

Top turning After the towing, there is a turn to align the kite such that it glides with the wind. This turn is executed by banking the kite to one side. Then, a bank angle causes the lift to deflect as shown in Figure 6.2. The horizontal force component initiates a centripetal acceleration, which results in a circular turn trajectory with a constant radial velocity. The radial velocity is calculated with Equation 6.5[15] and the turn radius with Equation 6.6[15]. In addition to this, the deflection of the lift causes the kite to have a downward acceleration, changing the vertical velocity of the kite and therefore the trajectory calculated with Equation 6.7[15].

$$\omega = \frac{V_{turn}}{R_{turn}} \quad (6.5)$$

$$R_{turn} = \frac{V_{turn}^2}{g \cdot \tan(\phi)} \quad (6.6)$$

$$\Delta V_z = g \cdot (\cos(\phi) - 1)\Delta t \quad (6.7)$$

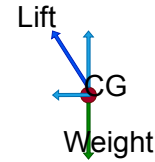


Figure 6.2: Deflection of the lift on a body due to a banking angle causing a circular turn

Here V_{turn} is the turn velocity, R_{turn} is the turn radius, g is the gravitational acceleration, ϕ is the bank angle, V_z is the velocity in the vertical direction and t is time.

Gliding Subsequently, the glide phase starts. In this phase, the kite glides down with the wind. The kite exploits its aerodynamic shape to glide longer tether lengths than its initial value. This allows for a tow phase with an increased final altitude. The glide has just as any lifting body a characteristic glide slope γ .

This can be calculated with Equation 6.8[16]. It can be seen that for a high lift over drag this slope can be very small, which is beneficial for the tether length increase.

$$\gamma = \arctan\left(\frac{D}{L}\right) \quad (6.8)$$

Bottom turning After this glide, the kite enters a second turn. The dynamics in this bottom turn are the same as for the top turn, but there is one difference; the kite enters already with a negative vertical velocity. Therefore, the kite will lose more altitude. This altitude loss will be taken into account by stopping the glide when it is at an altitude of 40 m .

After this bottom turn, the kite will be towed up again and the complete cycle will be repeated until the kite reaches the altitude where its lift-over-weight is larger than one, so the kite can sustain levelled flight.

The model The above phases modelled a feasible initial tether length. The model is, however, not finished, since some uncertainties about the applicability of the towing dynamics theory are unresolved. The uncertainties are mainly seen in the tether force. Namely, for a 0 m s^{-1} reeling speed, there is still a significant tether force. The large loads at low lift and reeling speed make

the launch unfeasible. Nevertheless, by combining knowledge from paragliding and the current launch of Kitepower (80 m initial tether length), it is known to be possible. Therefore, it is argued that the initial length of 85 m should be enough to have a feasible STL procedure.

6.2.3. Tower Take-Off

When the wind speed is sufficiently high (above 6 m s^{-1}), the STL is no longer needed and the kite can take off directly from the tower instead. For this, both the main tether and leading edge tether are slowly reeled out together while the kite climbs up to operational altitude.

6.3. Land Kite

The landing process of the kite consists of several phases. These are identified from the FFD in Chapter 3.

- FUN.7.1 Descend Kite
- FUN.7.2 Approach Tower
- FUN.7.3 Touch down on Tower

First, the kite needs to descend from its operational altitude. This is done in two steps, initially, the kite flies to the edge of the power zone to minimise the required reel-in force. Once the kite is closer to the ground station it flies to the Zenith position, this position requires more reel-in force but positions the kite in a more beneficial position for landing on the tower. At this point, the leading edge tether will be released from the KCU.

Before the kite can interface with the tower, the tower must be rotated such that it faces the direction of the kite. Since the tower can not rotate a full 360° , the kite might have to orient itself to compensate for the misalignment. The direction of the kite is mainly dictated by the wind orientation. With the tower in the right orientation the kite and KCU can be reeled in until it is right above the tower.

A kite on a short tether becomes difficult to control. A secondary tether directly attached to the leading edge of the kite is used to mitigate this problem and ensure reliable operation. This Leading Edge Tether (LET) is released from the KCU such that it can be used to pull the leading edge onto the RSS while the main tether pulls the KCU down to the foot of the tower. Lastly, the RSS latches onto the kite completing the landing procedure. In order to calculate the angle at which the kite will glide down with respect to the ground, Equation 6.9 is used.

$$\beta = \arctan\left(\frac{v_{glide} \sin(\gamma)}{v_{glide} \cos(\gamma) - v_w}\right) \quad (6.9) \quad \text{where } \gamma = \arctan \frac{C_D}{C_L}, \quad v_{glide} = \sqrt{\frac{mg \cos \gamma}{0.5 C_L \rho S}}$$

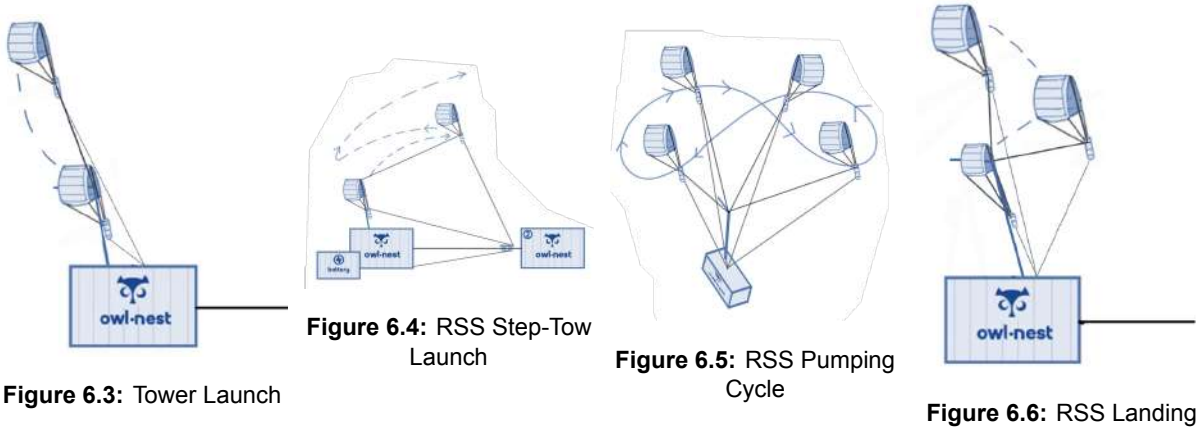
The angle of interest is not the aerodynamic glide angle γ , but rather the angle at which the kite descends with respect to the ground β . γ varies from 26.6° to 7.2° (depending on the glide ratio of the kite) but β depends on the wind speed and will be lowest at higher wind speeds. The maximum achievable beta at low wind speeds (4 m s^{-1}) is 37.9° . Thus, during low wind speed landing conditions, it is expected that the kite will fall down at an angle of less than 38° with respect to the ground.

At a wind speed of 6.5 m s^{-1} the kite will be able to descend at an angle of 80 degrees, and with lower wind speeds, the kite will have to be reeled in. The reeling speed and the powering of the kite at this stage will have to be controlled by the KCU. At low wind speeds and high reel-in speeds, the kite will have a high angle of attack and the apparent velocity will give the kite an induced (forward) tangential velocity, which will need to be corrected for by varying the reeling speed and the kite's form (controlled by the KCU). Aerodynamics and kite experts have assured us that this manoeuvre is indeed possible, but an analysis of the kite's behaviour during landing can be performed.

For a massless kite, the elevation angle β can be controlled by altering the L/D ratio of the kite and reel-in factor f . The elevation angle can be calculated with Equation 6.10 [13].

$$\beta = \arccos \left(\frac{\sqrt{1 + \left(\frac{L}{D}\right)^2(1 - f^2) + f\left(\frac{L}{D}\right)^2}}{1 + \left(\frac{L}{D}\right)^2} \right) \quad (6.10)$$

The operational sequence is illustrated in Figure 6.3, 6.4, 6.5, 6.6.



6.4. Store the kite

After landing, the kite must be stored to protect it from UV radiation and fluttering due to high winds. This task is performed by the RSS.

After touching down, the kite is clamped to the tower at the leading edge (next to the guiding tether), at which point the kite starts to deflate. Before full deflation, the KCU pulls on the bridles to adjust the position of the kite on the RSS horizontal cylinder, and once in the correct position, the kite is clamped in place from the trailing edge. The kite is then fully deflated, and the rolling motor engages. The cylinder with the kite starts rolling, and the kite folds on itself. After the needed rotations have been performed, the kite will have been folded around the cylinder in a final diameter of 1 m and a length of 5 m.



Figure 6.7: RSS storing system

6.5. Recommendations

To begin with, the STL lacks in theoretic knowledge since Airborne Wind Energy Theory [13] is for non-extreme reeling speeds. This theory should also assess the possibility of having a tailwind during launch. Additionally, the kite and reeling settings during launch should be optimised for minimal energy to make a STL possible with a tether load of 25 kN. Furthermore, the effect of the tension in the cable in the glide to limit the tether sag should still be investigated. Also, the turn dynamics are now fully based on banking the kite. To be more exact, a better turning model should be developed. The fifth recommendation is the implementation of the accelerations of the kite during launch. Especially the first acceleration is important to see if the kite does not fall on the ground when it is pulled off the tower. Lastly, a more complex model for determining an economically feasible operation should be made.

The tower is one of the main parts of the LLS where it has two main purposes: secure landing and storage of the kite and serves as a high point of launch in case sufficiently high-speed winds are present. The structure is located on top of the container. The tower is made of multiple components that work together to ensure a safe landing and storage of the kite.

In this chapter, the functions of the tower are analysed in Section 7.1, and in Section 7.2 the requirements for the tower are outlined. Section 7.3 gives a detailed overview of the design, which has the cost breakdown in Section 7.4, the verification in Section 7.5, the RAMS in Section 7.6, the sustainability in Section 7.7 and recommendations in Section 7.8.

7.1. Functional Analysis

In Table 7.1 the functions that the tower must perform are shown. They are taken from the functional breakdown structure in Chapter 3.

Table 7.1: Functions tower subsystem

Function ID	Function
FUN.2.3.3.1	Support and secure kite and KCU to RSS
FUN.2.3.5.1	Install LE tether
FUN.4.1	Rotate tower in take-off direction
FUN.4.2.2	Unroll kite
FUN.4.4	Detach kite from RSS
FUN.5.3.4.1	Reel-in LE tether
FUN.7.1.2.1	Reel-in LE tether
FUN.7.1.4.1	Reel-in LE tether
FUN.7.2.1	Rotate tower in kite direction
FUN.7.2.3.1	Reel-in LE tether until KCU is above tower
FUN.7.3.2	Lock kite to RSS
FUN.7.3.3	Reel-in LE tether completely until kite is on RSS
FUN.7.3.4.1	Lock kite to RSS
FUN.8.1.2	Roll kite around RSS
FUN.8.1.3.1	Apply a constant torque to the RSS to keep constant tension in the bridle lines
FUN.8.2	Rotate tower to default direction

7.2. Requirement Analysis

The landing tower subsystem needs to be designed to meet the requirements which flow from the functions defined in Section 7.1 and the risks in Appendix A. This will ensure that the functions are performed without overdesigning the system. These requirements are stated in Table 7.2. Moreover, system requirements LLS-GEN-OP-01, LLS-GEN-OP-15 and LLS-GEN-OP-16 and CON-LLS-GEN-03 on the damage and size of folded kite, as well as survivability and sustainability of the system are also driving.

Table 7.2: Requirements tower subsystem

ID	Requirement	Rationale	Flowdown
LLS-LT-STRUCT-01	The tower shall withstand the full weight of the kite and KCU	When the kite is secured on the tower, it will need to hold its weight and the KCU,	FUN.2.3.3.1, RSK-TCH-LT-01
LLS-LT-STRUCT-02	The guiding tether motor shall have a minimal reel-in force of 400N	During landing, this is the maximum force the kite is expected to pull on the guiding bridle: It will need to pull the 100kg kite from 8m/s to 0 in at least 2s.	FUN.5.3.4.1, FUN.7.1.2.1, FUN.7.1.4.1, FUN.7.2.3.1, FUN.7.3.3
LLS-LT-STRUCT-03	The rolling motor shall have enough torque to roll the mass of the kite and the KCU	The motor that wraps the kite around the cylinder in the RSS should be able to roll the full mass	FUN.8.1.2, RSK-TCH-LT-02
LLS-LT-STRUCT-04	The guiding tether motor shall be able to reel out at a speed of at least 15m/s	During Take-off and operation the LE guiding tether should reel out at the same speed as the winch, which is less than 15m/s.	FUN.4.4
LLS-LT-STRUCT-05	The clamp mechanism shall be able to hold the weight of the Kite and KCU under rotation	When rolling the kite around the storage system, the clamping mechanism should be able to hold the kite at all times	FUN.4.2.2, FUN.7.3.2, FUN.7.3.4, FUN.8.1.2, RSK-TCH-LT-05
LLS-LT-STRUCT-07	The kite shall be protected from sun radiation exposure for a period of at least 6 months when stored	The kite should be protected from harmful radiation, so no degradation occurs	STK-OEM-14
LLS-LT-STRUCT-08	The guiding tether motor shall be able to reel in at a speed of at least of 13 m/s	13 m/s is the speed at the highest gliding angle.	FUN.5.3.4.1, FUN.7.1.2.1, FUN.7.1.4.1, FUN.7.2.3.1, FUN.7.3.3
LLS-LT-STRUCT-11	The tower shall not weigh more than 15000 kg	The maximum payload of the container, and this is the budgeted maximum mass for the landing tower	LLS-GEN-STRUCT-01
LLS-LT-STRUCT-12	The failure mode the tower is designed towards shall be yield.	If the structure deforms under loading, then that is considered a failure and needs to be avoided	LLS-GEN-STRUCT-02
LLS-LT-STRUCT-13	The tower shall withstand a vertical impact from the Kite and KCU of 2.21kN without permanent deformation	It was calculated that the impulse is 2.21kN with a vertical speed of 13m/s and an impact time of 1s. 13 m/s is the speed at the highest gliding angle.	LLS-GEN-STRUCT-02
LLS-LT-STRUCT-14	The tower shall withstand a horizontal impact from the Kite and KCU of 1.02kN without permanent deformation	The Kite and KCU might impact the tower during landing.	LLS-GEN-STRUCT-02
LLS-LT-STRUCT-15	The length of the disassembled tower shall be less than 6m	The tower should fit in the container, which is around 6m long	STK-OEM-12

LLS-LT-STRUCT-17	The tower shall be designed with a safety factor of 2 for all load-bearing elements.	Common in civil engineering practices.	LLS-GEN-STRUC-02
LLS-LT-OP-01	The structure of the tower shall not interfere with the tether of the kite	The tower should not impede the landing and launching of the kite	FUNC-TOWER-06, RSK-TCH-LT-04
LLS-LT-OP-02	The tower shall rotate to a minimum angle of 45 degrees with the wind.	During landing, the tower should be positioned less than 45 degrees away from the direction of the incoming wind.	FUN.4.1, FUN.7.2.1, FUN.8.2
LLS-LT-OP-03	The tower shall be fully functional at temperatures of as low as 20 degrees Celsius below 0.	The tower should be able to function in harsh environments, and there need to be mechanisms that prevent failure of the tower during cold temperatures	RSK-TECH-LT-08

7.3. Design

To start off with the height of the mast, the minimum distance between the top of the container and the top of the mast has to fit both the bridle lines (currently 15 meters) and the half span of the kite (half of 20 meters). This height may differ on the scale of the system (higher/lower rated power generation) since it has a direct influence on the size of the kite, thus the span will change. It is also worth mentioning that the mast will not be perpendicular to the ground, but be slightly slanted outward to avoid tangling of the KCU and bridle lines.

The second section of the tower is the RSS: the storage subsystem consisting of a clamp to keep the kite secured once landed and a rotating motor to roll the kite itself. The number of revolutions needed by the RSS to fully roll the kite will differ depending on the dimensions of said component, this will be further described in the operations chapter. Additionally, a protection cover will be installed to protect the kite from UV radiation or any environmental hazards.

It is worth mentioning that in order to facilitate the landing sequence an additional tether will be installed on the top of the mast, together with its own winch. This will connect with the trailing edge of the kite and help guide it to a secure position on the tower.

In Section 7.3.1, research is done on the required angle of the tower, which will drive the structural analysis in Section 7.3.2, then in Section 7.3.3, the natural frequency is covered. In Section 7.3.4, the interface with the guiding tether is explained. In Section 7.3.5, Section 7.3.6 and Section 7.3.7, the clamping, rolling and covering mechanisms are covered. Finally, in Section 7.3.8 the interface with the container is discussed.

7.3.1. Tower Angle for Landing

The landing manoeuvre is important to consider for the design of the tower. From LLS-TOWER-STRUCT-12; the structure of the tower shall not interfere with the tether of the kite, it was decided that the kite's bridle lines and KCU need to land in front of the tower so that the lines will not tangle and the kite can take-off without having to disassemble and reassemble the bridle lines. Therefore, an analysis was done on the range of angles at which the kite is able to land at different velocities.

It is known that for the original kite, the L/D ¹ ratio can vary from 2 to 8. And using the theory

¹Lift over drag

described in Section 6.3 and Equation 6.10, it was calculated that β can be set to 90 degrees for almost any velocity (with an upper-bound wind velocity of 80 m s^{-1}).

Nevertheless, this is a preliminary value, as massless bodies are assumed, and the theory can not be applied to low windspeeds and manoeuvres close to the ground. After consulting with Dr. Ing. Schmehl, it was decided that an iterative analysis including the mass should be performed. Two provided Python scripts were used, an extensive version² and a simpler version³. Unfortunately, these scripts did not provide any useful results.

After contacting numerous experts⁴ it was found that this manoeuvre should be possible if the control software is adapted to perform this manoeuvre, but that a margin angle of the tower would still be of interest since the kite becomes nervous at short tether lengths. Since tower interference with the tether needs to be avoided at all times (LLS-LT-OP-01), the tower will be inclined 10° from the vertical.

7.3.2. Structural Analysis of Tower

The structure of the tower consists of three hollow thin-walled cylindrical sections as shown in Figure 7.1. The lowest section is inside the container and vertical, this allows for an easy rotation of the tower inside the container. The second section is 16 m long to facilitate the KCU and bridle lines hanging below the kite. The kite will land on the top horizontal section of the tower, after which it is clamped by two clamps, one on the leading edge and one on the trailing edge.

The loads stated in Table 7.2 are included in the FBD seen in Figure 7.1. The forces shown in the FBD are the weights of each component, the weight of the kite the force of impact of the kite and the pressure of the wind (see Table 7.3). The pressure of the wind is derived from sea-level wind hurricane conditions, of up to 30 m s^{-1} as stated in requirement LLS-GEN-STRUCT-03. Please know that this windspeed is considered the limiting case during landing since the system should be able to land the kite for wind speeds up to 25 m s^{-1} .

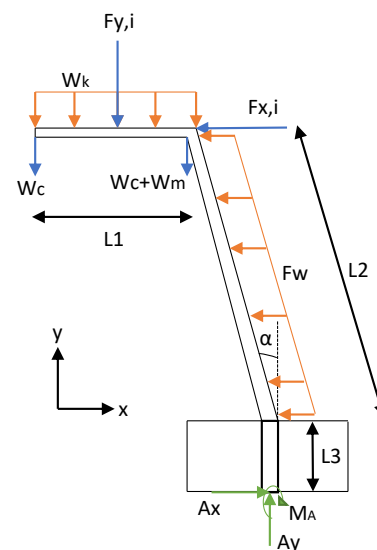


Figure 7.1: FBD of the tower. The external forces, as well as reaction forces, are drawn. The weights of the structure itself are not drawn, but are included in the calculation

²<https://github.com/awecourse/workshop>, Accessed on 09-06-2023

³https://github.com/TUD-AE/DSE2022-23-Q4-project20/tree/main/operation_model, Accessed on 09-06-2023

⁴Dr.-Ing. Roland Schmehl, Ir. Oriol Cayón Domingo, Ir. Jelle Poland Bryan van Ostheim and Ir. Eduard Ijsselmuiden

Table 7.3: External and reaction forces on the tower structure

Load	Value	Unit	Description
W _k	170·g	N	Weight of the Kite and KCU
W _c	10·g	N	Weight of clamping mechanism
W _m	10·g	N	Weight of rotating motor
F _{y,i}	2210	N	Vertical Impact force
F _{x,i}	1020	N	Horizontal Impact force
F _w	138	N/m ²	Wind pressure (drag)
A _y	6966	N	Vertical reaction force
A _x	1716	N	Horizontal reaction force
M _A	53017	Nm	Reaction Moment (z-direction)

The forces may be in multiple directions depending on the wind conditions and incoming kite, but the loading shown is considered to be the maximum loading case.

Now a choice of structure needs to be made. Conventionally, tall structures are often made of thin-walled cylinder cross-sections, take for example wind turbines and lamp posts. In order to not over-complicate the design, this design will stick to this method.

The highest stresses in all sections will be due to bending, which follows the following formula:

$$\sigma_{bending} = \frac{My}{I} \quad (7.1)$$

Where the area moment of inertia is:

$$I = \frac{1}{4}\pi(R^4 - r^4) \quad (7.2)$$

With R and r being the outer and inner radii respectively.

For the choice of material, the team looked into composites, steels and aluminium alloys. It was found, however, that similar cylindrical structures (such as lighting poles) are usually made of aluminium or steel, and composites are rarely used. The design team then performed a trade-off on both steel and aluminium with criteria on sustainability (CON-LLS-GEN-03), cost, mass and corrosion resistance.

Table 7.4: Structure properties for an Aluminium 6061-T6 and Grade 301 Temper ASTM A666 Steel (1/16 hard) structure

Material	Mass [kg]	Loading [Nm]	Corrosion	CO ₂ [kgCO ₂ e]	Material Cost [\$]
Aluminium	284.9	53017	Resistant	137	997.15
Steel	773	56736	Vulnerable	1469	1932.50

Stainless steel was used in these calculations, specifically Grade 301 Temper ASTM A666 Steel (1/16 hard), which has a yield strength of around 310 MPa⁵. It was found that both materials would require equal values of thickness and radii, and thus of volume. The cost that has been used for aluminium 6061 T6 is \$3.5⁶ or €3.24 and the cost for stainless steel that has been used is \$2.5⁷ or €2.31⁸. This cost does not take into account the manufacturing costs, but for the

⁵<https://www.azom.com/article.aspx?ArticleID=960> Accessed on 14/06/2023

⁶<https://www.navstarsteel.com/6061-t6-aluminium-plate.html>, accessed on 14-06-2023

⁷[https://blog.thepipingmart.com/metals/steel-vs-stainless-steel-prices-whats-the-difference/#:~:text=The%20cost%20of%20stainless%20steel,%242%2C500%20per%20ton%20or%20more!](https://blog.thepipingmart.com/metals/steel-vs-stainless-steel-prices-whats-the-difference/#:~:text=The%20cost%20of%20stainless%20steel,%242%2C500%20per%20ton%20or%20more!,), accessed on 14-06-2023

⁸<https://www.xe.com/currencyconverter/convert/?Amount=1&From=EUR&To=USD>, accessed on 14-06-2023

other criteria, aluminium still performs best and is thus the material of choice. With this material, and taking a safety factor of 2 with respect to the yield strength of aluminium, the design of the tower was chosen to be as indicated in Table 7.5.

The material of choice is aluminium 6061-T6 with a yield strength of 270 MPa⁹. Aluminium 6061 is a universal grade of aluminium that is commonly used in aerospace as well as structural applications. Finally, the sustainability of aluminium has been regarded as the best of its competitors, as its production emissions are low, it can be produced in Europe and it is recyclable. All of the estimated stresses are below 133 MPa in compression as well as tension. The total mass of the structure is estimated to be 284.9 kg.

Table 7.5 shows the characteristics of the tower per section. The tower is made of three different sections: section 1 is the 5.5-meter long horizontal cylinder which composes the RSS, the second section is the 10-degree slanted mast with helical strakes, as discussed in the following section, and section 3 is the vertical section interfacing with the container. Furthermore, section two is divided into three pieces of approximately 5.33 m, to meet LLS-LT-STRUCT-15; The length of the disassembled tower should be less than 6 m. These pieces slide into each other and are also bolted together by 6 M8 x 80 mm steel bolts each.

Table 7.5: Main geometrical and structural characteristics of tower

Section	Radius [cm]	Thickness [mm]	Length [m]	Mass [kg]	Crosssection
1	10	3	5.5	27.6	Circular
2	16	5	16	224.2	Circular
3	16.5	5	2.4	33.1	Circular

After contacting numerous companies, it was found that Senfalighting¹⁰ is able to produce aluminium 18.5 m high towers with a diameter of 32 cm and a thickness of 6 mm with equal diameter (no tapering) for \$1355 (Ex Works). Considering that the material cost of the tower is expected to be \$997.15, this seems like a reasonable price. Nevertheless, this company is based in China, and would thus not be sustainable to source products from that far. Since no information could be found on the prices of similar towers in Europe, the design team assumed a value of \$2710 (€481.3), which should account for the higher cost of the material and manufacturing in Europe and for the added complexity of the structure due to the many interfaces and the unusual angles.

⁹<https://www.makeitfrom.com/material-properties/6061-T6-Aluminum/> Accessed on 13/06/2027

¹⁰<https://www.senfalighting.com/> Accessed on 19-06-2023

7.3.3. Natural Frequency Analysis

Thin structures, like the tower, are prone to natural frequency vibration failure, so a thorough analysis of the vibration needs to be performed. There are two main modes of vibration that are relevant to thin pole design as illustrated in Figure 7.2.

Calculating the First and Second Mode Natural Frequency

For a cantilever beam with a point load on top, Equation 7.3 and Equation 7.4 can be used [17]. Where n is the mode number, E is Young's modulus, I is the area moment of inertia, ρ is the density and L is the length of the section. Keep in mind that these equations do not

$$f_1 = \frac{1.875^2}{2\pi L^2} \sqrt{\frac{EI}{\rho A}} \quad (7.3)$$

$$f_2 = \frac{4.694^2}{2\pi L^2} \sqrt{\frac{EI}{\rho A}} \quad (7.4)$$

With Equation 7.3, the natural frequencies of each section in the tower, as named in Figure 7.1, are displayed in Table 7.6.

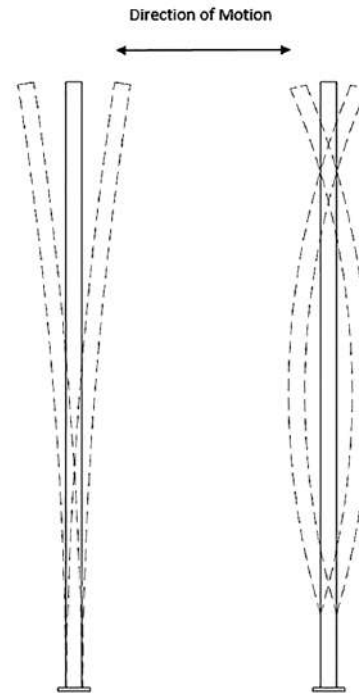


Figure 7.2: Relevant Vibration Modes for Pole Design. From left to right, first and second modes [18].

Table 7.6: Tower natural frequencies per section

	First mode natural frequency (Hz)	Second mode natural frequency (Hz)
section 1	2.03	12.72
section 2	0.38	2.40
section 3	11.65	72.99

Impact of the Natural Frequency

The critical wind gust frequencies for the first mode are 0.8 Hz to 1.2 Hz [19]. This means that section two could be affected by larger oscillations since it is below and close to this range.

The second mode is normally the most critical in the design of slender poles [19]. When the wind reaches speeds of at least 3 m s^{-1} vortex shedding causes the pole to be driven in the direction of the vortex. Once that vortex spins off into the wind stream, another vortex is formed on the opposite side of the pole, causing it to be driven to that side. This process repeats itself and the pole will start to vibrate back and forth, in the perpendicular direction to the wind.

The frequency f of this vortex shedding can be calculated with the Strouhal number St which depends on the Reynolds number Re and can be calculated with Equation 7.5 [20]. Where L is the characteristic length, in this case, the diameter. Furthermore, u is the free-stream velocity and ν is the kinematic viscosity of the air. The range of the Reynolds number will be calculated with Equation 7.6.

$$f = \frac{St \cdot u}{L} \quad (7.5) \quad Re = \frac{u \cdot L}{\nu} \quad (7.6)$$

The maximum wind velocity at which vortex shedding occurs is 11.1 m s^{-1} [19]. It is calculated

that the Reynolds number varies roughly from 0 to 200.000. For the calculated range of Reynolds numbers the average Strouhal number is 0.21 with a maximum deviation of 0.02 from empirical data [20]. Rewriting Equation 7.5, it is found that the maximum shedding frequency is equal to 7.28 Hz. If the second mode natural frequency of the pole is close to or coincides with this, large vibrations can occur. Therefore, it would be desirable to have the second mode natural frequency above this value. From Table 7.6, it can be seen that for section two this is not the case.

Prevention of Resonance Problems

It was found that the area moment of inertia of section two would have to increase by a factor of roughly 40 to meet the second mode natural frequency of 7.28 Hz. This would drastically increase the mass and therefore, the cost of the tower. Therefore, other options have been explored.

Another option that is regularly used in tall poles is a helical tube installed on the outside of the tower as in Figure 7.3. This technology is able to reduce vortex shedding with about 98 % [21].

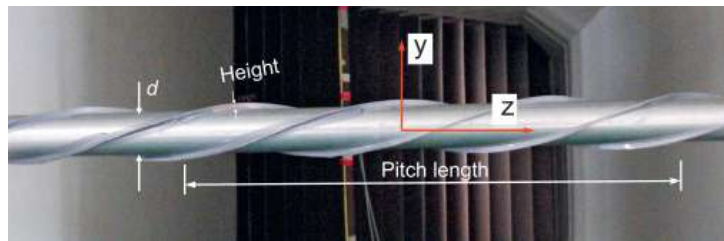


Figure 7.3: Rod with helical strakes in a wind tunnel [21]

Thus, for the design of the tower, helical strakes will be put on the side of section two. Studies have shown that the optimal number of strakes is three [21]. Furthermore, the optimal height of strakes h for Vortex Induced Vibrations (VIV) suppression is about $0.12d$ and a pitch p of about $10d$ has generally been accepted as optimal [21]. Where d is the diameter of the cylinder.

For section 2, the same proportions as those named in the previous section will be implemented. The weight of the rakes can be calculated with Equation 7.7.

$$m_{rakes} = 3 \cdot d \cdot \sqrt{100 + \pi^2} \cdot \frac{L_2}{p} \cdot t \cdot h \cdot \rho \quad (7.7)$$

Where ρ is the density of aluminium 6061-T6, 2700 kg m^{-3} . And the thickness (t) is set to 2 mm. This results in a total additional mass of 10.43 kg from the three helical rakes. And h is the height of section 2, which is 16 m long.

7.3.4. Guiding tether interface

In order to guide the kite towards landing the design it was chosen to perform this with the help of a guiding tether. After thorough brainstorming and contacting experts, it was found that a tether was the only reasonable option. And after carefully considering LE and TE tethers, it was found that TE tethers could make the kite unstable due to the added weight and would power the kite when engaged, which is dangerous, especially for short tether conditions, as concluded in Section 13.3.

This tether is always slack and is only tensioned during landing and touchdown. It needs to be pulled on when the KCU is at the height of the RSS, and the kite is (slowly) descending. At this stage, the kite will be moving with a speed of 6 m s^{-1} in the best-case scenario, and 13 m s^{-1} in the worst. This is the gliding velocity of the maximally and minimally powered kite respectively.

The guiding tether will guide the kite towards touch down on section 1 of the tower, where the horizontal rolling cylinder is. The guide would need to position the LE of the kite at the location of the clamping mechanism, close to the connection with section two.

The tower has been designed to withstand the loading in Figure 7.1, but in case the kite was to pull on the tower through the LE tether, it would be able to resist a pulling force of 2.8 kN horizontally and upwind of the tower. Which means that should be the maximum loading of the tether. The winch of this tether should thus reel out for forces higher than 2 kN (for safety).

The guiding tether will need a winch, which can be positioned on top of the tower near the location where the LE will need to be, or on the bottom of the container. The first has the advantage of reducing the length of the tether by at least 18 m, however, it would restrict the size of the winch and would increase the complexity of the electrical layout of the tower. Therefore, the tower will have a guiding tether running through its centre, and a set of pulleys will guide it to a winch attached to the base of the tower. This motor will need to reel out at the same speed as the kite moves without providing resistance. During operation, the reel-in speed will not be limiting, as the tether will just be dragged behind by the kite. However, during landing the tether will need to pull on the kite for touch down. At this point, the kite will be approaching the tower with a maximum speed of 13 m s^{-1} as this is the maximum gliding speed of the kite. So following requirements, LLS-LT-STRUCT-02, LLS-LT-STRUCT-04, LLS-LT-STRUCT-08, a winch will need to be commanded to Dromec, who can make a customised winch with 400N reel-in force at 6.5 m s^{-1} , a holding force of 2 kN, a big enough drum to hold 500 m of a 2.5 mm thick tether, and reel out at a speed 15 m s^{-1} without providing measurable resistance.

7.3.5. Clamping Mechanism

The kite needs to be secured to the tower after touchdown. The LE guiding tether pulls the kite into place, and where the entrance of the LE tether to the tower is, a solenoid locking actuator holds the ring on the kite in place. This way the load on the tether is relaxed, and the kite is held by the pin and ring of the LE. From LLS-LT-STRUCT-05; The clamp mechanism shall be able to hold the weight of the kite and KCU under rotation.

The Kendrion LHP025 with an edge dimension of 25 mm is used for this design.¹¹ The price for these components ranges from €50 to €2000, but for this report €1023.1 (\$1118) will be taken for the 1333550 Kendrion locking solenoid.¹² The design team believes that making customised high-lateral loading locking solenoids is possible and should not cost more than €1023. In the kite design, the LE clamping loading has been estimated to be as high as 5000 N, and that will be what is needed from the pin.

After the KCU centres the kite on the RSS horizontal bar (or cylinder), the TE also needs to be clamped. This is to ensure the kite does not move and the RSS is able to fold it around the cylinder. Therefore the choice has been made for a bar that folds on top of the fabric of the kite, with foam padding on both the clamp and the location the clamp is pushing on the tower, it is held in place. This is similar to a robotic claw. The foam also helps to prevent damage to the kite from the clamp.

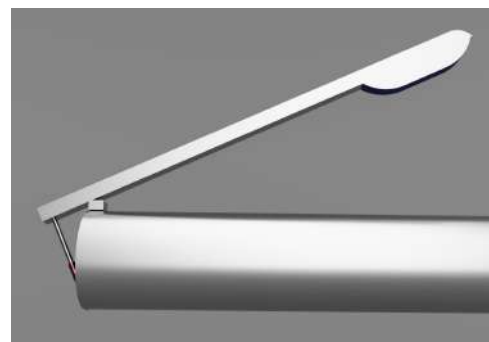


Figure 7.4: Clamp positioned on the trailing edge end of the tower

¹¹<https://www.kendrion.com/en/products/solenoids-actuators/linear-solenoids/high-performance-linear-solenoids>, accessed on 16-06-2023

¹²<https://solenoid-ninja.com/locking-solenoid-24v-dc-10mm-1333550/>, accessed on 20-06-2023

The required force of the trailing edge clamp on the kite to keep it from moving is set to at least 50 % of the total weight of the kite and KCU, which is 835 N. In reality, this will be less because at the moment of the critical case, where the RSS is halfway through its first rotation, a part of the weight will still be held by the main structure.

The TE clamp works with a lever mechanism, as shown in Figure 7.4. The long arm has been designed to act at a distance of 0.7 m and the short arm has been designed to be 0.1 m long. This means that the actuator needs to be able to push with a force of at least 5837 N. For this a linear actuator rated for 12 000 N static force is selected¹³

7.3.6. Rolling Mechanism

The RSS mechanism makes use of a rotating cylinder on top of which the kite hangs, to roll the kite folded kite around this cylinder and itself. This means that the cylinder needs to rotate itself, as well as the kite hanging from it. Once the rolling of the tower is started, the load on the motor would ideally only be due to the mass of the cylinder itself, as half of the kite will be going down, and the other hand will be going up. After half a rotation, the rolling motor will half to pull up half the kite as well as the remaining part of the other half of the kite that has not been rolled around the cylinder already. At this point, the motor will be rolling against this kite mass on one side of the cylinder as well as the KCU still hanging from the kite. The weight of the kite rolled around the cylinder after a first rotation will be approximately 3.14 kg, and thus this effect can be neglected. An illustration of the RSS is shown in Figure 7.5.



Figure 7.5: Illustration of the RSS rolling sequence

The sizing of the motor will be dominated by the torque needed to pull the kite and KCU around the rolling cylinder, as the acceleration from rest to rolling speed can be arbitrarily slow and the force needed to rotate the cylinder itself can thus be ignored. In conclusion, it can be determined that the torque the rolling motor requires is that of the KCU and Kite mass on one side: 170 kg at a distance of 10 cm from the centre of the cylinder. This translates into 166.77 N m.

With a safety factor of 1.2, the motor has been chosen to have 200 Nm torque. This is the Jefa 200 Nm transmission drive DU-TS8-12 (see Figure 7.6). The cost of this motor is approximately €1850¹⁴ the dimensions are 162 mm in length and 158 mm in maximum diameter and it has a mass of around 6 kg. This motor has a peak power consumption of 250 W, at 8 rpm. This means that it will take less than 50 s to roll the kite (around 6 revolutions).

The motor is positioned at the end of the rolling cylinder, between the first and second sections (see Figure 7.1). With a cylinder diameter of 20 cm and a kite thickness of 3.5 cm, the final stored kite will have a diameter of less than 1 m.¹⁵

¹³<https://nl.rs-online.com/web/p/electric-linear-actuators/8855325>, accessed on 19-06-2023

¹⁴<https://sailboat-spareparts.com/shop/jefa-autopilot-motor/>, accessed on 13-06-2023

¹⁵<https://www.handymath.com/cgi-bin/rollen.cgi?convodia=m&convthic=cm&convidia=m&convlen=m&odia1=&thic1=7&idia1=0.2&len1=10&submit=Calculate&numnum=1&moreless=1&decimal=5>, accessed 15-06-2023



Figure 7.6: Jefa 200 Nm transmission drive DU-TS8-12¹⁶



Figure 7.7: Internal gear slew bearing. In this image, the inner slew bearing ring rotates, while the outer is stationary and holds the structure. The small gear represents the motor rotating the inner ring.

7.3.7. Covering Mechanism

The requirement of the covering of the kite is LLS-LT-STRUCT-07; The cover of the kite shall protect it from sun radiation exposure for a period of at least six months.

Both a mechanical cover and an UV coating are considered to achieve this goal. A trade-off between these concepts is shown in Table 7.7.

Table 7.7: Trade-off table for the covering mechanism, 4 is the best score, 1 the worst

	Effectiveness	Reliability	Cost	Total
Mechanical covering	3	3	2	8
UV coating	2	4	4	10

For effectiveness, the mechanical covering has the potential to keep the kite completely dry, therefore it has a better score for the effectiveness criterion. Also, UV coating has a small negative impact on the kite's performance since it adds some weight to the kite. UV coating has the highest score for reliability because there are no mechanical parts which can break down. Finally, Mechanical covering is expected to be significantly more expensive because of moving parts. As can be concluded from Table 7.7, UV coating is the preferred design option.

Only the outer part of the kite needs to be covered by a coating since it is the only exposed part when the kite is rolled up. To keep the kite in balance, both sides of the kite will be covered by the coating, also allowing for alternating the rolling direction, doubling the lifetime of the coatings.

The diameter of the rolled-up kite is 1 m, therefore the area to be coated (half of the outer diameter) is 5 m x 1.57 m. including a safety factor of 1.2, and applied to both sides this is 18.84 m² in total. The type of coating and application will be described in Section 13.3 of the kite design chapter.

7.3.8. Interface with container

The tower will suffer heavy loading, which all needs to be transmitted to the container of the ground station and via the anchors to the ground. To allow rotation, the tower is mounted to a slew bearing. These bearings are used in applications such as construction equipment and wind turbines since they can resist high loading in all directions.

¹⁶<https://www.jefa.com/steering/products/drives/trans-150.htm>, accessed on 13-06-2023

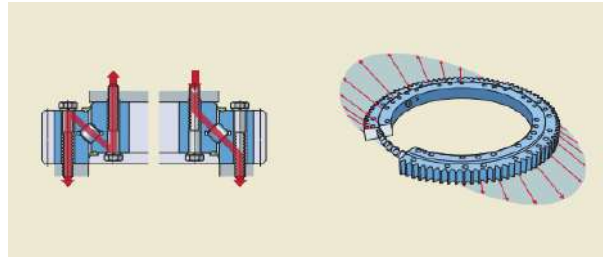


Figure 7.8: Transmission of moments in a supported slewing bearing ¹⁷

AB SKF is the world's largest producer of bearings and has many types of slew bearings available on the market.¹⁸ However, for this purpose, a custom bearing would be needed. The required loading would be that of Table 7.3, and would thus be loaded mostly in moment. To drive the rotation, the outside of the bearing is equipped with gear teeth.

The tower will be mounted off centre of the bearing since the tower should orbit a point. To ensure proper load introduction a frame will connect the base of the tower to the top of the bearing, this ensures loads are distributed over the entire circumference of the bearing.

Looking at the ground station layout and minimising the angle between the wind and the tower at all times as per LLS-LT-OP-02, it was found that the bearings should be designed for a maximum radius. Only 2.3 m is available in width, so the bearing will be designed with a diameter of 2 m to fit comfortably. Considering that the cable cart interface is about 90 cm, obtained from Section 12.3.4, it is found that with this radius, the tower would be able to rotate approximately 314° . This means that when the wind is exactly in the direction of the cables and cable cart, the tower will be positioned 23° off the wind's axis. This could become a problem for the control of the kite during landing, however, in case the wind is high enough, the kite will produce enough lift to remain controllable, and it will be able to fly crosswind towards touchdown, while in low wind conditions, the wind will not affect the movement of the kite measurably, since its apparent wind will be dictated mostly by its reeling and descend.

SKF's RKS.161.20.1904 slew bearing has an external gear, weights 305 kg, an external diameter of 2.0734 m an internal diameter of 1.796 m and a thickness of 68 mm ¹⁹ BSPD has been contacted and has agreed to sell one piece for \$4230 or 40 for \$3260 a piece (see footnote 19); although other manufacturers have prices as low as \$2769.3 a piece.²⁰

The tower will be rotated by a motor driving the gear teeth of the slew bearing, and it should do this in less than the time it takes the kite to descend from operational altitude to the container. This can be estimated to be at least 35 s seconds: from a height of 200 m on top of the container, and with the kite depowered completely, it will have a vertical speed of less than 5.6 m s^{-1} . So the kite will fall in at least 35 s. This is a lower bound, as the kite could also be descended with a lower rate of descent (for instance gliding the kite fully powered). This means that the bearing should rotate 180° in 35 s. For constant acceleration and deceleration, the motor will need to apply a force of 1 kN on the outer gear of the slew bearing. This comes from the fact that slew bearings have friction coefficients less than 0.2, which means that a 284.9 kg tower, a 152.5 kg outer slew bearing ring, and a 100 kg beam, would require slightly more than 850 N m to rotate [22]. With a small gear of for instance 23 cm for the drive gear, less than 200 N m will be required. The motor selected for the RSS meets these specifications.

¹⁷<https://www.skf.com/uk/products/slewing-bearings>, accessed on 15-06-2023

¹⁸<https://www.skf.com>, accessed on 16-06-2023

¹⁹<https://www.bspdbearing.com/product/RKS-161-20-1904/>, accessed on 16-06-2023

²⁰<https://www.tradebearings.com/rks-161-20-1904-crossed-cylindrical-roller-slewing-bearing-price-product-167610.html>, accessed on 17-06-2023

7.3.9. Summary of Design

In Table 7.8 all the components of the tower are listed, and the producer and part number are listed, accompanied by the estimated mass. All of the components are outsourced to companies in Europe, although for the cost estimated, quotes were enquired from companies outside of Europe. Moreover, as indicated in the table, not all fit producers have been found, and some parts will need to be custom-built. Lastly, the masses in parenthesis are estimates from similarly sized products.

Table 7.8: Component description of the tower, with fitting producer, part number and mass

Component	Producer	Part Number	Mass [kg]
Base Bearing	SKF	RKS.161.20.1904	305
Base motor	Jefa	DU – TS8 – 12	6
Main Structure Tower	TBD	Customised	298.4
RSS motor	Jefa	DU – TS8 – 12	6
RSS bearing	SKF	Customised	20
TE Linear actuator	Ewellix	CAHB-21	6.5
Solenoid locking	Kendrion	LHP025	(6.5)
LE Winch	Dromec	Customised	(500)
Hinge TE clamp	Steinbach & Vollman	Customised	(1)
Nuts and Bolts	TBD	M8x80	0.03686

7.4. Costs

Table 7.9 shows the costs of all the components in the tower. These costs are guiding and have been sourced from companies producing products similar to that stated in Section 7.3. The only cost that could not be estimated from similar products was the LE guiding tether winch. This product is highly application specific and after contacting Dromec²¹ and failing to get an estimate, an upper value of €10000 was decided. This estimate is reinforced by the fact that the main winch is considered to be around €100000, and the LE winch will be 30 times less powerful and will be a lot simpler.

Table 7.9: Overview of the prices of the tower components

Part	Cost per part [EUR]	Number of parts	Total cost [EUR]
Base Bearing	2983.23	1	2983.23
Base Motor	1850	1	1850
Main structure	2481.3	1	2481.3
RSS motor	1850	1	1850
RSS Bearing	500	1	500
TE Linear Actuator	592	1	592
Solenoid locking	1023.1	1	1023.1
LE winch	(10000)	1	(10000)
Hinge TE clamp	7.85	1	7.85
Nuts and Bolts	0.8	18	14.4
TOTAL	-	-	21301.88

²¹Sales and Geerart de Vree

7.5. Verification and Validation

The verification of this subsystem consisted of verifying the kite trajectory and tower stress and frequency analysis, as well as compliance of the design with the requirements.

7.5.1. Calculations

All the calculations performed, use simple physics with simple mathematical relations. These relations have been extracted from reliable sources as stated in the appropriate sections but it is important to consider the calculation's limits. Firstly, the angle of the tower was deduced from the trajectory of the kite during descent. For this purpose, an analytical as well as numerical analysis was performed of the angle of descent. The Python program was further assumed to be validated by the authors of the program themselves. To further validate the results numerous experts were contacted.

Secondly, the stress estimations of the tower largely relied on simple calculations. And these calculations are thus limited to idealised structures with perfectly cylindrical structures, negligible deformations, and moderate loading. Unexpected loads have not been accounted for, but a safety factor of 2 ensures that the design team is confident that the tower will stand for the designed loads.

Finally, the frequency analysis calculations were limited because the structure was considered ideal, only point loads were considered and the three different sections were considered to be independent, which is in reality not the case. The effect of the helical strakes was not quantified and the structure was assumed to be ideally straight and cylindrical. However, comparing the resulting product with existing structures gave the design team confidence in the results and the proposed solutions.

7.5.2. Requirements

The tower subsystem design must comply with the requirements set in Table 7.2. Each one of them was studied independently in Table 7.10, showing whether each requirement has been complied with and where it has been addressed in the tower design. In green are the requirements that have been complied with, in yellow are the ones for which a novel solution has been chosen and in orange is the requirement that has not been complied with yet.

Table 7.10: Compliance matrix tower subsystem

Requirement ID	Requirement	Compliance	Shown In
LLS-LT-STRUCT-01	The tower shall withstand the full weight of the kite and KCU	YES	Section 7.3.2
LLS-LT-STRUCT-02	The guiding tether motor shall have a minimal reel-in force of 400N	YES	Section 7.3.4
LLS-LT-STRUCT-03	The rolling motor shall have enough torque to roll the mass of the kite and the KCU	YES	Section 7.3.6
LLS-LT-STRUCT-04	The guiding tether motor shall be able to reel out at a speed of at least 15m/s	YES	Section 7.3.4
LLS-LT-STRUCT-05	The clamp mechanism shall be able to hold the weight of the Kite and KCU under rotation	YES	Section 7.3.5
LLS-LT-STRUCT-07	The cover of the kite shall protect it from sun radiation exposure for a period of at least 6 months when stored	YES	Section 7.3.7

LLS-LT-STRUCT-08	The guiding tether motor shall be able to reel in at a speed of at least 13 m/s	YES	Section 7.3.4
LLS-LT-STRUCT-11	The tower shall not weigh more than 15000 kg	YES	Section 7.3.2
LLS-LT-STRUCT-12	The failure mode the tower is designed towards shall be yield.	YES	Section 7.3.2
LLS-LT-STRUCT-13	The tower shall withstand a vertical impact from the Kite and KCU of 2.21kN without permanent deformation	YES	Section 7.3.2
LLS-LT-STRUCT-14	The tower shall withstand a horizontal impact from the Kite and KCU of 1.02kN without permanent deformation	YES	Section 7.3.2
LLS-LT-STRUCT-15	The length of the disassembled tower shall be less than 6m	YES	Section 7.3.2
LLS-LT-STRUCT-17	The tower shall be designed with a safety factor of 2 for all load-bearing elements.	YES	Section 7.3.2
LLS-LT-OP-01	The structure of the tower shall not interfere with the tether of the kite	YES	Section 7.3.1
LLS-LT-OP-02	The tower shall rotate to a minimum angle of 45 degrees with the wind.	YES	Section 7.3.8
LLS-LT-OP-03	The tower shall be fully functional at temperatures of as low as 20 degrees Celsius below 0.	NO	Section 7.3.9

Please note that the tower has been designed to withstand the landing loads at wind speeds of 30 m s^{-1} as seen in Figure 7.1. However, at higher windspeeds, the kite shall be stored and it will not impact the tower. The corresponding impact forces ($F_{y,i}$ and $F_{x,i}$ as shown in the FBD) can thus be ignored, and in this case, the tower can handle wind speeds (F_w shown in the figure) of at least 60 m s^{-1} .

7.6. RAMS Characteristics

The RAMS of the landing tower, a crucial component of design, is discussed hereby.

7.6.1. Reliability

Structurally, the tower is relatively reliable, since it has been designed for reasonable impact and operational loads. The lifecycle fatigue should not be a big problem since the number of launching, landing and storage cycles is low. The tower had the requirement to survive with wind speeds up to 30 m s^{-1} , but this did not turn out to be a driving requirement so somewhat higher wind speeds will also be survivable. Indeed, if no impact of the kite occurs, the tower is designed to withstand windspeeds up to 50 m s^{-1} . Operationally, there are some other failure points, discussed in Chapter 6.

7.6.2. Availability

The tower is designed to be structurally redundant; there is a safety factor. It can withstand the loads required for landing, launching and storing the kite. This ensures a higher availability of the system, in order to have at least a 100% uptime during the six months of operation. However, should the tower fail, the system will not be able to launch and land autonomously, but a traditional human-aided launch will still be possible.

7.6.3. Maintainability

The moving and thus more fragile systems of the tower are the kite clamps, the rolling motor and the rotating base. To maintain the latter, the tower may need to be disassembled and removed from its place. For the former two, the kite needs to be removed from the mast.

7.6.4. Safety

While maintenance is done on the tower, there should not be any extreme weather conditions such as a storm. This is because the risk of the system failing is higher than usual and necessary.

7.7. Sustainability

The landing tower contains about 274.4 kg of aluminium excluding the clamp and motor. With aluminium's emissions being around $0.5 \text{ kg}_{\text{CO}_2\text{e}}/\text{kg}_{\text{Al}}$ as per Section 19.2, this amounts to about 137.2 kg carbon equivalent emissions.

With a capacity factor of 0.5 on a rated power of 100 kW, and a grid carbon intensity of $523 \text{ g}_{\text{CO}_2\text{e}}/\text{kWh}$ as per Section 19.1, this amounts to an emissions payback period of approximately 5 h.

7.8. Recommendations

Firstly, the descend manoeuvre of the kite should be studied in depth. This manoeuvre should be tested, and the use of detailed simulations should be considered for the behaviour of the kite and the landing tower requirements.

Furthermore, to get a more accurate prediction of the resonance, Finite Element Method (FEM) can be used to analyse the modes. This can get a more accurate value for the natural frequency of the tower. Similarly, this could be used for the structural and life cycle fatigue analysis of the tower.

Also, in the future, the stability of the kite on the landing tower should be investigated. The addition of side rods may be beneficial to ensure that the kite does not slide to the left or right side.

In the present chapter, the guiding cable is explained. Starting with the functional analysis of the guiding cable in Section 8.1, then its requirements in Section 8.2, the design in Section 8.3, costs in Section 8.4, V&V in Section 8.5, RAMS in Section 8.6, sustainability in Section 8.7 and recommendations in Section 8.8.

The guiding cable functions as a guiding rail over which the cable cart with the swivel access point drives. The cable guide is tensioned between the main container and the offset container, which functions as the offset winching point.

8.1. Functional Analysis

The guiding cable is functionally the most simple part of the LLS. The functions listed in Table 8.1 are obtained from the functional breakdown diagram from Chapter 3. Some functions belonging to the cable cart subsystem are also listed since the guiding cable interfaces with the cable cart.

Table 8.1: Functions guiding cable subsystem

Function ID	Function
FUN.2.3.1	Tension guiding cable
FUN.5.1.1.7	Support cable cart throughout movement
FUN.5.4.2.6	Support cable cart throughout movement

8.2. Requirement Analysis

The subsystem requirements are listed in Table 8.2. These are derived from the functions in Section 8.1 and risks in Appendix A.

Table 8.2: Requirements guiding cable subsystem

Requirement ID	Requirement	Rationale	Flowdown
LLS-GUID-STRUCT-01	The guide cable shall experience stresses lower than 1.5 times its ultimate stress at the maximum operational rated combined tension of 150 kN	Exceeding the ultimate stress would result in catastrophic failure of the system.	FUN.2.3.1, RSK-TCH-GC-02, RSK-TCH-GC-03
LLS-GUID-OP-01	The guide cable shall allow the winch point cart to move unobstructed between the ground station and offset container	The cable must function as a guide on which the cart drives, any obstructions would prevent the functioning of the system	FUN.5.1.1.7, FUN.5.4.2.6

LLS-GUID-STRUCT-02	The guide cables shall experience a combined tension lower than the maximum rated tension of 100 kN (without safety factor) when the winch point is at the middle of it and the kite experiences the maximum rated gust speed of 40 m s^{-1}	In this loading case, which is the most extreme design case, the tension can not exceed the maximum allowed force	RSK-TCH-GC-02, RSK-TCH-GC-03
LLS-GUID-STRUCT-03	The guide cable system shall undergo controlled failure (breakage) at a tension between 149 kN and 151 kN	The cable must fail before the anchors subsystem suffers catastrophic failure	LLS-GEN-STRUC-02, RSK-TCH-GC-02

8.3. Design

The design of the cable revolves around sizing for feasible tension and sag. A model was used to simulate the cable and optimise for these parameters.

8.3.1. Cable Sizing

The guiding cables need to support the cable cart under different loading conditions. During normal operation, the cable cart needs to be kept upright, and the tension must be sufficiently high to prevent it from sagging too low so as not to obstruct the cable cart (LLS-GUID-OP-01).

Additionally, the cable sizing includes a “breaker” piece that, when exposed to forces that would result in catastrophic failure of the anchoring system (150 kN), will yield and ultimately break, thus containing the total damage incurred to the LLS system (LLS-GUID-STRUCT-01, LLS-GUID-STRUCT-02).

Hanging Cable Model

To size the cables accordingly, the problem must be analysed. A cable with a cross-sectional area A , density ρ and an undeformed length l_u will deform under its own weight, forming a catenary curve. Many exact, analytical methods for solving this problem have already been developed and online calculators¹ are available to find what tension is needed for a given cable to have a given sag.

The sizing of the guiding cable is more complex since, besides experiencing the loads from its own weight, it needs to bear a point load from the kite tether that includes aerodynamic loads from the kite in addition to the weight of the cart. It has been chosen to develop a numerical FEM solver in three dimensions. A cable is discretised by nodes connected by chain elements that can only be loaded in tension, with each of these elements functioning as a spring and damper as shown in Figure 8.1.

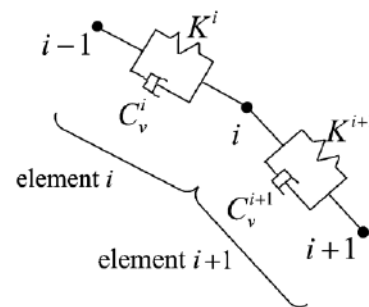


Figure 8.1: The i th element of the discretised cable is bounded by the $i-1$ st and i th nodes. [23]

¹<https://www.spaceagecontrol.com/calccabm.htm>, accessed on 07-06-2023

To solve this problem a direct integration method is needed instead of the more typical static analysis since the assumption of small deformation angles is invalid and the stiffness matrix is singular for loading acting perpendicular to the cable. The direct integration method mitigates these problems, as these assumptions are not made. The explained implementation is based on the approach done by B. Buckham et al. (2003) [23]

The forces acting on the nodes can then be calculated as shown in Equation 8.1.

$$(m^i + m^{i+1}) \cdot \ddot{\mathbf{u}}^i = (\mathbf{T}^{i+1} + \mathbf{P}^{i+1}) - (\mathbf{T}^i + \mathbf{P}^i) + \mathbf{F}_{ext}^i + \frac{m^i + m^{i+1}}{2} \mathbf{g} \quad (8.1)$$

Where \mathbf{T} is the tension in the tether due to the elastic deformation, \mathbf{P} is the force due to the damping. The loads acting on the cable are \mathbf{F}_{ext} , which is a point load acting in a node. The weight of the cable is modelled as a force on each node using a lumped mass approach, taking masses from neighbouring elements. The position of each node is \mathbf{u}^i , and the double time integral of the position is the acceleration and is denoted by $\ddot{\mathbf{u}}$. The superscript i indicates which element or node the quantity belongs to.

The tension in an element with cross-sectional area A , Young's modulus E and an undeformed length l_u can be obtained using Hooke's law, assuming elastic deformation. This is shown in Equation 8.2.

$$\mathbf{T}^i = \mathbf{n}^i \cdot AE \frac{l_u^i - l^i}{l_u^i} \quad (8.2) \quad l^i = |\mathbf{u}^i - \mathbf{u}^{i-1}| \quad (8.3)$$

The orientation of the element is given by its unit vector \mathbf{n} , this vector points from u_{i-1} to u_i .

The damping in an element is emulating the dissipation of energy due to the elongation of the cable. The damping constant is not of importance for the final design, but sufficient damping is needed to have a stable numerical method, the value of c is thus obtained with trial and error. The damping coefficient is denoted as c . The damping force is calculated in Equation 8.4.

$$\mathbf{P}^i = \mathbf{n}^i \cdot c |\dot{\mathbf{u}}^i - \dot{\mathbf{u}}^i| \quad (8.4)$$

The equation Equation 8.1 can be solved for the acceleration of each node, which then can be related to the displacement of the nodes by integrating with a time-stepping method, in this case, the central difference. At each time iteration, this acceleration needs to be recomputed with the updated values at each node. This way, the tension at the attachment points and the shape of the cable can be obtained for a given cable geometry and loading.

Guiding Cable

The guiding cables are sized with the help of the previously described model. The guiding cables have a core made out of Dyneema® with a nylon mantle to protect it from UV radiation and wear of the cable cart. Dyneema® has an ultimate yield stress of $\sigma_y = 3GPa$ [24], and a density of $\rho = 713.89 \frac{kg}{m^3}$ [25]. The needed distance between the winch and the kite is 85 m. The actual straight distance on which the guiding cable is tensioned needs to be a bit longer, since not the entire length of the cable is usable. The distance designed for is thus 88 m.

To prevent the cables from sagging too low touching the ground, obstructing the cable cart's path, the tension is sized to allow for a maximum sag. Assuming the guiding cable is attached near the top of the containers, at a height of approximately 2 m. From this, the maximum allowable sag was arbitrarily chosen to be 0.80 m. This ensures sufficient clearance from the ground. Similarly, a minimum resonant frequency of 3 Hz was arbitrarily chosen to ensure that cable resonance will not happen in high wind conditions. The fundamental resonant frequency of the cable is calculated as per Equation 8.5.

$$f = \frac{\sqrt{T \cdot \mu}}{2L} \quad (8.5)$$

By performing multiple iterations using the model, varying the cross-sectional area A and the undeformed length l_u , final values of all parameters are obtained such that the sag is less than 0.80 m and the lowest resonant frequency of the cable in any state is above 3 Hz. The stress in the cable is kept well under the ultimate stress, this is done based on the experience of Kitepower with their Dyneema® tether, which was prone to snapping if loaded close to its ultimate stress. The final parameters are listed in Table 8.3.

For the worst-case scenario of the kite being parked and experiencing a gust of 30 m s^{-1} while the cart is being moved through the middle of the guide cable, a disturbance C_d of 0.125 and a C_l of 0.126 with a projected surface area of the kite equal to 78 m^2 and standard ISO sea-level conditions were assumed, yielding a horizontal force equal to the pulling of the kite, about 7644 N split into two cables (the force is placed horizontally because this is force-wise the worst case scenario). The weight of the cart was also added in the vertical direction. Note that these calculations, for the sake of simplicity, neglect any moment imparted by the tether on the cable cart that could produce the load to be asymmetrically distributed between the two cables.

Table 8.3: Guiding cable parameters

Parameter	Symbol	Value
Cross-sectional area	A	$1.539 \times 10^{-4} \text{ m}^2$
Diameter	d	0.0014 m
Density	ρ	713.89 kg m^{-3}
Tenacity	σ_{max}	3 GPa
Untensioned length	l_u	87.913 m
Tensioned length	l	88.000 m
Max. tension	T_{max}	49.8 kN
Max. stress	σ_{max}	323 MPa
Ultimate stress	σ_{ult}	3 GPa
Sag with cart	s_{cart}	0.52 m
Sag without cart	s_{nocart}	0.03 m
Min. tension	T_{min}	38.4 kN
Min. resonance frequency	f_r	3.36 Hz
Controlled failure tension	T_{fail}	150 kN

Two of these cables are used in parallel, adding up to a total force on the attachment points of approximately 100 kN. As it can be seen, the maximum design force for the cables is optimised to be around 50 kN, which allows the use of the same dimensions as Kitepower uses, since it is the same as the maximum loading which the tether experiences.

8.3.2. Tension Adjustment

The correct tension in the cable needs to be maintained automatically, even if the length changes due to temperature variations or creep over time. This function will be achieved with a screw jack mechanism that can change the cable length based on tension readings in the cable obtained by a load cell. This load cell will also be part of the guiding cable health monitoring system, which sends a warning to the operator in case correct tension can not be maintained. This system will be installed at the side of the main container since it is simple to provide it with electrical power.

Assuming the system can operate in temperatures ranging from $-20 \text{ }^\circ\text{C}$ to $60 \text{ }^\circ\text{C}$, which is more than sufficient for most places on earth, the cable will experience an elongation as given in

Equation 8.6. Dyneema® has a thermal expansion coefficient of $\alpha_t = 12 \cdot 10^{-6} K^{-1}$ ². The guiding cable length l is 88 m.

$$\Delta l_{temp} = \alpha_t \cdot \Delta T \cdot l = 8.46 \text{ cm} \quad (8.6)$$

The creep of Dyneema® DM20 is stated to be “less than 0.02 %” per year.³ Assuming this value, the change in length due to creep over six months (STK-OEM-01) is calculated in Equation 8.7.

$$\Delta l_{creep} = 100 \text{ m} \cdot (1.0002^{0.5} - 1) = 0.00881 \text{ m} \quad (8.7)$$

A screw jack that has a travel length of at least a distance of $\Delta l_{temp} + \Delta l_{creep} \approx 0.10 \text{ m}$ distance and a rated force exceeding the tension in the cable of 100 kN (from LLS-GUID-STRUCT-04) is needed. Such a jack is shown in Figure 8.2. The specific model selected for reference is the 200 kN E Series Machine Screw Jack from PowerJacks⁴, rated for 20 t of tension.



Figure 8.2: Jack Screw Mechanism⁵

Weak link

To ensure that the anchors will not be torn off the ground during catastrophic failure and to design for the failure location, a weak link is added between the offset container and the cables themselves (LLS-GUID-STRUCT-03). This piece simply consists of two ASTM A36 Steel profiles with a cross-sectional area of $0.0001875 \cdot 10^4 \text{ m}^2$ each, which break at a stress of 400 MPa, resulting in “controlled” failure of the cable system when the total tension is the maximum rated for the anchoring system, 150 kN. By placing the weak link at the side of the main container, the energy in case of failure is directed away from the area with the most critical hardware.

8.4. Costs

The guiding cable was chosen to be the ultra-low creep Dyneema DM20⁶. It is quoted that 200 m of this line will cost about €4000, including a protective coating. Additionally, the jack mechanism that was discussed in Section 8.3.2 will cost around €250. Two are needed so that will total €500. For initial tensioning, turnbuckles are used and they are about €40 each⁷. Two are needed and it will total €80. As well, a ratchet strap that will be added in getting the cable onto the turnbuckle will also cost around €40. Lastly, a harp will cost €47⁸, €94 for two. In total, this is combined around €4700.

8.5. Verification and Validation

In order to verify the produced design, it is important to verify the model itself. This was done by comparison with analytic solutions. Furthermore, a compliance matrix was made to check that the design fulfils all main relevant requirements.

²<https://www.riggingdoctor.com/life-aboard/2020/4/10/dyneema-and-its-coefficient-of-thermal-expansion#:~:text=Dyneema%20has%20a%20Coefficient%20of,0.000012%20m%2C%20or%2012%20CE%BCm.,> accessed on 19-06-2023

⁴<https://www.powerjacks.com/perch/resources/DS/powerjacks-ds-screwjack-e-series-msj-200kn-202-01.pdf>, accessed on 12-06-2023.

⁵https://www.moremarine.nl/pdf/dyneema_dm20_specs.pdf, accessed on 21-6-2023.

⁵<https://www.powerjacks.com/perch/resources/DS/powerjacks-ds-screwjack-e-series-msj-200kn-202-01.pdf>

⁶<https://dynamica-ropes.com/products/dm20/>, accessed on 20-6-2023

⁷<https://www.indiamart.com/proddetail/10-ton-forged-turnbuckle-22733824391.html>, accessed on 21-6-2023.

⁸<https://www.hijsjob.nl/harp-sluiting-moerbout-extra-breed>, accessed on 21-6-2023

Table 8.4: Estimate of the guiding cable subsystem cost.

Part	Cost [EUR]
ultra-low creep Dyneema®	4000
jack screw mechanism	500
turnbuckle	40
harp	94
TOTAL	4634

8.5.1. FEM Model Validation

For verification, the equations and physical implementation used in the developed FEM were firstly checked by inspection, and then the results from a simple base case were compared to an analytical solution for the catenary equation.

The case used to compare with the analytical catenary solution consisted of a 85.026 27 m long steel cable connecting two fixed points 85 m apart, with a cross-sectional area of 0.000 225 m², a density of 8000 kg m⁻³ and a Young's modulus of 210 GPa, without any added forces, only its own weight. This yielded a sag and detensioned cable length within 0.01 % of the results obtained by the FEM for the given tension. For the analytical solution, the catenary equation was solved at an endpoint tension of 12 723.4 N, a straight-line length of 85 m, a linear density of 1.8 kg and a gravitational acceleration of 9.81 m s⁻². This data corresponds to the values from the sized cable used for the cable guides.

Parameter	FEM Value	Analytical Solution Value	Error
Tensioned Cable Length	85.0492 m	85.0493 m	0.000 12 %
Cable Sag	1.253 72 m	1.253 76 m	0.0032 %

8.5.2. Compliance Matrix

The compliance matrix for the guiding cable can be seen in Table 8.5.

Table 8.5: Compliance matrix guiding cable subsystem

Requirement ID	Requirement	Compliance	Shown In
LLS-GUID-STRUCT-01	The guide cable shall experience stresses lower than 1.5 times its ultimate stress at the maximum operational rated combined tension of 150 kN	YES	Table 8.3
LLS-GUID-OP-01	The guide cable shall allow the winch point cart to move unobstructed between the ground station and offset container	YES	Table 8.3
LLS-GUID-STRUCT-02	The guide cables shall experience a combined tension lower than the maximum rated tension of 100 kN (without safety factor) when the winch point is at the middle of it and the kite experiences the maximum rated gust speed of 40 m s ⁻¹	YES	Table 8.3
LLS-GUID-STRUCT-03	The guide cable system shall undergo controlled failure (breakage) at a tension between 149 kN and 151 kN	YES	Figure 8.3.2

8.6. RAMS Characteristics

The RAMS of the cable is fundamental to the functioning of the system, as cable failure under tension could result in total LLS system failure and significant damage. It is hereby discussed.

8.6.1. Reliability

The reliability of the system is high since the functions the guiding cable needs to fulfil are simple and the cables and tensioner are oversized. It is unlikely that this subsystem fails during operations.

8.6.2. Availability

The guiding cable is always available except during maintenance and replacement. During the operational life, these events result in an insignificant amount of downtime.

8.6.3. Maintainability

The nylon mantle of the guiding cable needs to be inspected every six months for excessive wear or tears. If the mantle is in good condition, it can be assumed that the core is also undamaged. The guiding cable needs to be replaced when the nylon mantle is worn out.

8.6.4. Safety

Tensioned cables are a safety risk to anyone near them. When a cable breaks a phenomenon called "snapback" occurs; the broken cable will rapidly accelerate to the point where the load is applied and can damage equipment or hurt personnel in the process. To avoid this happening regular inspections are scheduled and maintenance is performed when needed. Additionally, harm to people is avoided by having a danger zone that must be kept clear of people during operation in case a cable rupture does occur. All personnel entering this safety zone must be properly educated on the dangers of cable 'snapback'. Damage is minimised by designing a rupture point such that a snapback happens away from the battery since any damage to the battery can cause a thermal runaway [26].

8.7. Sustainability

The main components of the guide cable subsystem are the cables themselves, the cable anchoring points, the screw jack, and the breaker piece. From the cross-sectional area, density and untensioned length which can be seen in Table 8.3, it can be calculated that the cables will use a total of about 32 kg of Dyneema®, accounting to around 48 kg_{CO₂e} with emissions of 1.5 kg_{CO₂e}/kg_{PE} according to Section 19.2.

The screw jack, as per the manufacturer, weights 49.58 kg plus 0.52 kg for every 25 mm of stroke above 150 mm. This yields a total weight of 58.94 kg of steel for a 600 mm stroke. The breaker piece is just two 50 mm long, square profiles with cross-sectional area 0.000 187 5 m², amounting to 0.1 kg of steel, and the clamping anchors are arbitrarily assumed to use a maximum of about 10 kg of steel each to have a good safety margin. This results in about 69 kg of steel, or about 131 kg_{CO₂e} at 1.9 kg_{CO₂e}/kg_{Steel}, as per Section 19.2, yielding total emissions of 179 kg_{CO₂e}. Taking a capacity factor of 0.5 with a rated power of 100 kW, and a grid carbon intensity of 523 g_{CO₂e}/kWh according to Section 19.1, this yields an emissions payback time of the guide cable subsystem of approximately 7 hours of operation.

8.8. Recommendations

Improvements and optimisations are still possible beyond the scope of this report, given more time and resources. The exact loading acting on the guiding cable is unknown, forcing the team to perform sizing with safe, significant, estimates. The subsystem can be sized to smaller loads by identifying the actual aerodynamic loads. When implementing the LLS system into an existing AWE system, it is recommended to first measure the actual loads in the tether.

The cable cart, carrying the swivel access point, allows the launching of the kite with low wind speeds, acting as a movable offset winch point. Its functions and requirements will be discussed in Section 9.1 and Section 9.2 respectively. The cable cart must resist the loads introduced by the tether on the pulley system and guide it properly without inducing large amounts of wear. Its design will be thoroughly described in Section 9.3. Additionally, costs will be treated in Section 9.4, the V&V in Section 9.5, the RAMS in Section 9.6, the sustainability in Section 9.7 and finally recommendations in Section 9.8.

9.1. Functional analysis

The cable cart is a crucial component in the operation of the launching sequence. Below, the functions that the cable cart must be able to perform are shown, and they flow down from the ones in the functional breakdown structure in Chapter 3.

Table 9.1: Functions of the cable cart subsystem

ID	Function
FUN.5.1.1.1	Undock from main container
FUN.5.1.1.2	Move to offset position
FUN.5.1.1.3	Dock to offset container
FUN.5.3.4.1	Redirect the tether from the ground station to the kite
FUN.5.4.2.1	Undock from offset container
FUN.5.4.2.2	Move to main position
FUN.5.4.2.3	Dock to main container

9.2. Requirements Analysis

Following the functions outlined in Section 9.1, a series of requirements the cart subsystem should comply with, must be set. These will ensure that the subsystem operates nominally and safely. Every subsystem requirement is a flow down of either a function (Table 9.1), a system/stakeholder requirement (Table 4.1 and 4.2) or a risk (Table A.3).

Table 9.2: Requirements cable cart

ID	Requirement	Rationale	Flowdown
LLS-CART-OP-01	The cart shall be able to move on the guiding cables between both containers	The cart should move the winch point to the offset container and back to the main container	FUN.5.1.1.2, FUN.5.4.2.2
LLS-CART-OP-02	The cart shall redirect the tether in any direction in which the kite can be positioned.	To use the cart as an offset winch point, the tether has to be able to be redirected in any direction the kite can move	FUN.5.3.4.1, RSK-TCH-CC-04, RSK-TCH-CC-03

LLS-CART-OP-03	The cart shall be able to remain stationary when connected to the offset container.	To limit oscillations of the cables, the cart must be able to be safely connected to the offset container.	FUN.5.1.1.3
LLS-CART-OP-04	The cart shall be able to remain stationary when connected to the main container.	To limit oscillations of the cables, the cart must be able to be safely connected to the main container.	FUN.5.4.2.3
LLS-CART-OP-05	The cart shall not come in contact with the ground at any point of nominal operation.	The cart must always keep some clearance from the ground to prevent any damage.	FUN.5.1.1.2, FUN.5.4.2.2
LLS-CART-STRUCT-01	The cart shall not deform plastically due to the loading experienced during operation.	The cart can not function if it is deformed	LLS-GEN-STRUCT-02
LLS-CART-STRUCT-02	The cart actuators shall be fully redundant	The cart must be able to drive, even if one motor fails	RSK-TCH-CC-03

9.3. Design of the Cable Cart

As a first step in the design of the cable cart, it is important to recognise all the major parts of the subsystem. Six main components have been identified and listed below. Each one of them will then be investigated separately in Section 9.3.1, 9.3.2, 9.3.3 and 9.3.4. The following parts of the cable cart can be identified:

- **Swivel access point** A combination of pulleys, adopted to align the tether to the kite's orientation (made out of Steel). Figure 9.1 shows an example of the swivel access point of Kitepower.
- **Cable wheels** Small wheels riding over the guiding cable. These wheels also provide the driving and braking force required (made out of Steel).
- **Clamping System** A spring system is used to provide sufficient normal forces to make sure the wheels don't slip.
- **Electric motors** Two electric motors power the wheels through a transmission belt. Disk brakes are used to slow down the cart.
- **Battery & Motor Controller** A battery is used to provide enough power to the two electric motors. One motor controller per engine is needed to convert the electricity from DC to AC.
- **Cart Body** The load-bearing component of the cart includes side panels that the containers will clamp on too (made out of Aluminium).

This subsystem will be discussed in more detail compared to the other subsystems described in this report, as it needs to be designed from the ground up (apart from the battery and the motors).

9.3.1. Swivel Access Point

The swivel access point is a combination of pulleys that guide the tether exiting from the tether drum, located inside the ground station, and aligns it with the flying kite. It is important to keep the curve radius of the main tether large to minimise the wear these pulleys cause on the tether. To achieve this the swivel access point comprises two large fixed pulleys that guide the tether to a third pulley that is allowed to rotate 360° around a vertical axis, to align with the direction of the kite. Four small wheels ensure that the tether does not fall off the pulleys and direct it in the direction of the kite (LLS-CART-OP-01).

An example of a swivel access point is shown in Figure 9.1. The radius of the large pulleys is dictated by the allowed bending radius of the main tether, preferably this is kept large to reduce wear. A diameter of 20 cm is chosen to cause minimal fatigue in the 14 mm Dyneema® main tether. The pulleys will be made out of steel and the contact surface of the pulley with the tether will be polished to provide a smooth interface, minimising wear.



Figure 9.1: Swivel access point¹

Stresses and Sizing

In order to size the structural components of the swivel access point, it is necessary to perform a stress analysis. Starting from the analysis of the lower pulleys, the free body diagram showing the forces acting on it is shown in Figure 9.2. To simplify the calculations, the weight of the structure of the pulley has been assumed to be acting in the middle, where the pulley is. The torque created by the offset tension force has been neglected, as it is not a critical load. The equation governing these stresses is:

$$\sigma_z = \frac{(M_x I_{yy} - M_y I_{xy})y + (M_y I_{xx} - M_x I_{xy})x}{I_{xx} I_{yy} - I_{xy}^2} \quad (9.1)$$

Where M_x and M_y are the moments around the base of the pivot analysed. These are calculated using a simple moment equation, given in Equation 9.2, where d is the moment arm on which the force F acts. Only the second moments of inertia I_{xx} and I_{yy} (Equation 9.3.1) are non-zero, due to the symmetrical solid circular cross-section of the structure.

$$M = d \cdot F \quad (9.2) \quad I_{xx} = I_{yy} = \frac{\pi r^4}{4}$$

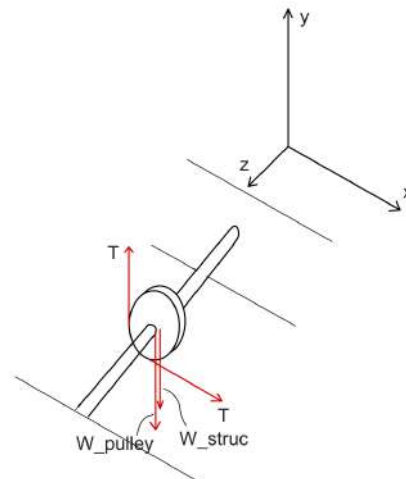


Figure 9.2: Simplified free body diagram pulley

Where r is the radius of the structure. It is minimum when the maximum stress matches the tensile yield stress of aluminium.

The torque created by the offset tension force has been neglected, as it is not a critical load.

The structure will be attached to the side metal sheet of the body of the cart through titanium bolts. Performing the bearing stress analysis allows sizing the thickness of the cart body metal sheet. This will also be the thickness of the end plate of the aluminium beam where the bolts are attached. The bearing stress p of the sheet is given by:

$$p = \frac{D \cdot t}{P_{bearing} \cdot n_{bolts}} \quad (9.3)$$

Where $P_{bearing}$ is the bearing force applied to the metal sheet by every bolt. The minimum thickness is found when the bearing stress is equal to the bearing yield stress of aluminium (the body is made out of aluminium).

¹<https://www.innovationquarter.nl/en/kitepower-secures-e3-mln-for-innovative-airborne-wind-energy-system/#next>, accessed on 30-05-2023

After sizing the metal sheet, each bolt must be able to sustain the load applied in shear:

$$\tau = \frac{4P_{bolt}}{\pi D^2 \cdot n_{bolts}} \quad (9.4)$$

The allowable shear stress of the bolts must be higher than the shear stress applied.

Applying the same procedure, also the structure of the upper pulley can be analysed according to the FBD shown in Figure 9.3. The structure beam will be hollow, so to allow the tether to be guided through it. For this reason, the second moment of area will be:

$$I_{xx} = I_{yy} = \frac{\pi r_o^4}{4} - \frac{\pi r_i^4}{4}$$

Where r_o is the outer radius and r_i is the inner radius.

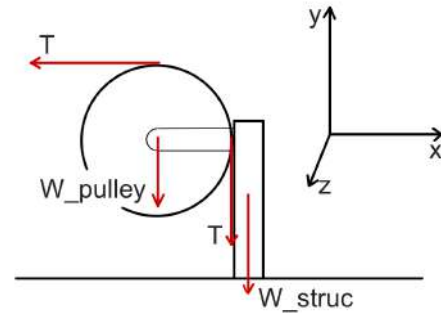


Figure 9.3: FBD upper tether pulley

The results of this analysis are summarised in Table 9.3. The radii indicated here have been rounded up to the closest millimetre.

Table 9.3: Pulley supports dimensions

Parameter	Value	Unit
Outer radius Upper Pulley support beam	44.0	mm
Inner radius Upper Pulley support beam	16.0 ¹	mm
Radius Lower Pulley support beam	39.0	mm
Radius upper wheel support beam	14.0	mm
Radius lower wheel support beam	11.0	mm

9.3.2. Cable Wheels

The cable wheels ride over the guiding cable, allowing the entire cable cart to move. These wheels have a relatively small diameter since the guiding cable is not bending around them. A total of four sets of wheels will be adopted, each set comprising two wheels, one above and one below the steel cable connecting the main and offset container. This is chosen since the cart needs the most support from the top wheels and less support from the bottom wheels due to the normal load case. Four wheels will be placed on one cable and four on the other cable. The four wheels on the bottom are needed in order to ensure stability in case of an abnormal loading case induced by unexpected tether forces, and only the four wheels located above the cable are driven by an electric motor. The choice of having four sets of wheels is because it is a minimum number to ensure the stability of the cart during nominal operations, while still maintaining the wheels equally distributed over the two cables.

The wheels will be solid and made out of steel to limit their wear caused by the rolling motion they are subjected to. It has been chosen to have wheels with a radius of 0.075 m. Based on the size of the wheel, then the minimum torque needed on these can be calculated, and eventually, the motor will be sized accordingly.

¹2 mm more than the diameter of the tether to reduce its friction wear

Rolling Mechanism

The wheels will be connected directly to the body of the cart through an aluminium shaft that will go through a hole drilled into the body's metal sheet and clamped to it through bolts. Ball bearings will be used to reduce the rolling friction between the wheels and the shaft. Two load cases will be analysed: one with an upwards tension in the tether limiting the minimum size of the lower shaft and one without it for the upper wheels. The shafts can be sized as described in Section 9.3.1. The FBD used to analyse the upper wheel structure is shown in Figure 9.4.

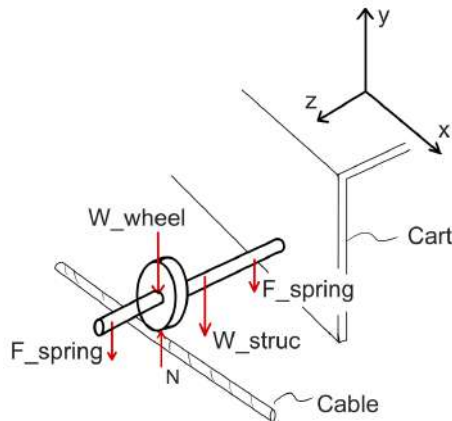


Figure 9.4: FBD upper wheel structure

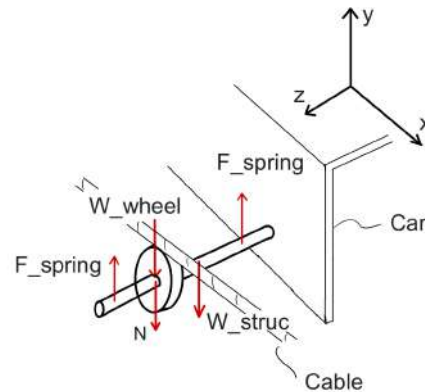


Figure 9.5: FBD lower wheel structure

The case analysed is considering there is no upwards tension force, so the wheels have to carry a fourth of the total mass of the cart (Normal force, N). From the result of the analysis, the shaft for the upper wheels will have a radius of 14.0 mm.

The bottom wheels will experience a normal force N given by the difference between a fourth of the vertical component of the tension force (including the safety factor) in the tether when the kite is parked ($T = 7644N$, see Equation 8.3.1) and a fourth of the weight of the cart. The FBD for the lower wheel structure is shown in Figure 9.5.

The shaft for the lower wheels will have a radius of 11.0 mm.

Clamping System

The cart must be designed in such a way that slipping is avoided at all times during operations. The worst scenario occurs when the cart is located in proximity to the offset container, where the tension in the tether needed is maximum. The following assumptions to design the clamping system have been made:

- $\xi = 0$: Given the large horizontal distance of the guiding cable of 85 m, the angle can be neglected
- $F_{roll} = 0$: The friction created by rolling is negligible

Where ξ is the angle between the line connecting the main and offset container and the tether section connecting the cart and the KCU. The first assumption results in having both tension forces acting parallel to the ground, leading to a more critical load in this direction. This effect can be neglected because the final resultant force needed to accelerate the system will be multiplied by the safety factor of 1.5. Neglecting F_{roll} leads to a slightly lower force F needed to accelerate the cart. This effect will be taken into account by the safety factor.

The free-body diagram of the car subsystem when accelerating is shown in Figure 10.6. Here W is the total weight of the cart, N is the normal force exerted by the guiding cable on one wheel of the cart and F is the resultant force exerted by the motor. For the first iteration, the

force is assumed to be as shown in the diagram, later it will be provided by the static friction force of the wheels rolling on the cable.

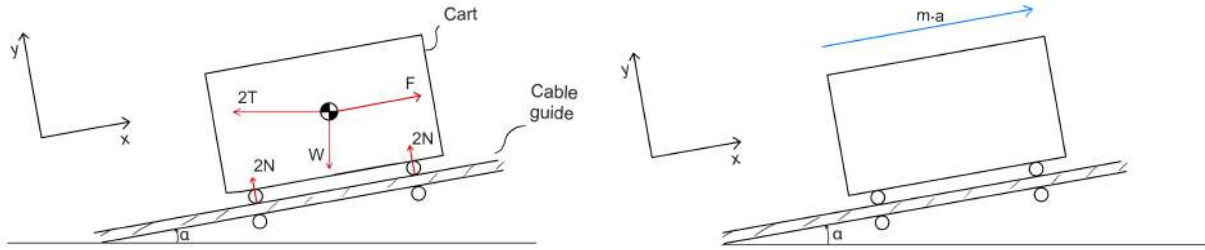


Figure 9.6: FBD of the cart subsystem (note that the diagram is not up to scale)

The tether cannot come in contact with the ground during operations (LLS-CART-OP-05). Assuming a flat terrain, the tether is allowed to sag until a maximum height of 50 cm above the ground. To achieve this, a tension force of 426.2 N is needed. Using a validated software for catenary curves² applied to the cable guide, it has been found that the cart when in the proximity of the offset container, will be positioned at an angle α from the ground which is 3.97° .

The directions of x and y are assumed positive in the directions shown in the reference system of the diagram. In the load case scenario described above, the cart should be able to accelerate from zero velocity to 2 m s^{-1} in 5 s, with no slipping motion. Taking the sum of forces in the x-direction:

$$\sum F_x : -2T - m_c g \sin(\alpha) + F = m_c \cdot a \tag{9.5}$$

Where:

$$a = \frac{v}{t}$$

The force F that results from Equation 9.5 needs to be multiplied by the safety factor of 1.5 and needs to be provided by the static friction force of the 4 wheels above the cable as shown in Equation 9.3.2. To ensure that the wheels don't slip, a clamping mechanism is needed to provide the additional normal force acting on the wheels to increase the friction force to the force calculated previously.

The static friction force generated by the two powered wheels, with no clamping force, is given by:

$$F_f = \mu_s \cdot N \tag{9.6}$$

Where:

$$N = (-2T \cdot \sin(\alpha) + m_c \cdot g \cdot \cos(\alpha)) / 4 \tag{9.7}$$

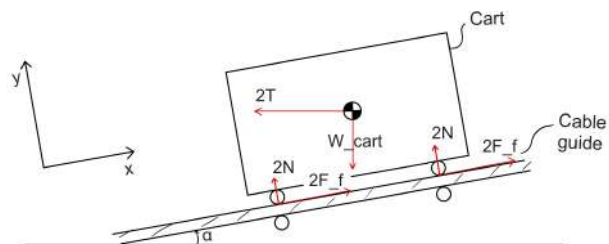


Figure 9.7: FBD of the cart subsystem, showing the action of friction force (the diagram is not drawn up to scale)

In order to increase the value of N and hence the magnitude of the static friction force, a clamping system is required. The required clamping force needed is given by:

$$F_{clamp} = \frac{F}{\mu_s} - \frac{F_f}{\mu_s} \tag{9.8}$$

²https://www.peacesoftware.de/einigewerte/seile_e.html, accessed on 12-06-2023

This force is the minimum force needed to not slip during the acceleration under a tension T of 426.2 N. With a mass of the cart of 136.6 kg, an angle of 3.97 degrees and an acceleration of 0.4 m/s a final clamping force on 1 wheel is 228.6 N.

To achieve this clamping force, two tension springs will be attached to each set of wheels. The chosen springs are *TR2280 tension springs*.³ These springs deliver a total force of 122 N each at an elongation of 66 mm, assuring that the required clamping force is reached. This force can't be exact since off-the-shelf springs are used and the most fitting spring had to be chosen.

Table 9.4: Parameters for the clamping mechanism

Parameter	Symbol	Value
Wheel Radius	r_w	0.075 m
Static Friction Coefficient	μ_s	0.4
Cart Mass	m_c	136.6 kg
Elevation Angle	α	3.97°
Max. Speed	v	2 ms ⁻¹
Max. Acceleration	a	0.4 ms ⁻²
Clamping Force per wheel	F_{clamp}	228.6 N

9.3.3. Power subsystem

A crucial requirement for the cart subsystem is that it must be able to move along the cable guides (LLS-CART-OP-01). To satisfy this requirement, a motor and a battery to provide power to the motor will need to be considered and sized.

Electrical Motor

Two electrical motors will be used to power the cart. they will be positioned on the sides of the two lower swivel access points, so they don't interfere with the tether and pulley system. Each motor will power the two wheels on the same side. Only the wheels located above the cable will be powered. The power will be transmitted from the engine to the wheel through a dented transmission belt. Each one of the two wheels will be connected to the motor through a separate belt. Because the resultant force of the tension acting on the pulley system on the cart is always acting towards the main container, the motor will only have to provide power to move towards the offset container.

The cart is designed to work in the worst load-case scenario, with a tension T of 426.2 N as described in Figure 9.3.2.

Knowing the magnitude of the force F (including the safety factor already) and the wheel radius r , the torque required T_{req} in the 4 driving wheels can be found with Equation 9.9.

$$T_{req} = F \cdot r \quad (9.9)$$

From the gear ratio theory, assuming the efficiency of the power transmission to be 100 %, the torque provided by the motor on the wheel can be found from the following relation:

$$\frac{T_w}{r_w} = \frac{T_m}{2r_m} \quad (9.10)$$

where the subscript w stands for wheel and m for motor. The torque of the motor is divided by 2, because it is connected to two wheels, with two different transmission belt systems connected

³<https://webshop.alcomexsprings.com/tension-spring-stainless-o-3-60x36-40x114-00-mm-tr2280>, accessed on 14-06-2023

to the same motor. The T_w found is the torque that the motor provides to each wheel. It must be greater than the minimum torque required to provide the acceleration of 0.4 m/s^{-1} .

The motor that resulted in providing the closest torque to the required one was the "QS138-A 72V 3000W"⁴. The relevant parameters for the performance of the motor and its dimensions can be found in Figure 9.5 and Figure 9.8 respectively.

Table 9.5: Relevant parameters for the performance of the motor

Parameter	Symbol	Value
Min. Force Needed	F	1496.06 N
Min. Torque per Wheel Req.	T_{req}	28.1 Nm
Max. Motor Torque	T_m	56 Nm
Radius Motor	r_m	0.0275 m
Torque per Wheel provided	T_{prov}	76.36 Nm

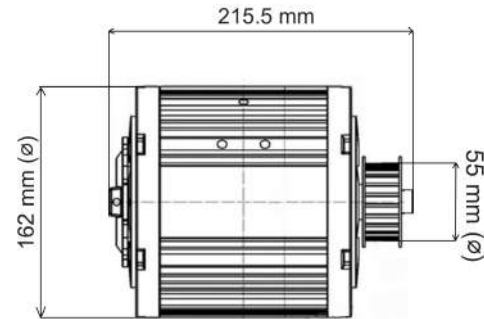


Figure 9.8: Sizes of the electrical motor

Battery

A battery will be used to provide the required power to the motors. The motors will only need to provide 38 % of their maximum torque, which will then relate to 38 % of their maximum power output, resulting in 2242 W given a maximum power output of 5900 W. The battery will be designed for a nominal output of 3000 W, including a safety factor for efficiency and battery lifetime losses. To deliver 3000 W to each motor, the battery needs to output 6000 W of power. Since the motors work with a voltage of 72 V, also the battery will need to be designed to output the same voltage and with a current of 83.333 A derived from Equation 9.11.

$$P = V \cdot I \quad (9.11)$$

Where P is the power, V is the voltage and I is the current intensity. The battery will comprise a series of cells connected in series and parallel to reach the right amount of power. The *Sanyo UR18650RX 1950mAh - 30A* batteries will be used to act as cells for the total battery.⁵ These batteries have a voltage of 3.6 V so they have to be put in a series of 20 batteries to achieve 72 V. The current of each cell is 30 A, meaning that three batteries have to be put in parallel to achieve a current of 90 A (which will be higher than the 83.333 A that is required).

The general layout of the battery will comprise 60 cells in total, distributed in three blocks in parallel containing 20 cells each connected in series. This would allow for active balancing of the cells, to make sure they are discharged at similar rates.

Finally, the total energy and Depth of Discharge (DoD) have to be determined to make sure the batteries can deliver the amount of energy that is required. The total energy required by the cart subsystem is calculated using Equation 9.12, and is equal to 285 000 J or 80 W h, assuming

⁴[⁵](https://nl.aliexpress.com/item/1005005651952169.html?spm=a2g0o.detail.0.0.145e2c47U32t2x&gps-id=pcDetailBottomMoreThisSeller&scm=1007.13339.291025.0&scm_id=1007.13339.291025.0&scm-url=1007.13339.291025.0&pvid=db7b3be6-77f4-4f56-b046-9a6ab3f149ba&t=gps-id%3ApcDetailBottomMoreThisSeller%2Cscm-url%3A1007.13339.291025.0%2Cpvid%3Adb7b3be6-77f4-4f56-b046-9a6ab3f149ba%2Ctpp_buckets%3A668%232846%238107%231934&pdp_npi=3%40dis%21EUR%21267.93%21267.93%21%21%21%21%21%21%40211b444016860, accessed 9-6-2023</p>
</div>
<div data-bbox=)

that the energy is only needed to move the cart over a time $t=47.5\text{ s}^6$, from the main to the offset container. When moving in the opposite direction, the horizontal component of the resultant force of the tension in the tether will be sufficient to move the cart.

The individual batteries have a capacity of 1950 mAh. Having three batteries in parallel will lead to a total capacity C of 5850 mAh ($1950\text{ mAh} \cdot 3$). To calculate the total energy E of the battery, Equation 9.13 can be used.

$$E = P \cdot t \quad (9.12) \quad C = \frac{E}{\eta \cdot V} \quad (9.13)$$

Where a voltage V of 72V and a total efficiency η of 90 % are assumed for a series of 20 batteries. This results in total energy of the complete battery of 379 Wh.

The battery will have a DoD= $80/379 = 21\%$ which means that the battery has more energy than is needed in one cycle. The battery may seem over-designed, but this battery has been chosen however since it is a cheaper option than the batteries with a lower capacity and a lower DoD also means that the lifetime of the battery increases, which is desirable for the design.

The Battery will be charged in the main container during operation when power is produced. Two conductive plates will be mounted on the side facing the ground station, which will interact with 2 conductive pins that are attached to the ground station. This will serve as a charging mechanism.

Motor controller

For the motor controller, a *3000W Brushless Controller* has been chosen.⁷ The motor controller will turn the DC current from the battery into an AC current which is needed for the motors. Two of these controllers are needed since it is not desirable to put two motors in parallel after a motor controller. The final configuration of the electrical system is shown in Figure 9.9.

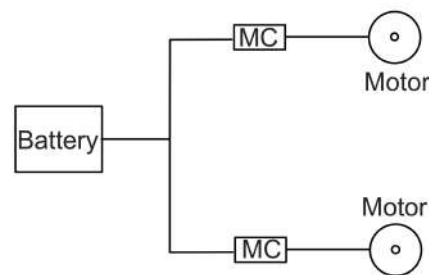


Figure 9.9: Sketch of the battery, motor controllers and motors

Braking System

The cart must also be able to reduce its speed to avoid bumping into the containers or damaging any other subsystem that interacts with the cart during its nominal operations.

A disk brake will be mounted on the powered wheels. The disc will have a diameter of 140 mm and is made out of alloy steel⁸. The weight of the disc is 100g, and the brake callipers weigh 239g⁹ and the cables have been estimated to have a mass of 25 g per wheel, for a total of 364 g

⁶Assuming an acceleration of 0.4 m/s^2 and a maximum velocity of 2 m/s for a distance between the two containers of 85 m

⁷https://nl.aliexpress.com/item/1005005538429917.html?pdn_pi=2%40dis%21EUR%21%E2%82%AC130%2C89%21%E2%82%AC65%2C45%21%21%21%21%40211b441f16866507542773331e9c2c%2112000033459027634%21btf&t=pvid%3Ae3a5e67b-d111-44ba-9a08-245d2a839a53&afTraceInfo=1005005538429917__pc__pcBridgePPC__xxxxxx__1686650754&spm=a2g0o.ppclist.product.mainProduct&gatewayAdapt=glo2nld accessed on 13-06-2023

⁸https://www.amazon.co.uk/Bynccca-140mm-160mm-180mm-Mountain/dp/B08CMR9XQN/ref=sr_1_5?crid=3QWOX0JVODQTM&keywords=brake%2Bdisc%2B140mm&qid=1686651033&sprefix=brake%2Bdisc%2B140mm%2CCaps%2C87&sr=8-5&th=1, accessed on 13-06-2023

⁹https://www.amazon.co.uk/Hydraulic-Brakes-Set%EF%BC%8CMountain-Pulling-Caliper/dp/B093R7K4K6/ref=sr_1_2_sspa?keywords=disc%2Bbrake%2Bcaliper&qid=1686899909&sr=8-2-spons&sp_csd=d21kZ2V0TmFtZT1zcF9hdGY&th=1, accessed on 13-06-2023

per disk brake system.

9.3.4. Cart Body

The cart body is the structural part of the cart, on which the pulleys, motors, wheels and various bearings are attached. It will consist of a sheet of aluminium, a light and sustainable material with optimal mechanical properties, shaped as a box with the bottom and the two ends perpendicular to the wheels' axes open. This would ensure an easy inspection of the components mounted on the cart. The cart will also comprise a plate at both ends with a hole in the middle to be attached to the main or offset container (LLS-CART-03, LLS-CART-04). It will have rounded edges, so to ease the hooking procedure.

Sizing of the Body

The load that is introduced into the metal sheets and the clamping plate is mainly bearing stress, and it will be analysed as seen in Section 9.3.1. The critical load that determines the thickness of the side and upper sheets is given by the lower and upper pulleys respectively, due to the large tension force directly applied to them (see Section 9.3.1 for the FBD). The clamping plate has to sustain forces only when attached to either container. It is designed to be able to withstand twice the tension force in the tether, as this is the worst-case scenario, depending on the position of the kite ($2T = 100000N$). Since the diameter of the clamping hole is insignificant compared to the width of the plate ($W/D = 11.5$), according to [27] the stress concentration factor can be neglected.

The final numerical results for the various thicknesses of the body of the cart are collected in Table 9.6. All the thicknesses have been rounded up to the nearest millimetre. The complete mass breakdown of the cart subsystem is shown in Table 9.8.

Table 9.6: Relevant thicknesses of the cart body

Parameter	Value	Unit
Thickness body side sheet	5.0	mm
Thickness body upper sheet	9.0	mm
Thickness clamping plate	9.0	mm

Table 9.7: Relevant cart sizes

Parameter	Value	Unit
Body width	367.0	mm
Body height	330.0	mm
Body Length	650.0	mm
Cart Length	1580.0	mm

Lateral Stability

In case of sudden wind gusts, while the cart is moving between the containers, the lateral stability of the cart could be a critical aspect of the design. The wheels and the clamping system keep the cart safely constrained to the cable guides, so the most likely accident would consist of the cart tipping over and entangling the cable guidelines, bringing the AWE system to a halt. The cart is only moved in case of a launch in low wind conditions, between 4 and 6 $m s^{-1}$. Assuming a gust of 30 $m s^{-1}$ exactly perpendicular to the side plate of the cart's body, the wind would exert on it a force F given by Equation 9.14.

$$F = \frac{1}{2} \rho V_{wind}^2 S \cdot c_l \quad (9.14)$$

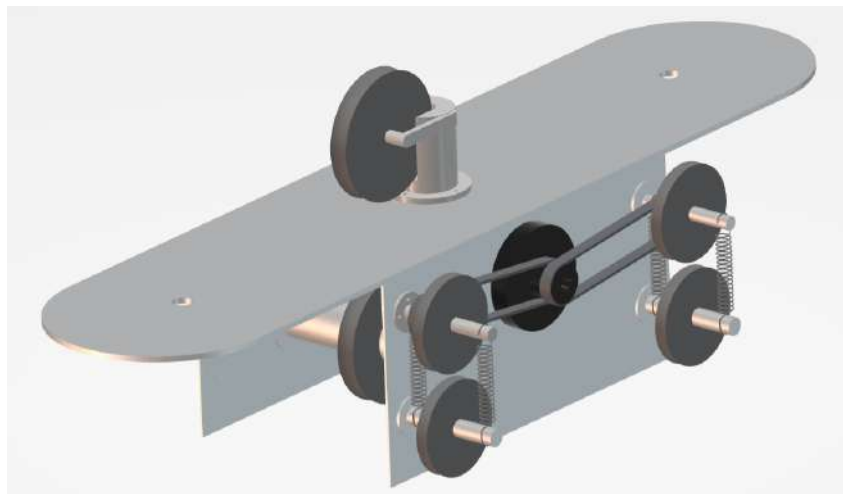
where the surface S is $0.2145 m^2$ ($w_{body} \cdot h_{body}$) and $c_l = 0.005$ for a turbulent flat plate¹⁰. This leads to a very low force of 0.59 N, meaning that its effect on the lateral stability of the cart can be neglected.

¹⁰https://www.engineeringtoolbox.com/drag-coefficient-d_627.html, accessed on 23-06-2023

Table 9.8: Overview of the components with the relative masses

Part	Mass per part [kg]	Number of parts	Total mass [kg]	Material
Pulley	4.88	3	14.64	Steel
Electric Motor	11.0	2	22.0	-
Wheel	2.77	8	22.16	Steel
Clamping Spring	3.75	8	30	Stainless Steel
Brake System	0.364	4	1.456	Steel(disc), Aluminium(caliper)
Transmission belt	0.19	4	0.76	Polyester
Roller Upper Pulley	0.17	4	0.68	Steel
Upper Pulley Arms	5.59	1	5.59	Aluminium 6061-T6
Upper Pulley Beam	1.85	1	1.85	Aluminium 6061-T6
Lower Pulley Beam	2.11	4	8.44	Aluminium 6061-T6
Upper Wheel Shaft	0.16	4	0.64	Aluminium 6061-T6
Lower Wheel Shaft	0.26	4	1.04	Aluminium 6061-T6
Clamping Plate	3.36	2	18.7	Aluminium 6061-T6
Body	11.43	1	11.43	Aluminium 6061-T6
Motor Controller	1.8	2	3.6	-
Cart Wiring	1.11	1	1.11	-
Charging inlet	1.11	1	1.11	-
Battery	0.046	60	2.76	-
Battery Case and Wiring	1.38	1	1.38	-
Bolts	0.0025	52	0.13	Titanium
TOTAL	-	-	136.69	

A visual representation of the complete cart subsystem has been included below in Figure 9.10.

**Figure 9.10:** 3D Model of the cart subsystem

9.4. Costs

A breakdown of the cost and the total cost of the system can be found in Table 9.9. Some parts are off-the-shelf and their price is taken from existing sources. These items include the clamping spring¹¹, brake system (disc brake¹² and caliper¹³), electric motor¹⁴, transmission belts¹⁵, motor controllers¹⁶, cart wiring¹⁷, the battery cells¹⁸ and the bolts¹⁹.

The parts that are not off-the-shelf have been calculated based on the material weight and the cost per weight of the materials. The cost that has been used for Aluminium 6061 T6 is 3.5 USD²⁰ or €3.24 and the cost for stainless steel that has been used is 2.5 USD²¹ or €2.31²².

The cost of the charging inlet, the battery case and case wiring have been assumed due to a lack of sources. For the charging inlet, the price is assumed to be twice as high as the cart wiring since an inlet can be quite expensive compared to wires. The battery case and internal case wiring are assumed to be half the cost of the battery cells similar to its weight estimation. The assembly of the cart has been assumed to be €2500. This price includes all the working hours and procedures needed to manufacture and assemble the parts.

All prices presented in Table 9.9 are the maximum possible price including shipping prices. Some off-the-shelf components can also be bought in stocks at discounted prices and on most components VATs are included which would not be taken into account during production inside an industry. This means that the final cost will be lower in reality than the one summarized in Table 9.9.

Table 9.9: Overview of the prices of the cart components

Part	Cost per part [Euro]	Number of parts	Total cost [Euro]
------	----------------------	-----------------	-------------------

¹¹<https://webshop.alcomexsprings.com/tension-spring-stainless-o-3-60x36-40x114-00-mm-tr2280>, accessed on 15-06-2023

¹²https://www.amazon.co.uk/Byncea-140mm-160mm-180mm-Mountain/dp/B08CMR9XQN/ref=sr_1_5?crd=3QWOX0JVODQTM&keywords=brake%2Bdisc%2B140mm&qid=1686651033&srefix=brake%2Bdisc%2B140mm%2CCaps%2C87&sr=8-5&th=1, accessed on 15-06-2023

¹³https://www.amazon.co.uk/Hydraulic-Brakes-Set%EF%BC%8CMountain-Pulling-Caliper/dp/B093R7K4K6/ref=sr_1_2_sspa?keywords=disc%2Bbrake%2Bcaliper&qid=1686899909&sr=8-2-spons&sp_csd=d2lkZ2V0TmFtZT1zcF9hdGY&th=1, accessed on 15-06-2023

¹⁴https://nl.aliexpress.com/item/1005005651952169.html?spm=a2g0o.detail.0.0.145e2c47U32t2x&gps-id=pcDetailBottomMoreThisSeller&scm=1007.13339.291025.0&scm_id=1007.13339.291025.0&scm-url=1007.13339.291025.0&pvid=db7b3be6-77f4-4f56-b046-9a6ab3f149ba&_t=gps-id%3ApcDetailBottomMoreThisSeller%2Cscm-url%3A1007.13339.291025.0%2Cpvid%3Adb7b3be6-77f4-4f56-b046-9a6ab3f149ba%2Ctpp_buckets%3A668%232846%238107%231934&pdp_npi=3%40dis%21EUR%21267.93%21267.93%21%21%21%21%21%21%40211b444016860, accessed on 15-06-2023

¹⁵<https://www.optibelt.com/fileadmin/pdf/produkte/keilriemen/Optibelt-TM-v-belt-drives.pdf>, accessed on 15-06-2023

¹⁶https://nl.aliexpress.com/item/1005005538429917.html?pdp_npi=2%40dis%21EUR%21E2%82%AC130%2C89%21%E2%82%AC65%2C45%21%21%21%21%21%40211b441f16866507542773331e9c2c%2112000033459027634%21bt&_t=pvid%3Ae3a5e67b-d111-44ba-9a08-245d2a839a53&afTraceInfo=1005005538429917__pc__pcBridgePPC__xxxxx__1686650754&spm=a2g0o.ppcList.product.mainProduct&gatewayAdapt=glo2nld, accessed 15/06/2023

¹⁷https://www.amazon.com/Devil-Dog-Connections-SJ00W-DDC10-3-SJ-M/dp/B09L6LW7N1/ref=sr_1_4?keywords=30+Amp+Wire&qid=1686735610&sr=8-4, accessed 15-06-2023

¹⁸<https://eu.nkon.nl/rechargeable/li-ion/18650-size/panasonic-ur18650rx-30a.html>, accessed on 15-06-2023

¹⁹<https://tibike.co.uk/shop/titanium-bolts/m6-titanium-bolts-tapered-head/>, accessed on 15-06-2023

²⁰<https://www.navstarsteel.com/6061-t6-aluminium-plate.html>, accessed on 14-06-2023

²¹[https://blog.thepipingmart.com/metals/steel-vs-stainless-steel-prices-whats-the-difference/#:~:text=The%20cost%20of%20stainless%20steel,%242%2C500%20per%20ton%20or%20more!](https://blog.thepipingmart.com/metals/steel-vs-stainless-steel-prices-whats-the-difference/#:~:text=The%20cost%20of%20stainless%20steel,%242%2C500%20per%20ton%20or%20more!,), accessed on 14-06-2023

²²<https://www.xe.com/currencyconverter/convert/?Amount=1&From=EUR&To=USD>, accessed on 14-06-2023

Pulley	10.30	3	30.90
Electric Motor	371.99	2	743.98
Wheel	6.41	8	51.30
Clamping Spring	13.37	8	106.96
Brake System	40.88	4	163.52
Transmission Belt	66.76	4	267.04
Roller Upper Pulley	0.39	4	1.57
Upper Pulley Arms	18.12	1	18.12
Upper Pulley Beam	6.00	1	6.00
Lower Pulley Beam	6.84	4	27.36
Upper Wheel Shaft	0.84	4	3.37
Lower Wheel Shaft	0.52	4	2.07
Coupling plates	30.30	2	60.59
Body	31.57	1	31.57
Motor Controller	130.69	2	261.38
Cart Wiring	47.00	1	47.00
Charging Inlet	94.00	1	94.00
Battery cell	2.99	60	179.40
Battery Case and Case Wiring	90.00	1	90.00
Bolt	4.18	52	217.36
Assembly	-	-	2500
TOTAL	-	-	4903.49

9.5. Verification and Validation

The verification of this subsystem consists in verifying the stress analysis performed and the compliance of the design with the requirements.

Calculations To accelerate the iterative process during the stress analysis of the cart subsystem, a Python program has been developed to size the structure to sustain the stresses introduced in the cart. The equations used have been taken from the book by Megson [28], therefore it can safely be assumed to be validated theory. The implementation of these formulas has been checked by manually performing the calculations and assessing any differences with the program's outputs.

The software has been considered verified, after assessing a discrepancy with the calculations in the order of 10^{-3} , justified by the rounding of the reference results to the third decimal place for simplicity.

The software could not be validated, due to a lack of resources. In order to properly validate it, a prototype of the cart should be tested in a real load case scenario.

Requirements The cart subsystem design must comply with the requirements set in Table 9.2. Each one of them will be investigated singularly in Table 9.10, showing whether each requirement has been complied with and where it has been addressed in the cart subsystem's design.

Table 9.10: Compliance matrix cart subsystem

Requirement ID	Requirement	Compliance	Shown in
LLS-CART-OP-01	The cart shall be able to move on the guiding cables between both containers	YES	Figure 9.5
LLS-CART-OP-02	The cart shall redirect the tether in any direction in which the kite can be positioned	YES	Section 9.3.1
LLS-CART-OP-03	The cart shall be able to remain stationary when connected to the offset container.	YES	Section 9.3.4
LLS-CART-OP-04	The cart shall be able to remain stationary when connected to the main container.	YES	Section 9.3.4
LLS-CART-OP-05	The cart shall not come in contact with the ground at any point of nominal operation	YES	Table 8.3
LLS-CART-STRUCT-01	The cart shall not deform plastically due to the loading experienced during operation.	YES	Section 9.3.4
LLS-CART-STRUCT-02	The cart actuators shall be fully redundant	YES	Section 9.3.3

9.6. RAMS Characteristics

The RAMS of the cart is vital for sans-maintenance functioning of the system since it is one of the most complex subsystems with the most moving parts of the LLS system. It is hereby discussed.

9.6.1. Reliability

The cart is the most complex subsystem with more failure points and generally lower reliability. To ensure the cart keeps working during the 6 months that it has to be autonomously operable (STK-OEM-01), it has been over-designed including high safety factors and extra "fail safe" components, such as the double motor. Those currently run at only 38% of their maximum power, meaning that if one of the motors fails the system would still be operable. The motors, motor controllers and battery are expected to be the most critical parts of the subsystem since they are the only electrical components. For the springs the redundancy strategy has been to include a safety factor of 1.5 which means the clamping force will be maintained after one or two spring failures.

9.6.2. Availability

The cart is moved only whenever the kite is launched with low wind conditions. Although its moving time is rather low, it will be subjected to very high loads for a prolonged period, which increases the probability of failure of the subsystem. The swivel access point on the cart, indeed, will be active during the entire operation and landing phase, since the tether will be permanently hooked to it. The introduction of safety factors in the sizing of the structure allows the cart to increase its stiffness and hence also availability. The cart will also be capable of performing its nominal functions with one single motor, meaning that it can continue its operations even in the unlucky event of a motor failure.

9.6.3. Maintainability

Every six months a planned maintenance will be performed. The health of all parts will be checked and a part such as the motor or a spring can be changed in case it failed during operation. In case heavy damage is sustained and the cart is not repairable on-site the entire cart can be replaced and repaired in adequate facilities.

9.6.4. Safety

The cart does not introduce a lot of safety hazards since the cart will travel at low speeds (2 m/s). A safety zone will still be introduced around the entire AWE system to make sure people won't come in contact and hurt themselves or the system. If the cable snaps the cart would experience high forces but since the direction in which the cart travels is located in the safety zone, the cart should not cause any danger to people or animals outside this zone. When maintenance is needed the cart will be parked in the ground station to make sure the maintenance personnel does not get in danger or injured by the cart.

9.7. Sustainability

From Table 9.8, it can be seen that the cart consists mainly of steel, aluminium and polyester.

The steel parts are the pulleys, the wheels, the clamping springs, the brakes and the roller upper pulley, adding up to about 69 kg of steel. DC electric motors have a copper content of 15% to 18%, therefore it is sensible to assume that the motors used consist of approximately 15% copper and 85% steel, which amounts to an extra of about 19 kg of steel. This works out to a total of around 88 kg of steel, which using an emissions intensity of $1.9 \text{ kg}_{\text{CO}_2\text{e}}/\text{kg}_{\text{steel}}$ as per Section 18.1 yields about $167 \text{ kg}_{\text{CO}_2\text{e}}$.

The aluminium parts are the upper pulley arms and beams, the lower pulley beams, the wheel shaft, the clamping plate and the body. This adds up to a total of around 48 kg of aluminium, amounting to about $24 \text{ kg}_{\text{CO}_2\text{e}}$ for an emissions intensity of $0.5 \text{ kg}_{\text{CO}_2\text{e}}/\text{kg}_{\text{Al}}$ according to Section 18.1.

The copper in the motor is estimated to be around 3.3 kg. For emissions purposes, the motor controller, cart wiring, charging inlet and battery case and wiring are going to be assumed to be composed of 100% copper. This adds about 7.2 kg of copper, corresponding to about $41 \text{ kg}_{\text{CO}_2\text{e}}$ with an emissions intensity of $3.9 \text{ kg}_{\text{CO}_2\text{e}}/\text{kg}_{\text{Cu}}$ as per Section 18.1.

The transmission belt is made of 0.76 kg of polyester, which amounts to about $3 \text{ kg}_{\text{CO}_2\text{e}}$ at an emissions intensity of $3.7 \text{ kg}_{\text{CO}_2\text{e}}/\text{kg}_{\text{PET}}$ according to Section 18.1.

The battery consists of 3x20 1950 mAh cells, which amounts to a total battery energy capacity of 0.42 kWh, at an emissions intensity of $75.5 \text{ kg}_{\text{CO}_2\text{e}}/\text{kWh}$ yields about $32 \text{ kg}_{\text{CO}_2\text{e}}$, as per Section 18.1.

The titanium for the bolts will be neglected because it is a very small mass compared to the other materials, and thus its contribution to the emissions payback time is estimated to be insignificant.

Added together, the cart is responsible for about $267 \text{ kg}_{\text{CO}_2\text{e}}$, which with a capacity factor of 0.5 and a rated power of 100 kW with a grid carbon intensity of $523 \text{ g}_{\text{CO}_2\text{e}}/\text{kWh}$, as per Section 19.5 contributes about 10 hours to the LLS system's emissions payback time.

9.8. Recommendations

With the current design, the cart shall be fully functional within the Landing, Launching and Storage system. The cart contains two electric motors and a battery powering 4 wheels which will ride over the guiding cables. The cart is also equipped with a swivel access point in order to perform its most important function by redirecting the tether to the kite at the offset container. Structural analysis of all load-bearing components is performed to assure that the cart will not fail under high stresses during operations. This results in a total mass of the cart of 136.69 kg and a total cost of the cart of €5009.49. For sustainability, the cart has an emissions payback time of 10 hours with a total emission of $267 \text{ kg}_{\text{CO}_2\text{e}}$ during its production (excluding maintenance).

Recommendations Currently, the battery is charged entirely by an external link with the battery in the main container. Part of the energy could also be recharged with the "regenerative braking" concept, which consists in recharging the battery during the deceleration of the cart, helping at the same time the cart to brake faster.

To make the cart body more lightweight, it is also recommended to make cutouts in the metal sheet wherever the stress concentration is low. This can be done through topology optimisation programs.

In this design, the normal force has been assumed to be equally distributed among the wheels. In reality, the acceleration and the tension forces introduced by the tether on the cart would generate a counterclockwise moment which would increase the load on the back wheels and reduce the reaction force of the upper wheels. It is worth investigating the use of a differential, which would allow the faster spinning of the higher-loaded back wheels than the front wheels. According to this new load, a new stress analysis would need to be performed on the rear wheels' shaft, as it will experience higher loads.

Meanwhile, the cart is moved back to the main container, the kite is expected to be kept parked at its operational altitude, so to limit the oscillations in the cable guide introduced by the tether on the cart. The case in which a sudden gust occurs while the cart is moving has not been investigated in this report. It would increase the tension in the tether very rapidly and this force would then lead to an oscillation of the cable guides. Since the lift force would be applied on the kite directly, and subsequently transmitted in terms of tension through the bridles, KCU, main tether and cart before reaching the cable guides, it is expected that some dampening will already occur with the current design. Even with this consideration, it is warmly recommended to investigate damping modes for these oscillations and assess their criticality in the design.

Scalability The cart subsystem was designed specifically for loads of the 100 kW system. Scaling up the system would inevitably lead to a significant increase in tension in the tether (the diameter of the tether would be bigger as well as the force the bigger kite would exert on it). This would have a direct impact on the stresses the cart will be subjected to, leading to larger thicknesses in the body and structures. On the same line, the power system will need to be sized to provide enough power to overcome the additional tension force introduced in the system and the pulleys will need to increase in size to accommodate the bigger tether. The braking and clamping system also needs to be adjusted accordingly.

Anchoring Mechanism

The guiding cable and tower introduce large additional forces on the system. To prevent the containers from moving, they will be held in place with the help of anchors as explained in this chapter. The chapter first goes through the functional analysis of the tower in Section 10.1. Then the requirements relevant to it are explained in Section 10.2. After this, the design itself in Section 10.3 is discussed. Further, the costs are analysed in Section 10.4. Then the V&V is discussed in Section 10.5. As well, the RAMS in Section 10.6 is outlined, then the sustainability is explained in Section 10.7 and lastly some recommendations are given in Section 10.8.

10.1. Functional Analysis

Earlier analysis showed that the external battery container would have to be attached to the ground in one way due to the loads induced by the high-tension tether [29]. The consequences of having no fixed connection to the ground were assessed; even though it has substantial weight, the battery container faces the risk of getting dragged along the ground surface. This is the product of a risk that shall be mitigated using a safe and reliable anchoring method. This can be seen in Table 10.1. With the anchoring system, the offset container does not have to be very heavy anymore, and as such, another container can be used, which coincidentally adds storage space. A 10-foot ISO container is chosen for the offset point.

Table 10.1: Functions anchoring subsystem

Function ID	Function
FUN.2.1.1	Evaluate site
FUN.2.1.2	Place main and offset container
FUN.2.1.3	Anchor system to site
FUN.10.3.1.1	Remove anchors

10.2. Requirements Analysis

The anchoring subsystem needs to be designed to meet the requirements which flow from the functions defined in Section 10.1 and risks in Appendix A. This will ensure that the functions are performed without overdesigning the system. These requirements are stated in Table 10.2.

Table 10.2: Requirements anchoring subsystem

Requirement ID	Requirement	Rationale	Flowdown
LLS-ANCH-STRUCT-01	The main- and offset- container shall be able to support limit loads without permanent deformation.	Plastic deformation would likely prohibit the system from operating nominally.	FUN.2.1.2, LLS-GEN-STRUCT-02
LLS-ANCH-STRUCT-02	The offset container shall not move under an applied load of 150 kN in the direction of the guiding cables.	150 kN is the guiding cable tension found in Chapter 8.	FUN.2.1.3

LLS-ANCH-STRUCT-03	The ground station container shall not move under an applied load of 150 kN in the direction of the guiding cables and a load of 50 kN in the direction of the tether.	50 kN is the maximum tether force from the kite.	FUN.2.1.3
LLS-ANCH-STRUCT-04	The ground station container shall not move under the maximum applied loads from the tower as stated in Table 7.3	The tower is connected at the bottom of the container.	FUN.2.1.3
LLS-ANCH-OP-01	There shall be anchoring systems available for rock	The ground units must be able to be installed on any type of ground	FUN.2.1.1, FUN.2.1.3, RSK-TCH-ANC-02

10.3. Design

The design of the anchoring subsystem depends largely on the anchorage effect, container properties and configurations and loads. All of these are discussed below.

10.3.1. Anchorage's Effect on the Anchor Design

The structural integrity of the LLS system relies on the adequate design of many aspects of the ground-based elements. One of these elements that should not be overlooked is the soil that the system rests upon. The ground surface quality is a critical factor that will determine the LLS system's stability and long-term performance. By assessing the characteristics of the soil, the anchoring structure can be designed accordingly and the reliability of the system can be improved drastically. This section will focus on the role of the ground surface in the anchoring system design.

Anchorage is the surface to which an anchor is attached. In this case, the anchor is what attaches the offset container to the ground surface, and the ground surface itself is the anchorage. The specifications and size of the anchoring method can only be determined after analysing the load-bearing capabilities of the soil the LLS system will be placed on the anchorage.

Standard Penetration Testing (SPT) is a common practice for many engineering projects, in which the soil is tested for its ability to provide adequate support to the structure to be constructed on top of it. By conducting SPT, engineers are able to assess the stiffness, flexibility, and strength of the soil. An SPT test is conducted by drilling a borehole to the desired sampling depth by dropping a 63.5 kg hammer repeatedly from a height of 76 cm until the sampler that is driven into the ground reaches a depth of 45 cm, with intervals of 15 cm. The number of blows required to reach the last 30 cm of depth is called the "standard penetration resistance" or the N-value¹. A higher N-value, thus, indicates a more resistant and strong soil, which comes at the expense of it being harder to penetrate - posing as a constraint on the ease of set-up. The N-value is considered to be an indication of the suitability of the ground for construction but can also be used as an anchor design driving parameter.

In the case of anchoring both the ground station and the offset container, it is critical that the anchor can direct all loads of the cable into the ground. For this reason, before they are anchored, the N-value of the soil should be determined and a sufficient amount of soil anchors should be used. If a certain soil type is deemed inoperable or when more than four large anchors are

¹[https://www.geoengineer.org/education/site-characterization-in-situ-testing-general/standard-penetration-testing-spt#:~:text=Standard%20Penetration%20Test%20\(SPT\)%20is,strength%20of%20stiff%20cohesive%20soils.,](https://www.geoengineer.org/education/site-characterization-in-situ-testing-general/standard-penetration-testing-spt#:~:text=Standard%20Penetration%20Test%20(SPT)%20is,strength%20of%20stiff%20cohesive%20soils.,) accessed 26-05-2023

needed, reinforcements may need to be added to the anchor, anchorage, or container itself. The N-values for different surface types are provided in Table 10.3.

Table 10.3: ASTM soil classification

Basic Soil Type	Sub Group	Compaction/Strength	SPT-N	ASTM Class
Sand	Sand	Very Loose	0-3	8
		Loose	3-8	5
		Compact	8-30	3
		Cemented	30-58	1
	Sand Clay / Sandy Silt	Soft	3-8	5
		Firm	8-30	3
Stiff		30-58	1	
Silts	Silts	Very Soft	7-14	6
		Soft	14-25	5
		Firm	25-60	4
	Silty Clay	Soft	7-14	6
		Firm	14-25	5
		Stiff	25-60	4
Clays	Clay	Very Soft	0-5	8
		Soft	4-8	7
		Firm	7-14	6
		Stiff	14-25	5
		Very Stiff	35-60	3
		Hard	>60	1
Peats	Organic Clay Silt or Sand	Firm	0-5	8
	Peat	Spongy	0-5	8
		Plastic	0-5	8
Chalks	Very Weak		0-25	6
	Weak		25-100	2
	Moderately Weak		100-250	1
	Moderately strong to very strong		>250	0

From Table 10.3, it is seen that soils have been classified from 0-8, indicating different properties at each level. Spirafix describes the compatibility between the individual soil types and the load limit of their 75 mm anchor as can be found in the load chart of Spirafix².

From this, two conclusions regarding anchor design and site selection can be made:

- Stiffer and harder soils (high N-value, low American Society for Testing and Materials (ASTM) class number) are able to bear heavier loads.
- The required depth quickly becomes infeasible for lower ASTM class soils, hence some applied loads can never be supported by certain surfaces making it impossible to operate on those grounds.

These effects necessitate setting a maximum allowable anchor depth. Installing the anchors deep will increase the associated costs as larger machinery may be required. This would also make maintenance and inspection more difficult. Thus, the most optimal solution would be to minimise the anchor installation depth.

To account for future changes to the loading on the anchor, lines for each ASTM class are fit to linear regression. Using the start and end point for each line, the slope can be found and,

²<https://www.spirafix.nl/uploads/files/producten/schroefanker-ac-m24-rond-75mm/Spirafix%2075mm%20Load%20Charts%202019.pdf>, accessed on 09-06-2023

in turn, used with the initial point to formulate a simple linear relation between the maximum working load and the required depth of anchor. This allows for estimating the necessary anchor depth at any given applied load. Table 10.4 shows the regression formula for each ASTM soil class.

Table 10.4: Required depth of a single anchor to support a load X acting axially on the anchor for all ASTM soil classes

ASTM Soil Class	SPT N-Range [-]	Depth of a single anchor at X kN [mm]	Max. Load at a single anchor [kN]	Operable Depth Range [mm]
0	>250	$29.429 \cdot X + 270.836$	81	1100-2700
1	60-250	$30.864 \cdot X + 306.128$	76	1100-2700
2	45-60	$32.944 \cdot X + 309.356$	71	1100-2700
3	35-50	$37.215 \cdot X + 279.413$	64	1100-2700
4	24-40	$39.541 \cdot X + 324.832$	59	1100-2700
5	14-25	$43.630 \cdot X + 298.298$	54	1100-2700
6	7-14	$47.847 \cdot X + 308.732$	49	1100-2700
7	4-8	$53.850 \cdot X + 308.551$	40	1100-2700
8	0-5	$66.596 \cdot X + 202.624$	35	1100-2700

Table 10.4 will provide the basis for anchor sizing since its final design will have to account for the properties of all anchorage types within the operational envelope. This shall be done by estimating, firstly, the total load experienced by the offset container due to the tensile forces from the tether connecting the offset container, ground station, and kite. The total loading will be distributed to several anchors, which will determine the magnitude of the load experienced by each one of them - thus, making it possible to size the anchors using the information provided in Table 10.4. If the required depth is too large for certain types of soils, more soil anchors could be used. Note that the load on the maximum load of the anchor is in the axial direction, while the anchor will be installed under an angle of 45° with the ground, and will be pulled under an angle of approximately 90° with respect to the anchor. These angles will increase the maximum load that the anchors can handle. Therefore, the values in Table 10.4 are conservative.

In the case of rocky ground, soil anchors will not work, and more effort is required to make sure the system will not move. The container and rest of the anchoring system can be the same, but there need to be holes drilled into the ground in which so-called rock bolts are placed. It needs a heavy mining-grade drill and a specially trained crew. There are many types of rock anchors on the market, but expanding anchors³ seem ideal since they require shallow holes.

A drilling system that is capable of drilling a 50mm diameter hole in hard rock is required for this. A jackhammer can also be used but the risk of making the hole diameter larger than it needs to be is high. The complexity of this method makes it a last resort, only for use in locations where there is no layer of soil at all in the vicinity of where the electricity should be provided.

10.3.2. Container Properties

From LLS-ANCH-STRUCT-01, it follows that it is important that the container does not bend too much or break under the loads that are applied by the cable guide and anchors. The 10-foot container has connection points, also called corner castings. These are designed for standardised transport and therefore also to carry the standard max load of the container. Thus, these corner castings are convenient to attach the ground anchors to. However, the corner castings

³<https://alliedboltinc.com/Earth-Anchor/Expanding-Rock-Anchor~17/1-inch-X-53-inch-EXPANDING-ROCK-ANCHOR~55509>, accessed on 20-06-2023.

or walls of the container should not critically deform under the loads. If there is a total horizontal load of 100 kN on the container, and this is directed at 45° into the ground, these corners each have to hold about 70 kN. ISO prescribes a minimum vertical corner load of 190 kN so this is well within its capabilities. For the loads that the container can hold, it is good to know that a standard shipping container consists of a square hollow beam on every corner with sheet metal of roughly 2 mm in between these beams.

ISO Container Required Test Loading

Since the sheets are thin, the compression and tension load is typically mostly carried by the structural members on the edges of the container. The skeleton of a container is displayed in Figure 10.1.

ISO1496 specifies that series 1 freight containers (10 feet) need to be designed such that they can withstand a longitudinal load of 75 kN and a transverse load of 150 kN applied on the top corners of the container (from the side), both tensile and compressive [30][31]. Steinecker, a company manufacturing containers [31] complies with this by making the top rail from a 60 x 60 x 3.0 mm rectangular hollow section steel.

Furthermore, the requirement for stacking the container states that every corner post needs to be able to carry 850 kN, which is a lot higher than the forces that could be introduced by the cables of the design at hand. Steinecker does this by having an inner part of 113 x 40 x 12 mm hollow section steel and an outer part of additional 6 mm steel.

Furthermore, the requirement for stacking the container states that every corner post needs to be able to carry 850 kN, which is a lot higher than the forces that could be introduced by the cables of the design at hand. Steinecker does this by having an inner part of 113 x 40 x 12 mm hollow section steel and an outer part of additional 6 mm steel.

10.3.3. Anchoring Configurations and Loads

In this section, the anchoring configurations for the main- and offset containers are discussed. This is not a trivial problem because the loads on the container and the positioning of the anchors are dependent on each other. The focus will be put on minimising the number of anchors needed. This is done to comply with requirement STK-OEM-11; The LLS shall fit in a standard 20ft container, and also requirement STK-OEM-07; The cost of one LLS system unit shall not surpass €40,000.

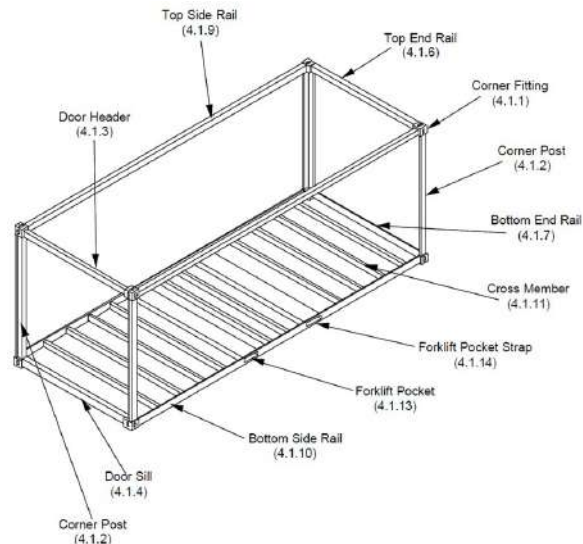


Figure 10.1: Skeleton of a standard shipping container⁴

⁴<https://www.shippingandfreightresource.com/anatomy-of-a-shipping-container/>, accessed 31-05-2023

Configuration for the Offset Container

This configuration is the simplest because the moment of the tower does not need to be taken into account. In this configuration, guy lines to the anchors are attached to the top four corner castings (like with a tent). This helps to reduce the load on the container because the majority of the load flows through the top of the container, while the resultant vertical force is carried by the stiff corners of the container. There is a shear force on the sides of the container, but it is negligible. Furthermore, the loads that act on the container are sketched in 2D for both the side view and the top view in Figure 10.2. Using Equation 10.1, Equation 10.2 and Equation 10.3, the loads on the container can be calculated.

It was decided to not rely on the frictional force of the container but only on the anchors. Also, α was set to 30° and θ to 15° . Furthermore, because of the long distance of cable F_1 , the small angles are neglected for now.

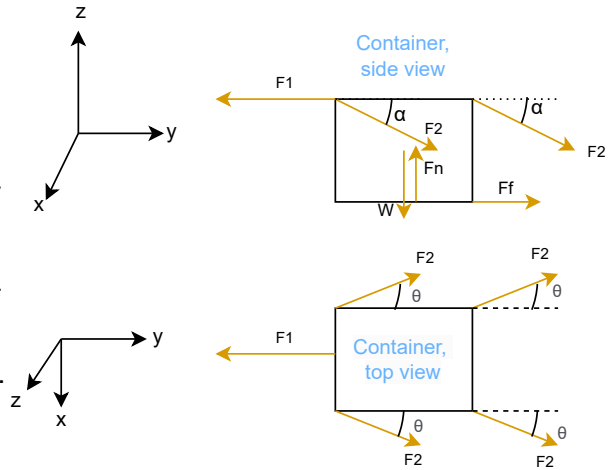


Figure 10.2: FBD of the offset container anchoring

$$\sum \vec{F}_x : 2F_2 \cos \alpha \sin \theta - 2F_2 \cos \alpha \sin \theta = 0 \quad (10.1)$$

$$\sum \vec{F}_y : 4F_2 \cos \alpha \cos \theta + F_f - F_1 \quad (10.2)$$

$$\sum \vec{F}_z : F_n - W - 4F_2 \sin \alpha \sin \theta \quad (10.3)$$

It was found in Section 10.3.1 that each anchor can readily hold 50 kN in most surfaces, so this is the assumed tension force F_2 for now. Therefore, for this configuration, the maximum force F_1 would be 167.5 kN. However, the loads that go through the top of the container longitudinally on one side are a fourth of the force in the y-direction, 41.9 kN. This is slightly above 37.5 kN, half of the longitudinal requirement set by the ISO standard. This means that the maximum force F_1 reduces to 150 kN for this configuration unless the container is reinforced in the longitudinal direction.

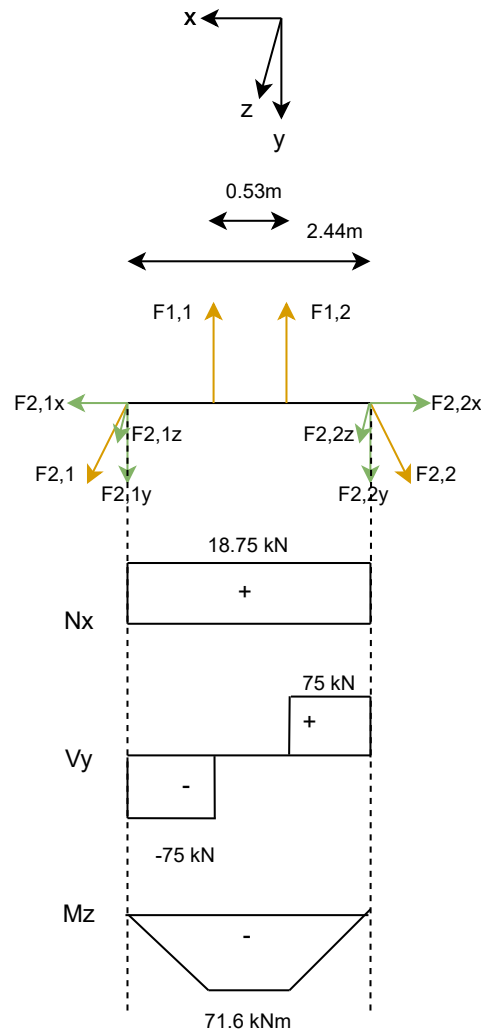


Figure 10.3: Most important forces and moments for the 'door header'

Furthermore, with Equation 10.3, it can be calculated that the forces put on the container in the z-direction is 6.47 kN. Assuming that the sheet and 'door header' do not carry the load in the ver-

tical direction, the corner post, which has a maximum load of 850 kN, as found in Section 10.3.2, will carry this load without problems.

The edge on the top front (door header) will have to get two extra attachment points in the middle to connect to the guiding cables. Furthermore, a bending moment will be put on this part because of the three point-forces. The most important forces and moments that are put on this front edge are shown in Figure 10.3. The maximum bending moment is calculated by multiplying half of the length of the short side of the container, 1.15 m [30]. The analysed stresses within the acceptable values for the container. the attachment points will however need to be added.

From Figure 10.3, the moment on the door header is equal to 71.6 kNm. The door header section is typically made out of a cross-section of alternating 3 mm and 4 mm, and a height and width of 60 mm[31]. From this, the maximum stress can trivially be calculated to be 6 GPa with Equation 10.4 for the standard door header. Therefore, the door header would need to be heavily reinforced. However, this can be circumvented by redirecting the forces of the guiding cables to the corners of the container. Thus it is recommended to insert a clamp between the guiding cables to be able to redirect the forces.

$$\sigma_{bending} = \frac{My}{I} \quad (10.4)$$

This configuration was chosen such that the container is stable because it is tied down at every corner point. Also, it makes sure that the load is only transferred through the top part of the container.

Configuration for the Main Container

For the main container, the tower adds extra forces and moments to the container. From Table 7.3, it can be concluded that the moment M_A , which has a magnitude of 53 kN is the critical case when acting over the short side of the container. For this case the additional Equation 10.5 is important, the critical case has also been illustrated in Figure 10.4. In the case which is drawn, the left anchor rope, $F_{2,1}$ does not carry any of the loading. Thus this has not been taken into account by Equation 10.5. It has been decided that the anchor configuration will be the same as for the offset container, with the addition of two extra anchors at the middle point of the long side of the container with θ set to ninety degrees and α also set to thirty degrees.

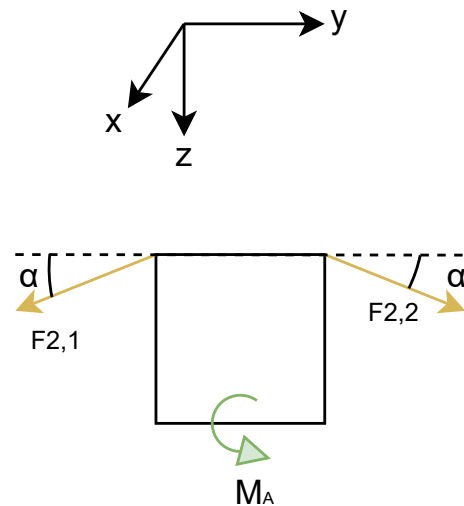


Figure 10.4: Critical loading case of the tower on the container

$$\sum M_A = M_A - F_{2,2z} \cdot h - F_{2,2y} \cdot \frac{w}{2} \quad (10.5)$$

From this, it can be calculated that the force in $F_{2,2}$ is equal to 35.6 kN. This is well below the established limit for the anchor and the anchor cables can handle it. However, the container is not designed for this load on the side of the container. That is why the main container will get two extra reinforcing bars welded on the top long sides of the container, on these bars a ring is welded to which the anchor cables can be connected. The reinforcing bars shall be able to

handle a moment of 50 kN m over the six-meter-long container. The thickness of the bar hollow square cross-section bar needs to be 5mm if it has a diameter of 16 cm. These two additional anchors to the main container will bring the total number of anchors to ten.

10.3.4. Connection Cables and Corner Casting Connection

The cables between the anchors and the attachment points will be Ratchet strap cables. These cables have a tensioning device in between and can be connected to the eye of the anchor and the corner castings of the container. Except for the two additional tower cables which are connected to the reinforcement bar mentioned in the previous section.

10.4. Costs

In Table 10.5 an overview of all the prices is given. Spirafix provided a quote for the anchors, in which a price of €366 was stated per anchor, assuming an order size of fifty anchors. The manufacturing of the reinforcement bar with the attachment point is outsourced to a company that has yet to be determined, but it is a trivial part so it will not be a problem. Furthermore, a ratchet strap costs around €10 per strap⁵.

Table 10.5: Overview of the prices of the cart components

Part	Cost per part [Euro]	Number of parts	Total cost [Euro]
Ratchet strap (5m)	10	15	150
Reinforcement bar	100	2	200
Attachment point	50	2	100
Anchors	366	10	3660
TOTAL	-	-	4110

10.5. Verification & Validation

The verification of this subsystem consists in verifying the stress analysis performed and the compliance of the design with the requirements.

Compliance Matrix

requirements set in Table 11.2. Each one of them will be investigated singularly in Table 10.6, showing whether each requirement has been complied with and where it has been addressed in the cart subsystem's design.

Table 10.6: Compliance matrix anchoring subsystem

Requirement ID	Requirement	Compliance	Shown In
LLS-ANCH-STRUCT-01	The main- and offset- container shall be able to support limit loads without permanent deformation.	YES	Section 10.3
LLS-ANCH-STRUCT-02	The offset container shall not move under an applied load of 150 kN in the direction of the guiding cables.	YES	Section 10.3.3

⁵<https://www.theratchetshop.com/ratchet-straps/ratchet-straps-above-3000kg/10-000kg-ratchet-strap.html>, accessed on 21-06-2023

LLS-ANCH-STRUCT-03	The ground station container shall not move under an applied load of 150 kN in the direction of the guiding cables and a load of 50 kN in the direction of the tether.	YES	Section 10.3.3
LLS-ANCH-STRUCT-04	The ground station container shall not move under the maximum applied loads from the tower as stated in Table 7.3	YES	Section 10.3.3
LLS-ANCH-STRUCT-05	The anchors shall fail before the container structure fails	YES	Section 10.3
LLS-ANCH-OP-01	There shall be anchoring systems available for rock	YES	Section 10.3.1

10.6. RAMS Characteristics

As the reliability of the anchors is vital for system stability, it is important to discuss the RAMS of the anchoring subsystem.

10.6.1. Reliability

The quality of an anchor is measured by its lack of movement. A reliable anchor is therefore one that resists movement for a long time with little probability of failure. Because the anchors are relatively light for the amount of force that they can withstand, and the tension in the cable is variable because of possible (unaccounted) vibrations, it is good to overdesign the anchoring system with a moderately high safety factor.

10.6.2. Availability

As long as the cable is under tension, the anchor needs to be able to provide resistance to this tension. There must be no intermittence in its operation, as this will cause instant catastrophic failure of the system. Furthermore, the battery container will be positioned behind the main container, such that it does not interfere with the anchor guy lines.

10.6.3. Maintainability

The anchor should not have to be able to be maintained, and should therefore be able to last for the full six months of operation. After the system is packed up, it must be assessed whether the parts can be used again or must be discarded and replaced. Inspection should still be able to be done by making possible failure points accessible to visually assess whether, for example, the environment will not degrade certain parts beyond their ability to perform their respective function.

10.6.4. Safety

The anchoring system is the point where all loads of the cable, kite, and cart combine. These loads flow through small parts like tensioners and hooks in a concentrated manner. Each of these stress concentrations, especially those that are under tension, can release a lot of energy when they fail catastrophically. Overdesigning is key to preventing this. In addition to this, those who tension the cable must consider strict safety measures that take into account the danger zones in case of possible cable-, anchor- or another equipment failure.

10.7. Sustainability

There is little information available about the mass of the Spirafix ground anchors. For the present report, it will be assumed that each anchor has 30% of the mass of a solid 75 mm diameter cylinder of steel. For 8 2600 mm anchors, this works out to about 221 kg of steel which, at $1.9 \text{ kg}_{\text{CO}_2\text{e}}/\text{kg}_{\text{steel}}$ as per Section 19.2, is associated to about $420 \text{ kg}_{\text{CO}_2\text{e}}$ emissions.

This yields an emissions payback time of about 16 hours with a capacity factor of 0.5 on a rated power of 100 kW with a grid carbon intensity of $523 \text{ g}_{\text{CO}_2\text{e}}/\text{kWh}$ as per Section 19.1.

10.8. Recommendations

The load analysis and anchor configuration are related in quite a complex manner, and pre-tensioning or de-tensioning of anchor lines will have an impact on the loading but has not been explored yet, researching this further would be beneficial to improve the loading model.

Furthermore, the anchoring subsystem turned out to be more expensive than expensive due to the high cost of the anchors. For further design, the option of a driven pole could be researched to save costs.

As mentioned in Section 10.3, it is recommended to redirect the loads from the guiding cables to the corners of the container to reduce the load on the door header. A cable clamping of the two guiding cables just before the anchors is recommended for this. The exact design for this has yet to be determined.

Electrical System

In the present chapter, the electrical system is explained. Starting with the functional analysis of the system in Section 11.1, then the relevant requirements in Section 11.2, the overall design in Section 11.3, costs in Section 11.4, V&V in Section 11.5, RAMS in Section 11.6, sustainability in Section 11.7 and recommendations in Section 11.8.

The electrical system of the LLS is of great importance since the main objective of an AWE is to create energy in the most efficient way possible. The three most important electrical components are:

- The battery
- The cable connecting battery and winch
- The winch

11.1. Functional Analysis

This section will state the main functions the electrical system has to perform. These functions are derived from the functional breakdown structure in Chapter 3 and the stakeholder requirements in Table 4.1.

Table 11.1: Functions electrical subsystem

Function ID	Function
FUN.2.2	Connect to power infrastructure
FUN.2.4.1	Ensure the appropriate power-on of the system
FUN.5.2	Reel-in main tether
FUN.5.3.4.2	Reel-in main tether
FUN.7.1.2.2	Reel-in main tether
FUN.7.1.4.2	Reel-in main tether
FUN.7.2.3.2	Reel-in main tether until KCU is above tower
FUN.7.3	Reel-in main tether completely
FUN.12.1	Provide power to every subsystem
FUN.12.2	Store power from Electrical Machine (EM) in battery

11.2. Requirements Analysis

The anchoring subsystem needs to be designed to meet the requirements which flow from the functions defined in Section 11.1 and the risks in Appendix A. This will ensure that the functions are performed without overdesigning the system. These requirements are stated in Table 11.2.

Table 11.2: Requirements electrical subsystem

Requirement ID	Requirement	Rationale	Flowdown
LLS-ELEC-BATT-01	The battery shall have a capacity of at least 300 kWh	This capacity was provided by the people at Kitepower	FUNC-ELEC-04/STK-OEM-16

LLS-ELEC-BATT-02	The battery shall function at temperatures between -15°C to 40°C	The battery should be able to work in a wide range of temperatures, including freezing or extreme heat	LLS-GEN-OP-16
LLS-ELEC-BATT-03	The battery shall function as an energy supply regulator for the microgrid	There has to be a constant flow of energy even when the kite is not producing energy and serves as a voltage/frequency regulator as well	STK-PGO-02/FUN.2.2
LLS-ELEC-WNCH-01	The winch shall have a minimum reel-in speed of 12 m/s	It is the minimum speed necessary to successfully do step-towing	FUNC-ELEC-06
LLS-ELEC-WNCH-02	The motor shall have a rated power of at least 100 kW	It is a customer requirement that the system is at least 100 kW	FUNC-ELEC-06

11.3. Design

The design of the electrical system consists basically of the battery, the winch and the interface with the other subsystems.

Battery

The battery is a critical component for the proper functioning of the LLS system, its main purpose is to feed energy to both the microgrid and all the components so the system may land, launch or store the kite. Because this design is supposed to work disconnected from the grid, the battery will serve as an energy storage unit that will allow this system to function autonomously for at least 6 months. Some components that make use of this energy are: the cable cart needs to move along the cable guides, the tower should be able to rotate in order to align itself with the kite, the winch needs to reel in or out the tether, and the RSS's motor has to roll in the kite. The battery container will be at the side of the ground station, close to where the power is generated and consumed. Additionally, the battery feeds energy to the microgrid when the AWE is not producing any energy. It serves as a constant supply of energy and doubles as a voltage/frequency regulator that ensures that the power grid does not over-power and gets damaged.

Rather than designing a battery from scratch, an off-the-shelf battery shall be used. Currently, Kitepower is using a battery from the company Greener Power Systems. Specifically, the 336 models will be used for the LLS as they comply with the sustainability requirements.

Table 11.3: Parameters for Greenpower 336 Battery

Parameter	Value
Length Container	10 ft.
Weight	8100 kg
Capacity	336 kWh
Power	318 kVA
Voltage	230/400Vac
operating Temperatures	-20 to +40°C
Grid Frequency	50 Hz.

Because this battery can be grid-connected, there is no need to charge the battery with a DC current. An in-built rectifier in the battery allows for the battery to be connected to the 3-phase motor generator.

Winch

This component creates electrical energy from the reeling-out action of the tether. The winch that stores the tether is directly connected to the machine and depending on the mode of operation it will produce or consume energy. The winch has two main parts: the first one is the drum where the tether is stored, and one motor-generator attached to the side.

During the operation of the kite, there are multiple modes in which the kite flies and pulls on the tether. When performing the pumping cycle, the kite reels out the tether. During this type of manoeuvre, the winch creates energy which is then transmitted to the battery so it may be stored. When the kite has to be reeled in towards the ground the machine works as a motor. As such, it consumes energy from the battery.

The EM will be securely attached to an internal frame in the container so it may remain immobile when the kite is applying force. Additionally, the winch possesses a spooling system that prevents the tether from tangling when being reeled in/out. The spooling system consists of two pulleys moving side to side over the drum, guiding the tether, illustrated in Figure 11.1.



Figure 11.1: Spooling system for tether



Figure 11.2: Winch produced by Dromec for Kitepower systems ground station 2

Currently, the company Dromec is the supplier of winches for Kitepower. One of their previous models is shown in Figure 11.2. Some of its specific parameters are shown in Table 11.4. This information was provided by the personnel of Dromec¹.

Table 11.4: Parameters for EM

Parameters	Value
Weight	5500 kg
Motor power	160 kW
Voltage	400 V
Nominal reel out speed	2.8 m/s at 40 Hz
Maximum reel in speed	10 m/s
Nominal reel in force	5 kN
Maximum reel out force	70 kN
Drum (smooth section)	∅866mm x1770mm
Tether diameter	∅14 mm
Tether storage	300 meters (+ additional safety windings)
Operating temperature	-10°C to +50°C

⁰<https://www.nswinches.co.uk/case-studies/swedish-polar-research-gme500>, accessed on 15-06-2023

¹<https://www.dromecwinches.com/product/esp-5500-op-kitepower-kite-groundstation/>, accessed on 09-06-2023

The winch needs to be adjusted to perform an efficient Stepped Tow Launch (STL). The winch should be able to reel-in at 12 m s^{-1} with an applied force on the tether of 25 kN. Additionally, the drum must be resized such that a longer tether of 500 m can be used. Super-capacitors are installed and connected directly to the winch so that the energy output is kept constant and does not vary too much, this ensures a more secure transmission of energy.

The dimensions of this custom winch are assumed to be similar to the original winch². The drum has a diameter of 866 mm and length 1800 mm. The EM is assumed to have a diameter of 610 mm and a length of 1600 mm and is mounted to the side of the drum. The total length of the winch system is thus 3.400 m. This custom part will be provided by Dromec.

Interface and Architecture of Electrical System

To visualise this better, a basic electrical diagram has been created in Figure 11.3. Looking from left to right, the first component to appear is the 3-phase AC motor-generator. The characteristics of such a machine have previously been specified in Table 11.3. When the winch is generating energy during the pumping cycle, the power may be transmitted in 3 different AC lines.

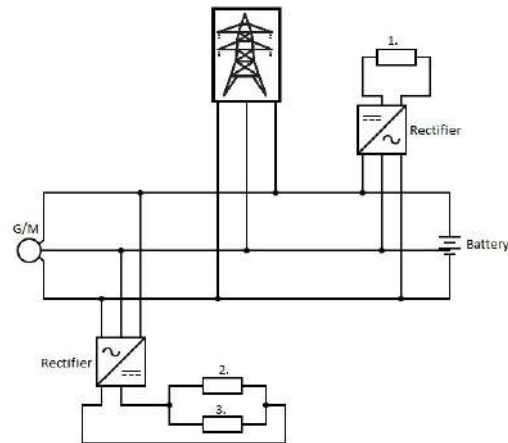


Figure 11.3: Circuit diagram of the electrical system

Most of the devices used by the subsystems work with DC current, for this reason a rectifier will be installed³ ⁴. This rectifier will rectify the 3-phase AC to DC to provide electricity to the landing tower, the cable cart charger and the guiding cable tensioning system. Since these devices have a lower functioning voltage, each electric component will have a buck converter⁵. Since it is difficult to electronically connect the offset container to the main container it is opted to have a small solar panel and battery which provide the small amount of energy needed to operate the cart docking system on the offset container side.

Lastly, the grid tower represents any loads that are needed to supply energy by the battery. Some examples can be agricultural machinery, households or electric vehicles.

11.4. Costs

Both the winch and the battery form part of the AWE system rather than the LLS, which is why their costs will not be included. Asking people who have worked on previous generations of the AWE, they stated that the estimated price for the Dromec specialised winch was around $\approx \text{€}100000$. The Greener contact centre gave a price for a 336 kWh battery of $\text{€}3000/\text{month}$. Considering a minimum autonomy of 6 months the final cost is $\text{€}18000$. The buck converters are estimated to cost around $\text{€}250$. Since 3 of these will be needed for those subsystems, a total of $\text{€}750$ will be needed⁶. Adding around 31 metres of internal wiring to interconnect everything,

²<https://www.dromecwinches.com/product/esp-5500-op-kitepower-kite-groundstation/>, accessed on 15-06-2023

³<https://symbols.radिकासoftware.com/229/single-line-symbols/78/power-supply-rectifier-ac-dc>, accessed 09-06-2023

⁴<https://www.arrow.com/en/research-and-events/articles/how-rectifiers-work-types-of-rectifier-s-and-their-uses>, accessed 09-06-2023

⁵<https://learnabout-electronics.org/PSU/psu31.php>, accessed 09-06-2023

⁶<https://www.dwe-oss.eu/product/400v-to-24v-dc-dc-converter-400w/>, accessed on 09-06-2023

a total of around €950 will cost the final electrical system of the LLS⁷. The specific amount of wiring will have to be quantified by the electricians in charge of setting up the device. The cost is summarised in Table 11.5.

Table 11.5: Estimate of the electrical subsystem cost.

Part	Cost [EUR]
buck converter	750
wiring	950
TOTAL	1700

11.5. Verification & Validation

To conduct the verification of this subsystem, a compliance matrix will be included, illustrated in Table 11.6. Those requirements that have been highlighted express that the requirement has been fulfilled.

Table 11.6: Compliance matrix electrical subsystem

Requirement ID	Requirement	Compliance	Shown In
LLS-ELEC-BATT-01	The battery shall have a capacity of at least 300 kWh	YES	Table 11.3
LLS-ELEC-BATT-02	The battery shall function at temperatures between -15°C to 40°C	YES	Table 11.3
LLS-ELEC-BATT-03	The battery shall function as an energy supply regulator for the microgrid	YES	Section 11.3
LLS-ELEC-WNCH-01	The winch shall have minimum reel-in speed of 12 m/s	YES	Table 11.4
LLS-ELEC-WNCH-02	The motor shall have a minimum rated power of 100 kW	YES	Table 11.4

All the components used will be off-the-shelf and developed by a third-party company. In the case of the battery, Greener Power Solutions B.V.⁸ ensures that their models have been tested and will perform as expected. Dromec B.V. specifically designed the winch for Kitepower, which is not being produced in series yet. Because this product is still in an early or prototype phase it is expected that it is not as reliable as is if it were mass-produced, and had received all the necessary testing and certification. When choosing the cable, the team will get in contact with multiple companies to see which one complies with the performance requirements and safety regulations.

11.6. RAMS Characteristics

The RAMS of the electrical subsystem will be assessed below. This is an important part since from other sectors electronics are prone to fail.

11.6.1. Reliability

As stated in Section 11.5 the reliability of the system will depend on the companies from which the components are acquired. It is expected from these companies that their products will meet the performance promised and comply with all the regulations necessary. Though, when looking at the reliability of the electrical subsystem of a wind turbine you can expect an annual failure

⁷<https://www.amazon.com/Welding-Battery-Flexible-Inverter-WindyNation/dp/B00Z8XF6QM>, accessed on 09-06-2023

⁸<https://www.greener.nl/nl/>, accessed 21-06-2023

rate of 0.4%^[32] which is, due to the similarity of the system, comparable to that of the AWE system.

11.6.2. Availability

The electrical system may be one of the most crucial subsystems. It is in charge of harnessing the energy from the wind, transmitting it to the battery and storing it for later use by the subsystems to perform the different phases. If one of these three main components were to fail the LLS system would not function and could not carry out the customer's needs.

11.6.3. Maintainability

This system is relatively easy to access and maintain. It can be shut down whenever necessary and it isn't necessary to completely dismantle the entire system to change a specific part. Unfortunately, most electric/electronic devices are challenging to repair⁹. Consequently, it is expected that when there is a failure of any electric component it will be necessary to replace the part. Maintainability can also be improved with a health monitoring system installed in the most crucial components communicating with remote operators.

11.6.4. Safety

According to the International Electrotechnical Commission, the winch and battery are low-voltage systems since their rated voltage is below 1000 V¹⁰. A series of precautionary measures will be implemented to ensure that maintenance personnel, wildlife or people in the vicinity are not at risk of electrocution. Some other risks that may compromise safety are water leakage, exposed cabling and mechanical failure of the winch. If a short circuit is detected by the monitoring system an automatic shut-down procedure will engage.

11.7. Sustainability

The 3-phase cables used by the electrical system for power transmission between the ground station and the battery use a total of around 122 kg of copper, resulting in roughly 477 kg_{CO₂e}. The battery has a capacity of 336 kWh, which at an emissions intensity of 75.5 kg_{CO₂e}/kWh as per Section 19.2, yields 25 200 kg_{CO₂e}. The generator weights 5500 kg which, assuming a copper content of 15%, implies about 4675 kg of steel and 825 kg of copper, resulting in about 12 100 kg_{CO₂e} at an emissions intensity of 1.9 kg_{CO₂e}/kg_{steel} and 0.5 kg_{CO₂e}/kg_{Al} respectively, per Section 19.2. This yields an energy payback period for the electrical system of approximately 1445 h, or about 60 days, with a capacity factor of 0.5 on a rated power of 100 kW and a grid carbon intensity of 523 g_{CO₂e}/kWh as per Section 19.1.

11.8. Recommendations

It is clear how this subsystem is vital for the proper functioning of the Landing, Launching and Storage (LLS) system. This electrical system was specifically designed for the 100 kW system, but customers may want more powerful systems. If this were the case a redesign of the electrical components would have to be done. If more power is needed a higher power rated motor-generator would be installed, if more energy has to be supplied a battery with more capacity can be placed and the cable connecting these systems would have to be recalculated depending on the loads.

To do more accurate estimations on the sizing of parameters for the different components it is necessary to know the required energy from the subsystems, how much is necessary to supply to the grid and also the wind condition of the site to predict the energy created.

⁹<https://securis.com/news/is-it-better-to-repair-or-replace-devices/>, accessed on 09-06-2023

¹⁰<https://www.electricityforum.com/what-is-considered-high-voltage>, accessed on 09-06-2023

In the present chapter, the ground station is explained. Starting with its functional analysis in Section 12.1, then the ground station's requirements in Section 12.2, its design in Section 12.3, costs in Section 12.4, V&V in Section 12.5, RAMS in Section 12.6, sustainability in Section 12.7 and recommendations in Section 12.8.

The containers making up the ground station form a large part of the system, they function as an anchor for all other subsystems and thus need to be sized to resist high loads. The main container is a standard 20ft container, these are 20ft in length, 8ft in width and 8ft 6" in height, which corresponds to 6.06 m by 2.44 m by 2.59 m. The current ground station, houses the winch and generator (with batteries in early versions), the tether guiding system and has space for several spare kites (estimated to be 5). In the new configuration, however, the main container needs to interface with the tower, the guiding cable and the cable cart while also providing storage space for the transport of the system. The offset container is a standard 10ft container. Its function is to be an anchor point for the guiding cable and provide a storage area for the system during transport.

12.1. Functional Analysis

The functions listed in Table 12.1 are obtained from the functional breakdown diagram from Chapter 3.

Table 12.1: Functions main container subsystem

Function ID	Function
FUN.2.3.1	Install guiding cable
FUN.2.3.4	Install landing tower with RSS
FUN.5.1.1.4	Unlock cable cart from the main container
FUN.5.1.1.5	Lock cable cart to offset container
FUN.5.1.1.6	Charge the cable cart
FUN.5.4.2.4	Lock cable cart at main container
FUN.5.4.2.5	Unlock cable cart from offset container
FUN.10.4.1	Provide storage for the AWE system

12.2. Requirements Analysis

The ground station subsystem needs to be designed to meet the requirements which flow down from the functions defined in Section 12.1, the requirements stated in Chapter 4, and the risks stated in Appendix A. These requirements are stated in Table 12.2.

These requirements are the driving factors for the design of the ground station.

Table 12.2: Requirements ground station subsystem

Requirement ID	Requirement	Rationale	Flowdown
LLS-GS-STRUCT-01	The guiding cable attachment point to the main container shall be able to support a tension force of 150 kN without permanent deformation.	The guiding cable breaking piece fails at a load of 150 kN	LLS-GEN-STRUCT-02, FUN.2.3.1

LLS-GS-STRUCT-02	The tower attachment points shall be able to support loads of the tower as listed in Table 7.3 without permanently deforming.	The forces of the landing tower should not destroy the main container.	LLS-GEN-STRUCT-02, FUN.2.3.4
LLS-GS-STORE-01	The main container shall function as a storage area for the LLS system during transport	The system must be stored for transport inside a single 20ft container	FUN.10.4.1, STK-OEM-11
LLS-GS-STRUCT-03	The cable cart to main container locking mechanism shall be able to handle a load of 100 kN .	The cable cart should be securely locked to the main container during operation.	FUN.5.1.1.4, FUN.5.4.2.4
LLS-GS-STORE-02	Any moisture- or water sensitive components shall be raised above the container floor.	A water leak in the system could lead to (premature) failure of the complete system.	RSK-TCH-GS-08
LLS-GS-ELEC-01	The main container shall be able to make an electrical connection with the cable cart.	The battery of the cable cart needs to be charged.	FUN.5.1.1.6
LLS-GS-STRUCT-04	The cable cart to offset container locking mechanism shall be able to handle a load of 100 kN .	The cable cart should be securely locked to the offset container during winching.	FUN.5.1.1.5, FUN.5.4.2.5
LLS-GS-STRUCT-05	The guiding cable attachment point to the offset container shall be able to support a tension force of 150 kN without permanent deformation.	The guiding cable breaking piece fails at a load of 150 kN	LLS-GEN-STRUCT-02, FUN.2.3.1
LLS-GS-STRUCT-06	The offset container shall not deform plastically due to the loads of the winch assembly.	The forces by the winching assembly should not cause the main container to fail.	LLS-GEN-STRUCT-02

12.3. Design

The design of the ground station subsystem mainly concerns the main and offset containers, as well as the interface with other subsystems, mainly the tower, guide cables and cable cart.

12.3.1. Main Container

The 20ft container shall be a modified version of a standard container. On the side without the doors, an opening will be present for the guiding cables and on the top, a slot will be present to allow the cable cart to move uninterrupted from the anchoring to the ground station while tethered to the flying kite. The top will have a circular cutout to allow the rotation of the tower.

An internal structure will compensate for the reduced structural integrity due to the cutouts and provide mounting points for the winch, anchoring, tower and guiding cable (LLS-GS-STRUCT-01, LLS-GS-STRUCT-02).

12.3.2. Offset Container

For the offset container, a 10ft container will be used. This is in addition to the equally sized container that houses the battery. This container is sized such that the three containers making up the system utilise the same space a single 40ft container would utilise, which is standard for shipping containers.

This 10ft container is fitted with mounting points for the guiding cable, anchoring, and a locking mechanism for the cable cart (LLS-GS-STRUCT-04, LLS-GS-STRUCT-05). Since no holes are made in this container, no additional reinforcement is needed. The empty space inside the container can be used for storing parts of the AWE system during transport.

12.3.3. Interface of guiding cable with main ground station

The heavily loaded guiding cables will require a sturdy attachment point to the container. Any forces on the guiding cables will be transmitted to the container. These cables can not go all the way to the back of the container, since there must be room for the tower to rotate around the cable ending point. Instead, they will be connected to a supporting structure mounted to the top of the container. This will require an additional supporting structure, which is connected to the rest of the container and anchored in a way that the loads of the cable are transferred into the ground. The guiding cable is designed to fail at a load of 150 kN, obtained from Figure 8.3.2. The attachment point thus needs to be sized to resist the same loads and provide a load path to the anchors (LLS-GS-STRUCT-01).

12.3.4. Interface with cable cart

During operation, the cable cart moves to the end of the guiding cable where it will dock to attachment points. The attachment points on the main container both lock the cart in place and provides an electrical connection to charge the battery onboard the cart, while the attachment point on the offset container only locks the cart in place. To interface with the cart, a metal pin is extended by a solenoid actuator that goes through the coupling plate of the cart, locking it in place (LLS-GS-STRUCT-03, LLS-GS-STRUCT-04). Electrical contact is made by spring-loaded pins that touch contacts on the cable cart (LLS-GS-ELEC-01). The dimensions of the cart are obtained from Table 9.6 and the width of the cable cart is 0.70 m. To allow for easy docking with the main container, a margin on each side of 0.05 m is included, giving a required width of the slot of 0.80 m. Flanges that function like a funnel compensate for any misalignment and allow the cart to slide into the slot reliably. The spacing of the cables is 538 mm.

12.3.5. Interface with tower

On the top side of the container, an opening is made from where the tower will stick out, so the kite may land on it. The dimensions of the lower section (Section 3 in Figure 7.1) of the tower are given in Table 7.5 and need to be taken into account when sizing the hole in the top of the container.

The tower, as stated in Chapter 7, is attached to a slewing bearing to allow rotation. This bearing will be securely attached to the container. The bearing will be positioned on the bottom of the container right behind the winch assembly, directly underneath the end of the guiding cable such that the tower can rotate around the parked cable cart. The mounting points for this bearing need to bear the loads of the tower, specified in Table 7.3. The tower can rotate 314° before it collides with the frame.

12.3.6. Interface with winch

The mounting points for the winch need to resist the heavy loads that the kite exerts on the winch. In Table 11.3, the properties and dimensions of the winch are given.

The maximal loading on the winch is 50 kN, given by [14]. This load acts on the spooling mechanism since this is the point where the tether is redirected. Assuming the spooling mechanism is at a height of 1 m, a maximum moment of 50 kN m can occur.

Considering the tether can leave the drum at an angle, a possible moment depending on the arm needs to be designed for in addition to the forces.

12.3.7. Internal Frame

The internal frame is the structure implementing the aforementioned interfaces. The goal of this section is to show a possible implementation of such a frame to demonstrate feasibility, however, it is not the goal to provide a final, detailed design. For this reason and due to a lack of resources, the beams making up the frame have not been sized. Instead, the mock-up assumes square steel tubing with sides of 5 cm and a wall thickness of 5 mm.

In addition to implementing the interactions, the frame must also allow for moisture-sensitive components, such as the capacitor bank, to be elevated from the floor (LLS-GS-STORE-02). This is achieved by creating low shelves on which to mount these components.

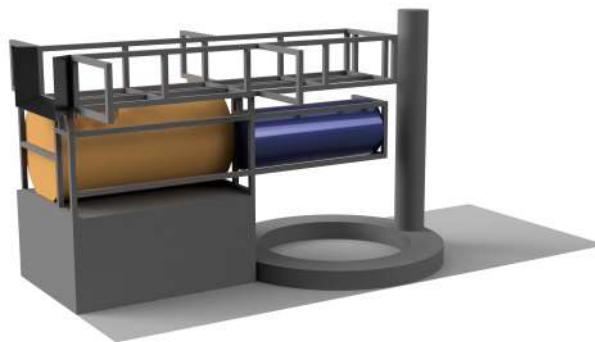


Figure 12.1: Mock-up of the main container internal layout

For scale, the system is placed on a bottom plate with the same size as a 20ft container. The yellow and blue components, respectively representing the winch and spooling mechanism, and EM, make up the winching assembly. These are attached to a frame which also functions as the interface with the cable cart and guiding cable (the channel on top). This frame is attached to the top of the main container.

The circular bearing with the bottom section of the tower gets directly attached to the structural members making up the bottom of the container. Below the winching assembly, there is room for capacitors for short-term energy storage, this is the ideal place since it is next to the EM.

The CAD model gives a total frame mass of approximately 100 kg. This mass will be used for further analysis, despite being obtained from a mock-up of the ground station.

12.3.8. Storage space

The remaining empty space of the main container is dedicated to storing the LLS system during transport, as required by LLS-GS-STORE-01. For this, a distinction needs to be made between

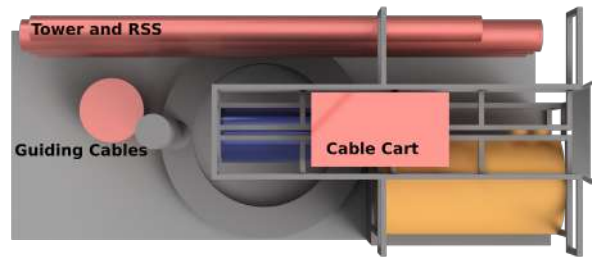


Figure 12.2: Storage of systems in the main container

equipment belonging to the AWE system and that belonging to the LLS system. The equipment that is considered part of the LLS is listed as follows:

- Tower
- Cable Cart
- Guiding Cable
- RSS

Items such as the kites, anchors, and battery are not considered part of the LLS since they are a necessary part of any AWE system. These items can thus be excluded from requirement LLS-GS-STORE-01 and will be stored in the 10ft offset container.

The tower consists of three sections, as seen in Table 7.5. The third section remains attached to the bearing, the first section fits lengthwise in the 20ft container, while the second section needs to be further disassembled into three sections of 5.33 m each. These four sections are then stored vertically in a rack on the free wall of the main container. The cable cart simply gets removed from the guiding cable and stored in the same location where it docks at the main container during operation.

The guiding cables are connected end to end and are rolled on a spool. This is then stored in the main container behind the tower base. Assuming a spool with a diameter of 40 cm and height of 50 cm, the Dyneema[®] guiding cables with a total length of $2 \cdot 100 = 200m$ and a diameter of 14 mm needs to have less than 3 layers of cable on the drum to contain the entire length. The final dimensions of the spool with cable would be $0.40 + 2 \cdot (0.014 \cdot 3) = 0.484 \approx 0.50m$.

All these parts are secured inside the container with ratchet straps to prevent things from moving around inside the container during transportation.

12.4. Costs

The cost of the ground station is that of the internal frame needed to integrate all other subsystems. Other parts of the ground station, such as the 20ft container itself, are considered part of the basic AWE system and thus are not considered for the cost of the ground station section of the LLS.

The frame has a mass of 100 kg, obtained from Section 12.3.7, and is made out of steel. Assuming steel costs 2.5 USD¹ or €2.31 per kg, the price of the material alone would be €231. A factor of 1.5 is used to account for labour costs such as welding and cutting, giving a final cost estimate of approximately €350.

¹[https://blog.thepipingmart.com/metals/steel-vs-stainless-steel-prices-whats-the-difference/#:~:text=The%20cost%20of%20stainless%20steel,%242%2C500%20per%20ton%20or%20more!](https://blog.thepipingmart.com/metals/steel-vs-stainless-steel-prices-whats-the-difference/#:~:text=The%20cost%20of%20stainless%20steel,%242%2C500%20per%20ton%20or%20more!,), accessed on 19-06-2023

12.5. Verification and Validation

A compliance matrix of the ground station subsystem is shown in Table 12.3. All requirements about loading are still uncertain since the ground station has not been sized. These uncertainties are depicted by yellow cells with 'TBD' in the compliance matrix.

Table 12.3: Compliance matrix ground station subsystem

Requirement ID	Requirement	Compliance	Shown In
LLS-GS-STRUCT-01	The guiding cable attachment point to the main container shall be able to support a tension force of 150 kN(Figure 8.3.2) without permanent deformation.	TBD	Section 12.3.3
LLS-GS-STRUCT-02	The tower attachment points shall be able to support loads of the tower as listed in Table 7.3 without permanently deforming.	TBD	Table 7.3
LLS-GS-STORE-01	The main container shall function as storage area for the LLS system during transport	YES	Section 12.3.8
LLS-GS-STRUCT-03	The cable cart to the main container locking mechanism shall be able to handle a load of 100 kN.	TBD	Section 12.3.4
LLS-GS-STORE-02	Any moisture- or water sensitive components shall be raised above the container floor.	YES	Section 12.3.7
LLS-GS-ELEC-01	The main container shall be able to make an electrical connection with the cable cart.	YES	Section 12.3.4
LLS-GS-STRUCT-04	The cable cart to offset container locking mechanism shall be able to handle a load of 100 kN.	TBD	Section 12.3.4
LLS-GS-STRUCT-05	The guiding cable attachment point to the offset container shall be able to support a tension force of 150 kN (Figure 8.3.2) without permanent deformation.	TBD	Section 12.3.3
LLS-GS-STRUCT-06	The main container shall not deform plastically due to loads of the winch assembly.	TBD	Section 12.3.6

12.6. RAMS Characteristics

Since all critical systems are connected or directly located on the ground station, it is important to discuss the RAMS of it.

12.6.1. Reliability

The RAMS of the ground station is analysed. For this analysis, the ground station is only considered to be the internal frame and not the subsystems that are integrated inside of it. As the frame is supposed to be stationary, the wear on it comes for a large part from the environment. Especially in coastal regions, rust forms a hazard to the integrity of this subsystem and its reliability. Just like with the other steel parts of the system, a good layer of protective paint must be applied in order to prevent this.

12.6.2. Availability

The system availability should comply with STK-OEM-01 and therefore be available for six months on end.

12.6.3. Maintainability

The internal frame is difficult to maintain during operation because of the load that it constantly carries. It should be made such that to inspect the system for corrosion or other wear that might weaken the system, the frame structure is accessible to the maintenance crew. However, during the six months of operation, this should not happen, and for this reason, no maintenance is expected during the operation. In fact, the stationery of it combined with its robustness, should warrant an uninterrupted service duration of a lifetime.

12.6.4. Safety

As long as the internal frame is properly sized for its loading there is no safety risk, either for humans, the environment, or property. If there are no sharp edges or other hazards to the crew that has to be around the system, it is deemed safe.

12.7. Sustainability

The welded steel frame weighs about 100 kg, and a 20 feet container weighs about 2300 kg. This adds to 2400 kg of steel which, at $1.9 \text{ kg}_{\text{CO}_2\text{e}}/\text{kg}_{\text{steel}}$ as per Section 19.2, amounts to $4560 \text{ kg}_{\text{CO}_2\text{e}}$.

The payback time for this amount of emissions, taking a capacity factor of 0.5 on a rated power of 100 kW with a grid carbon intensity of $523 \text{ g}_{\text{CO}_2\text{e}}/\text{kWh}$ as per Section 19.1, comes to about 174 hours.

12.8. Recommendation

Due to limited time and resources, only an initial, high-level design of the ground station was made which still leaves room for many improvements.

There are a lot of uncertainties in the ground station verification and validation, Section 12.5. To get more certainty the ground station needs to be properly sized and modelled. For this, computer tools such as FEM analysis provided in CAD packages can be used. This will help reduce the uncertainties in the design. Furthermore, the use of aluminium instead of steel could reduce the weight of the frame.

Another point where improvements can be made is in the storage of the system for transport. The storage is done in a way that complies with the requirement LLS-GS-04, but this is not the most sensible solution. If one were to disregard this requirement, parts of the LLS and AWE systems can be stored in both the 20ft and 10ft container, instead of storing all parts belonging to the LLS system exclusively in the 20ft.

This chapter discusses the kite and KCU subsystem and how the LLS system affects them. Firstly, the functions of the subsystem are provided in Section 13.1. Secondly, the requirements flowing down from the functions and risks are presented in Section 13.2. Thirdly, the existing design and changes to this design are discussed in Section 13.3. Fourthly, the added cost is listed in Section 13.4. Fifthly, the verification and validation is discussed in Section 13.5. Sixth, The RAMS of the subsystem is discussed in Section 13.6. Seventh, the sustainability is covered in Section 13.7 and lastly, recommendations are made for future designs in Section 13.8.

13.1. Functional Analysis

The functions of the Kite & KCU subsystem are either taken from the functional breakdown structure in Chapter 3 or are sub-functions of those. They are shown in Table 13.1 with the relative identifier (FUN).

Table 13.1: Functions of the kite and KCU including an identifier and the origin in from the functional breakdown

Function ID	Function
FUN.4.2.2.1	KCU controls the tension in the bridles.
FUN.4.2.3	Inflate the kite
FUN.5.1.2	Retract LE tether guide to KCU
FUN.5.3.1	Turn to face away from the wind
FUN.5.3.2	Glide in the wind direction
FUN.5.3.3	Turn to face into the wind
FUN.5.4.1	Park the kite
FUN.5.5.2	Retract LE tether guide to KCU
FUN.5.5.3	Park the kite
FUN.6.1	Perform pumping cycle
FUN.6.2	Perform reversed pumping
FUN.6.3	Park the kite in high wind conditions
FUN.7.1.1	Fly kite to edge of power zone
FUN.7.1.3	Fly kite to zenith
FUN.7.2.2	Point kite in tower direction
FUN.7.3.1	Release the LE tether guide
FUN.7.3.4.2	Dock kite to RSS
FUN.8.1.3.1	KCU controls the tension in the bridles.
FUN.8.1.1	Deflate kite

13.2. Requirements Analysis

The functions from Section 13.1 and the risk analysis in Appendix A impose restrictions on the system that we call requirements. Together with the requirements that have been developed previously, they are compiled below in Table 13.2. Each requirement has an identifier including Landing, Launching and Storage (LLS), Kite (KT), Leading Edge Tether (LET), Kite Control Unit (KCU) and Bridles (BRDL).

Table 13.2: Requirements of the kite and KCU including an identifier and the origin of the requirement

Requirement ID	Requirement	Rationale	Flowdown
LLS-KT-KT-01	The kite shall be compatible with the RSS system	To be able to store the kite, the interface with the RSS system should work	FUN.3.4.2
LLS-KT-KT-02	The kite shall be guided and attached to the landing tower during landing	To be able to land the kite and keep it on the landing tower of 16.5 m (Chapter 7)	FUN.3.4.2
LLS-KT-LET-01	The LET shall not break due to tensioning	The LET must be strong enough to not break to perform its purpose	LLS-GEN-STRUC-02
LLS-KT-LET-02	The LET shall not entangle with the bridles	Entanglement is a dangerous situation due to control loss	FUN.4.2.2.1/ FUN.5.3.1/ FUN.5.4.1/ FUN.5.5.3/ FUN.6.1/ FUN.6.2/ FUN.6.3/ FUN.7.1.1/ FUN.7.1.3/ FUN.7.2.2/ FUN.8.1.3.1
LLS-KT-KCU-01	The kite shall be controllable at all times	The kite must be controllable to prevent dangerous situations	RSK-TCH-KT-04/ FUN.4.2.2.1/ FUN.5.3.1/ FUN.5.4.1/ FUN.5.5.3/ FUN.6.1/ FUN.6.2/ FUN.6.3/ FUN.7.1.1/ FUN.7.1.3/ FUN.7.2.2/ FUN.8.1.3.1
LLS-KT-BRDL-01	The bridles shall not entangle during operations	Entanglement is a dangerous situation due to control loss	RSK-TCH-KT-01/LLS-KT-KT-01
LLS-KT-BRDL-02	The bridle length shall be compatible with the landing tower height	Compatibility of the bridles with the tower is important for the controllability of the kite since the two interact a lot with each other	LLS-KT-KT-02

13.3. Design

From the identified functions and requirements in Section 13.1 and Section 13.2 a design of the kite can be made. In this design, the existing kite subsystem will be altered to comply with the added requirements.

13.3.1. Existing kite

The existing kite is presented in Figure 13.1[33]. This design consists of the kite itself, the bridles and the KCU designed by Kitepower.

The power of the system is generated with the lift of the kite. The kite is made of nylon fabric in between an inflatable leading edge and longitudinal struts. Additionally, these struts are reinforced with solid battens. On the leading edge, there are air pumps located which regulate the pressure in the inflated parts of the kite.

The kite has multiple attachment points at the leading edge and the trailing edge for the bridles.

Two bridles at the tips of the kite are steering lines connected to a winch in the KCU. These bridles also control the power of the kite with a depowering winch. Another component is the safety line. This is not tensioned, but when a weak link is broken between the tether and the KCU, the kite will only be attached to the main tether by this safety line. This weak link is a pin which can be pulled out if necessary depowering the kite automatically. The distance from the kite to the leading edge is 15 meters. Additionally, there are pumps connected to the leading edge which are there to maintain the correct pressure in the inflatable parts of the kite.

The KCU is, as described, responsible for steering and depowering the kite. In this component, there is a little wind turbine of 200 W which charges a battery of 12.6 Ah to power the device. The energy is mainly used by two 180 W Maxon motors¹ with both a 3-stage gearbox² to drive the steering and depowering tapes according to Kitepower. Also, KCU communicates with the winch through a tension-measuring device and a radio link. The radio link is suitable for communicating up to 2 km away from the ground station³.

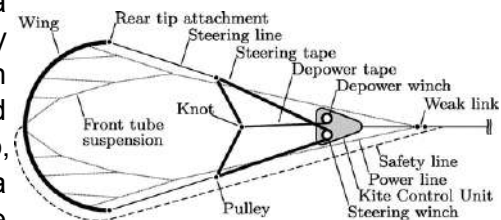


Figure 13.1: Existing kite layout[33]

13.3.2. Leading Edge Tether (LET) design

The kite will be landed by pulling on an additional line to a point on the landing tower. The choice of a LET is made instead of a trailing edge tether since pulling on the trailing edge will pose a large risk of generating undesired power due to the tension in the tether. The maximum load on the tower is 2 kN. This sets a constraint on the LET. For this load, a Dyneema[®] cable of 0.92 mm could be enough. Though for safety and convenience (buying off-the-shelf components) a diameter of 2.5 mm will be used.

13.3.3. LET retraction

An issue of the LET that needs to be solved is the entanglement with the bridles when the kite turns. The found solution is retracting the LET to the KCU before any manoeuvre will be made as described in Chapter 6. The responsible mechanism will be a line from the KCU to the LET which goes through a pulley which is presented in Figure 13.2 and is called the Leading Edge Retraction System (LETRS). The LETRS imposes the need for an additional third 180 W motor inside the KCU which pulls on the connection line with the pulley at the end through which the LET passes (see Figure 13.2). This motor must also have a drum with a 15 m cable capacity following from the tower design in Chapter 7. The retraction is very similar to the retraction of the depowering tape. Therefore the same type of motor can be applied. This additional winch will be added to the lower part of the KCU as shown in Figure 13.2. It is below the existing KCU since it is preferred to shift the centre of gravity down and not up.

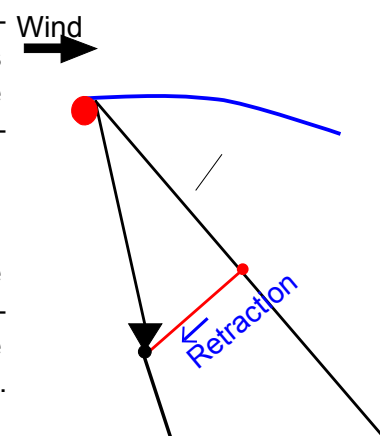


Figure 13.2: Leading edge-bridles interaction problem solution

³https://www.maxongroup.com/maxon/view/product/motor/ecmotor/EC-i/516068?etcc_cu=onsite&etcc_med=Header%20Suche&etcc_cmp=mit%20Ergebnis&etcc_ctv=Layer&query=180%20W, accessed on 19-06-2023.

³https://www.maxongroup.com/maxon/view/product/gear/planetary/GPX/GPX14/GPX14-3-Stufig-LN/GPX14LNKLSL0231CPLW?etcc_cu=onsite&etcc_med=Header%20Suche&etcc_cmp=mit%20Ergebnis&etcc_ctv=Layer&query=3%20stage, accessed on 19-06-2023.

³<https://thekitepower.com/product/>, accessed on 12-06-2023.

The connection line between the tether and the KCU will be little loaded since the LET has very low tension when the kite is operating, and the connection line is untensioned when the LET is tensioned. Therefore, an arbitrary diameter for the connection can be taken. Looking at Dyneema® distributors a diameter of 2.5 mm is very common which is therefore selected. With a failure stress of 3 GPa of Dyneema®⁴ this diameter still allows for a maximal load of 14.7 kN which is significant.

13.3.4. Kite-Landing Tower Attachment

Merely reeling in the LET does not lock the kite properly on the tower. Therefore clamps are designed in Chapter 7 and a ring-pin lock will be implemented where the ring must be attached to the kite.

Their ring is just behind the leading edge on the same line as is followed by the LET. This must ensure the exact alignment of the ring with the pin lock. The pin lock is a solenoid pin actuator and is located on the landing tower.

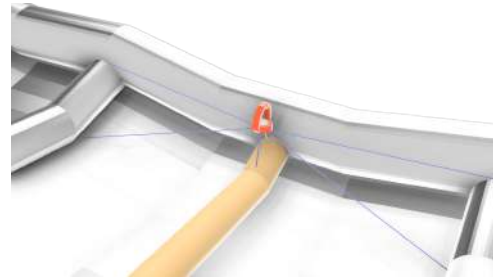


Figure 13.3: Load eye setup below the kite

The subsystem loading is constrained by the maximal loading of the landing tower which is equal to 2 kN. To implement some safety a load eye of 0.5 tons lifting weight⁵ will be used and will be attached to the leading edge, side struts and an additional mid-strut as shown in Figure 13.3 with bridles. The mid-strut is a new component and will only run from the LE to the quarter chord to save weight and aerodynamic impact. To mitigate the load singularity at the end of the mid-strut, the strut will be tapered towards the end to make it less stiff.

13.3.5. RSS Interface

When landed on the tower, RSK-TCH-KT-01 requires the bridles to be under tension when storing, so they will not get tangled. This requires the KCU to be able to reel in all bridles that are connected to it as they hang under some amount of tension. Since the steering bridles are connected to the same winch, as seen in Figure 13.1, the other winches are first reeled out until they are hanging under tension, then this winch is adjusted such that both steering bridles carry about the same amount of tension. Then the depower tape is adjusted such that it also hangs under some amount of tension, while at the same time keeping tension in the other bridles. The rolling has been tested multiple times with tensioned bridles and the results were positive since no entanglement was observed which makes the approach suitable for storage.

The kite will be stored in the open air. This causes the kite to be exposed to UV radiation during storage. This will add up to the degradation of the kite material and is, therefore, a loss of the system. To mitigate this problem the kite will be partially covered in a UV protection coating for 18 m² which consists of 9 m² for the exposed parts when the kite is stored and 9 m² to make the kite symmetrically loaded. Taking an area density of 0.224 kg/m² ⁶. Therefore a mass of 4 kg will be added to the kite.

13.3.6. Impact of Kite and KCU Design

In the new kite/KCU design a ring on the leading edge, a leading edge tether, a UV-resistant coating and an extra winch in the KCU are added compared to the existing design as explained

⁴<https://fibrxl.com/wp-content/uploads/2020/07/FibrXL-PDS-performance-0720-DEF-Dyneema.pdf>, accessed on 12-06-2023

⁵<https://www.mennens.nl/en/products/chains-components/lifting-eyes/female-swivel-eye-bolt-codipro-fe-seb-up-p322170?categoryId=491934#>, accessed on 14-05-2023

⁶<https://www.krylon.com/en/products/clear-coatings/uv-resistant-clear-coating#accordion-1e34218980-item-3c854fa17f>, accessed on 15-06-2023

in Section 13.3.1. It is important to analyse how the performance of the kite-KCU subsystem will change.

The ring at the leading edge is located just behind the leading edge. This ring is aligned with the chord of the kite which makes it quite aerodynamic. It will still cause a bit of separation, though the leading edge does already cause much separation. Therefore it is judged that the ring will not have a significant effect on the aerodynamic performance of the kite. In terms of weight, there is approximately 1.8 kg added⁷. Compared to the kite-KCU mass this is an increase of 1.06%. Noting that potential energy scales linearly with mass, the required energy for launching to operational height will also increase by 1.06%. In terms of performance, the kite is about energy production. Energy scales linearly with the potential energy. Therefore, an increase of 1.06% mass requires 1.06% of energy to compensate.

The addition of the leading edge tether causes additional drag on the kite. This is due to the additional frontal surface area. According to [13] the drag of a tether is calculated with Equation 13.1. In this equation ρ is the air density, d_t is the tether diameter, l is the tether length, C_τ is the tangential drag coefficient of the tether and $v_{a,\tau}$ is the tangential apparent velocity of the kite.

$$F_D^t = \frac{1}{8} \rho d_t l C_\tau v_{a,\tau} \quad (13.1)$$

For C_τ the drag coefficient of a cylinder was taken which is approximately 0.51[34]. This is 2D but since the tether is very long the 3D effects are negligible. The length is taken to be 500 m. Also, the average tangential apparent velocity is assumed to be 15 m s^{-1} which is derived from an optimal reeling factor of 0.14[13], a wind speed of 15 m s^{-1} , an elevation of 45° and using Equation 6.3. Combining this gives an additional drag of 9.9 N. The total apparent velocity equals 25 m s^{-1} . For this during operation ($C_D = 0.13$) the kite experiences a drag of 2986 N. The power equation scales with $1 + \left(\frac{L}{D}\right)^2$. Therefore the drag causes the performance to drop by 0.33%. The mass also has an effect on the launch of the kite like for the loading eye, but the tether is very lightweight which makes the effect negligible.

The UV-resistant coating adds 4 kg to the kite. Therefore, just as with the loading eye the launch performance is mostly affected by it. With the same reasoning, this leads to a launch performance drop of 2.35%.

The extra winch in the KCU adds 0.82 kg due to the motor. The gearbox does add around 0.02 kg and the most significant part is the drum with the line which is most probably around 10 kg by reasoning that it is the same cable capacity as in the Dromec Dynamic oil NP05 winch⁸. Though, the drum in the KCU only consists of the drum and can be lighter due to the lower load that will be applied. With the same reasoning as for the loading eye, the launch performance of the kite will drop by 6.38%. The aerodynamic aspect is minor due to the little surface area that has been added. In terms of power, there is an additional 180 W required. Though, the retraction will take place when the kite is on the tower when no or little steering and depowering are required. Therefore, the battery can stay as it is.

Combining all the changes as a whole should not produce excessive noise (requirement STK-PVS-01). This is already complied with in the existing kite design. The only part that can alter this is the addition of the LET and mid-strut. Though, since these are just minor changes to the design and are similar to parts that already exist, it is expected that the noise profile will not change.

⁷<https://www.msdirect.com/browse/tn/Material-Handling-Storage/Material-Lifting/Hoist-Rings/Pad-Eyes-Lifting-Eyes?navid=2105339>, accessed on 16-6-2023

⁸<https://www.dromecwinches.nl/product/dinamic-oil-np05/>, accessed on 19-06-2023

13.4. Cost

The addition of the tower attachment ring below the kite sum up to €10.2 for 15 meters of 2.5 mm Dyneema^{®9}, €20 for the load eye¹⁰ and €20 for the additional mid-strut (since it is just some material and stitches added). Further, the cost of the LET is purely cost for Dyneema[®] which is derived from footnote 9 and equals €250. Also, the coating cost €11 per m^2 ¹¹. Therefore, for a surface area of 18 m^2 a cost of €198 is applicable. Lastly, the addition of the LET retraction mechanism cost about €300 (motor and gearbox both €100 and the drum+line also €100). Therefore a total cost of €788

13.5. Verification & Validation

In Table 13.3 the requirements are restated and checked if they complied with the design performed in Section 13.3.

Table 13.3: Requirements of the kite and KCU including an identifier and the origin of the requirement

Requirement ID	Requirement	Compliance	Shown in
LLS-KT-KT-01	The kite shall be compatible with the RSS system	YES	Section 13.3.5
LLS-KT-KT-02	The kite shall be guided and attached to the landing tower during landing	YES	Section 13.3.2
LLS-KT-LET-01	The LET shall not break when it is tensioned	YES	Section 13.3.2
LLS-KT-LET-03	The LET shall not entangle with the bridles	YES	Section 13.3.3
LLS-KT-KCU-01	The kite shall be controllable at all times	YES	Section 13.3.1
LLS-KT-BRDL-01	The bridles shall not entangle during operations	YES	Section 13.3.5
LLS-KT-BRDL-02	The bridle length shall be compatible with the landing tower height	YES	Section 13.3.5

13.6. RAMS Characteristics

Since the kite is the subsystem that handles aerodynamic and control loads, its reliability and maintainability can be complex. Hereby the kite and KCU's RAMS are looked into.

13.6.1. Reliability

As the kite and KCU before their redesign are fully flight-proven, it can be taken that accessing their reliability lies mostly in the redesign and the interfaces with the LLS. To start with the bridles: the main concern is the Leading Edge Tether. As long as it is correctly retracted with the mechanism explained in Section 13.3.3, wear on it and the other bridles will be minimal. Should the retraction mechanism fail, or perform worse than expected, however, one or more bridles and/or the LET may fail prematurely. The bridles are redundant so catastrophic failure of the whole system is not expected to happen. This is also the case for LET; failure of this tether will lead to a landing that is not on the LLS system. In both cases, it will make it necessary for the crew to inspect the kite and perform maintenance before the end of the 6 months (CON-

⁹ <https://www.touw-staalkabel.nl/c-3214905/dyneema-lier-touw/>, accessed on 19-06-2023

¹⁰ <https://www.mscdirect.com/browse/tn/Material-Handling-Storage/Material-Lifting/Hoist-Rings/Pad-Eyes-Lifting-Eyes?navid=2105339>, accessed on 16-06-2023

¹¹ <https://www.techsil.co.uk/krylon-uv-resistant-gloss-clear-11oz>, accessed on 16-06-2023

LLS-GEN-01-04). It is important to state that entanglement is difficult to model and the handling of the LET by the KCU needs to be validated well.

For the KCU itself, it is changed by the addition of a winch, namely for the line that is attached to the LET. As the non-LLS model already houses two winches, it is concluded that adding a winch will make the system acceptably larger but not add much extra complexity. There is one thing that should be taken into account - each of the motors require 180W, and the turbine provides only 200 W. It also has a battery, so a higher than 200W peak load is possible as long it is not sustained. It is deemed feasible; this winch is only scheduled to operate just before launch and the battery will be powerful enough to power two winches at the same time.

13.6.2. Availability

Like in every other part of the LLS, the mean time between failures needs to be at least six months (CON-LLS-GEN-01-04, CON-LLS-GEN-01-13). Failure of the bridle lines can be due to roughly two things: the forces get too high and they fail naturally, which is also the case without the LLS, or the LET retraction system works less well than expected and extra friction of the lines causes failure. For the first failure mode, this has been flight tested and the probability is almost zero. A failure will not cause system downtime. However, the second failure mode is the most concerning one. If one bridle line gets damaged or snaps, the system can still stay airborne. The critical case is the snapping of the LET; as said before, this prevents the kite from landing on the LLS and will lead to downtime. Snapping of the line that is connected to the LET is not immediately critical on the other hand, as the kite will still be operable when this line is gone. There will be a risk of entanglement, however, but the kite will still be able to use the LLS.

To prevent this, the LET must be designed to deteriorate due to friction as little as possible, by covering it by a friction-lowering coating or mantle. It is also recommended that this tether is thicker than the bridles.

13.6.3. Maintainability

When maintenance needs to be done on the system, however, to minimise downtime, the system needs to be designed such that this is as easy as possible. Generally, systems should not be less accessible than necessary, and not require too many specialist tools to maintain them.

More specifically, in the case of the KCU, the integration of the third winch should be similar to the other two. The winch-type should be similar, including the motor type and motor controller. This way, spare parts will be already available and there is knowledge on how to replace them. Mechanics will require little extra instruction on how to do this type of maintenance.

Regarding the kite and the bridles, without the LLS it is assumed that crew knows how to replace bridles when they fail. Although the LET is new as well as the line that is attached to it, the maintainability will be similar and not more complex than other tethers and bridles.

13.6.4. Safety

The safety of a system is reliant on the lack of risks and hazards it poses to humans, property, and the environment. As for the first, the system will not operate near people. When the system is not in operating mode, and there need to be people close to the KCU, it should be landed and taken off the tower. A master switch should take power off the system before it is opened to minimise the risk of electric shock. No unnecessary sharp edges or objects should be included in the design. As for the kite, no work should be done on it when it is not taken off the tower as well. The enormity of it warrants careful handling in even light winds, as it might take off unexpectedly. When working on it, it should therefore stay deflated as much as possible.

During operation, there will be a no-go area around the flight regime of the kite in the form of a ground buffer zone of 450 meters, so the chances that anyone will be harmed by the kite or

any other part of the system are minimal.

Property damage is minimised by two things; the ground risk buffer, and redundancy in the kite design: if the main tether breaks, the kite will immediately be depowered and still be connected to the LET. In the improbable case that that breaks as well, the kite is still controllable up to a distance of 2 km. This scenario has been explored in Section 8.6.4. For more about this, the risks and hazards to the environment are mainly discussed in Chapter 19.

13.7. Sustainability

The tether and leading edge line are made out of Dyneema®. Both are 450 m long, but the tether has a 14 mm diameter while the leading edge line is 2.5 mm in diameter, corresponding to a mass of 49.5 kg and 1.6 kg of Dyneema® respectively. This yields about 77 kg_{CO₂e} at an emissions intensity of 1.5 kg_{CO₂e}/kg_{Dyn} as per Section 19.2. Further, the kite body itself is assumed to be made completely of Nylon and weights about 100 kg, which yields about 510 kg_{CO₂e} at an emissions intensity of 5.1 kg_{CO₂e}/kg_{Nylon} according to Section 19.2. Also, the KCU weighs 70 kg and, assuming it is 10% copper and 90% aluminium, contains about 7 kg of copper and 63 kg of aluminium. With the emissions from copper and aluminium being 3.9 kg_{CO₂e}/kg_{Cu} and 0.5 kg_{CO₂e}/kg_{Al} respectively, this results in a total of about 59 kg_{CO₂e}. The kite, thus, produces a total of 646 kg_{CO₂e}, implying an emissions payback period of about 25 h with a capacity factor of 0.5 on a rated power of 100 kW with a grid carbon intensity of 523 g_{CO₂e}/kWh as per Section 19.1.

13.8. Recommendations

The proposed kite design has some limitations which cannot be assessed in this report due to time constraints. Therefore, the recommendations for future detailed design of the kite will be discussed in this section.

First of all, the placement of the bridles that hold the attachment eye in place should be validated and possibly adjusted. The load on the bridles can be 2 kN. While it is very unlikely that the bridles will break, there is a considerable probability that the attachment of the bridles to the kite structure will fail.

Secondly, it should be investigated further what type of loading eye should be used. In Figure 13.3 a off the shelf eye is taken. To optimise the operation of the kite a different shape could be used. This might decrease the aerodynamic impact of the load eye and it could make putting the locking pin through the hole easier.

Thirdly, for landing it is desired to have an adjustable drag ratio by δ . This could decrease the $\frac{L}{D}$ which is beneficial for the glide slope. A glide ratio of 1 is already achieved by Skysails with a lift coefficient of 0.53 which translates to a descending angle of 80 degrees. The way to go is most probably a bleed air spoiler. Though, this is not implemented in the current design since it is not yet a fully validated concept.

Fourthly, the rolling of the kite on the RSS is only tested roughly for low wind conditions. Therefore it is recommended that more tests are performed with a more sophisticated prototype of the RSS in stronger winds.

Lastly, the aerodynamic impact of the attachment eye, coating and added KCU winch are difficult to assess. For this reason, a more practical assessment is required most probably involving a wind tunnel.

Communication and Data Handling

The Communication and Data Handling (CDH) of the LLS will be the framework of how every subsystem communicates with the relevant other subsystems. In Section 14.1, the functional flow diagram is used to derive the required data streams in the CDH. In Section 14.2, more detailed requirements on certain links are established. This chapter will touch upon communication of the different subsystems rather than the systems itself, or, in network-theory language, the links in the network rather than the nodes.

14.1. Data Streams

In this section, the necessary data streams in the LLS system are identified. To accomplish all functions related with communication present in Chapter 3, the following 9 data streams are needed:

- COMM.1 bidirectional communication between GCU and KCU
- COMM.2 bidirectional communication between GCU and off-site operator.
- COMM.3 communication from weather services to GCU .
- COMM.4 communication from on-site weather sensors to GCU .
- COMM.5 communication from GCU to cable cart
- COMM.6 communication from GCU to tower
- COMM.7 communication from GCU to RSS
- COMM.8 communication from health sensors to GCU
- COMM.9 communication from GCU to winch

The Ground Control Unit (GCU) is the brain of the LLS system, since it is responsible for controlling all actuators of the system and handling the in and outflow of data of the system. It collects the required weather data and instructions from the weather services and off-site operator and based on that decides what to do (COMM.2, COMM.3, COMM.4). The GCU then controls all actuators to be in the desired position (COMM.5, COMM.6, COMM.7, COMM.9) and continuously communicates with the KCU to control the flight plan (COMM.1). All data from the health monitoring system is logged at the ground station and communicated to the off-site operator is requested (COMM.2, COMM.8).

14.2. Requirements on Communications

Some of these data streams have more stringent requirements that they need to fulfil. These requirements are derived for each link based on top level requirements and risks.

Table 14.1: Command and Data Handling requirements

Requirement ID	Requirement	Rationale	Flowdown
LLS-CDH-KCU-01	COMM.1 shall have an operational range of at least 2 km.	Airborne system should be in communication with the ground system within the full operational range, as well as in case of tether rupture.	STK-PGO-02
LLS-CDH-KCU-02	COMM.1 shall be a redundant wireless link	System must be operable in case of main communication link loss	RSK-TCH-CDH-01

LLS-CDH-CRT-02	COMM.5 shall be a redundant data link between GCU and cart	A redundant link is needed in case the main link fails	RSK-TCH-CDH-02
LLS-CDH-ECC-01	COMM.2 shall be a redundant wireless communication link between GCU and an external command centre.	The system must be in wireless contact with the external command centre	STK-OEM-12, RSK-TCH-CDH-03

14.3. Design

Each data stream from Section 14.1 can now be worked out into detail, making sure to take the requirements from Section 14.2. Figure 14.1 shows the different communication stations and their links.

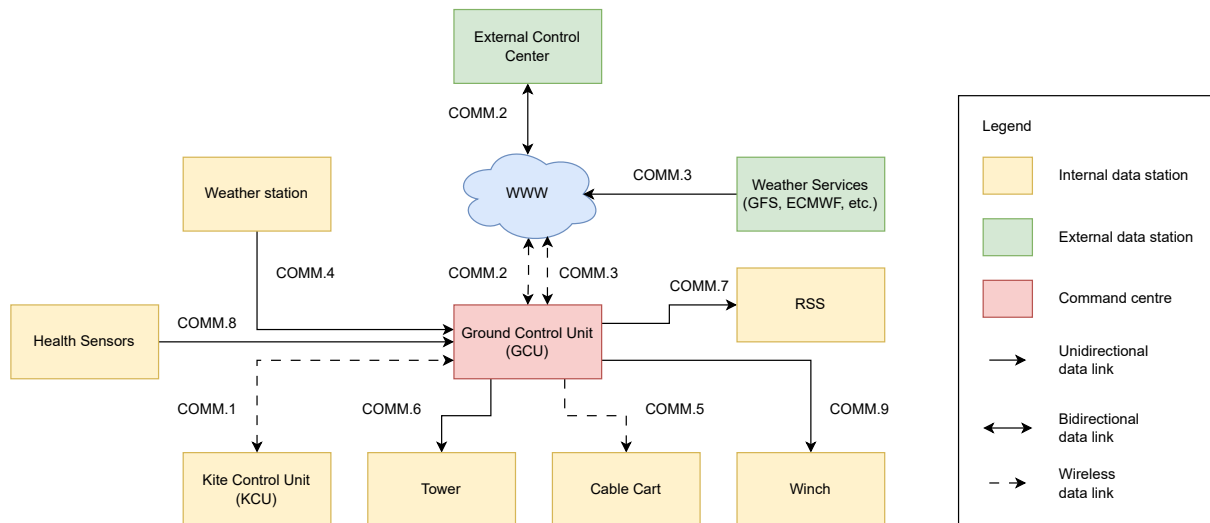


Figure 14.1: Diagram of the communications nodes and links

The data streams can be grouped together into communication buses. The communication to the parts on the ground station (COMM.6, COMM.7, COMM.8, COMM.9) is implemented on the same wired bus to reduce complexity and increase reliability. By utilising a protocol such as CAN-bus all actuators and sensors can communicate to the GCU over the same wired serial connection.

COMM.5, the connection with the cable cart, is a wireless connection to avoid additional cabling to the cable cart. LLS-CDH-CRT-02 states that this link must be redundant, to achieve this a 5GHz main link and a secondary 2.4GHz link for redundancy is used. This is a low-power link with a high-gain antenna, directed to the cable cart. With a refresh rate of 3Hz and a packet size of 100 bytes (position, timestamp, other metadata), the bitrate is expected to be around 2.3 kB/s. This bitrate is assumed to be similar to COMM.6, COMM.7 and COMM.9 due to the nature of the data.

COMM.1, the connection between the GCU and KCU, is a critical link of the LLS system. Communication will be ensured by a main 5GHz and secondary 2.4GHz link as to have a redundant link prescribed by LLS-CDH-KCU-02. These links need to function up to a distance of 2 km (LLS-CDH-KCU-01). This link is considered a part of the AWE system and does not require any modifications from the system currently used by Kitepower. Such a WiFi communication

method is Point-to-Point WiFi. Small systems that use this technology can reach 5km which is more than enough for LLS-CDH-KCU-01. With a refresh rate of 3Hz and a packet size of 300 bytes (Position, attitude, bridle line tension, other metadata), the bitrate is expected to be around 6.9kB/s. This is higher than for COMM.5 since the data size will increase due to COMM.1 being connected to a more complex system. A similar bitrate will be assumed for COMM.3, COMM.4 and COMM.8.¹

In total all data streams excluding COMM.3 will have a combined bitrate of 36.8kB/s. All this data will be sent to the External Control Centre which means that COMM.3 will have a bitrate of at least 36.8 kB/s. This data will be stored for 24 hours and the weather data or COMM.3 and COMM.4 will be held for 7 days. This means that an internal storage of 10.4 GB is needed to store all the data.

14.4. RAMS Characteristics

14.4.1. Reliability

Communications are an important part of any system. If contact between the GCU and another subsystem would fail the system itself would either cease operations or control would be lost. A redundant communication link has been installed to all individual wireless subsystems to make sure communication between the GCU and the other subsystem will not be lost. For wired subsystems, the reliability is assumed high enough as to not have the need for a redundant data link.

14.4.2. Availability

The communication links must be available all the time to guaranty successful and safe operations of the system. Due to the high level redundancy in the communication it is considered unlikely that it would cause any downtime.

14.4.3. Maintainability

The system needs to perform without interference for 6 months(CON-LLS-GEN-01-04). If a communication link fails within 6 months its redundant link will become active. The main link will be repaired after the 6 months. During this maintenance, all other parts that have not failed will be inspected and repaired. If a link and its redundant link(s) all fail then the system will stop operation and unplanned maintenance is required.

14.4.4. Safety

A communication subsystem does not introduce any major physical safety hazards. Low power data transfer over 2.4GHz and 5GHz is not considered harmful to humans and animals². However, there is the danger that the wireless communications can be intercepted or even spooked for malicious purposes. To ensure system data links are not compromised, encryption should be implemented. In case the wireless links are jammed by malicious actors, an emergency landing is performed using, relying only on the tension in the tether for communication.

14.5. Recommendation

The communication does not change significantly of the traditional implementation of an AWE system. The main link between the KCU and GCU remains unchanged, however, a more complex wired communication bus is needed for handling the large amount of actuators and sensors in the ground station needed for the LLS system.

¹<https://www.dlink.com/en/products/dap-3711-5-km-long-range-80211ac-wireless-bridge>, accessed on 23-6-2023.

²<https://ask.imeshforce.com/en/articles/2508878-is-wifi-safe-and-healthy-is-5ghz-wifi-safer-than-2-4ghz-wifi>, accessed on 19-06-2023

Now that all the subsystems have been detailed, it is possible to combine them and have a complete view of the final system. This chapter begins with the final configuration and layout in Section 15.1, followed by the compliance matrix in Section 15.2, the resource budget in Section 15.3 and the reliability, availability, maintainability and safety in Section 16.1, Section 16.2, Section 16.3 and Section 16.4 respectively.

15.1. Configuration and Layout

The final configuration of the OWL consists of a main container and an offset container connected by the guiding cable. The main container houses the tower with Rolling Storage System (RSS) and the winch. The offset container is empty and functions as storage for equipment belonging to the AWE. The cable cart drives over the guiding cable, allowing the swivel access point to move to an offset position. All these parts can be identified in Figure 15.1, depicting the system midway in the winch launching process. The interfaces of these subsystems are covered in detail in Section 12.3.

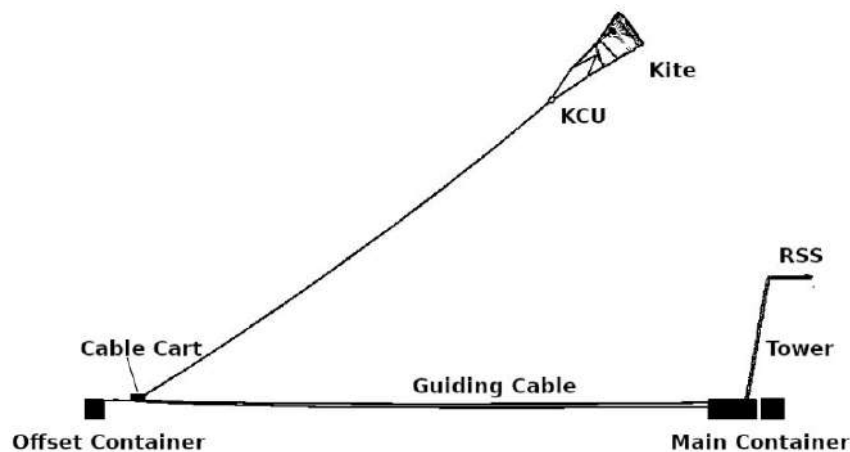


Figure 15.1: Complete system side view

15.2. Compliance Matrix

It is important to validate whether the design can actually fulfil its mission. Although a compliance analysis has been done for each subsystem, a similar analysis is needed at the level of the complete system to see if all top level requirements, listed in Chapter 4, are met. The compliance matrix with the stakeholder requirements is shown in Table 15.1

Table 15.1: Compliance with stakeholder requirements

Requirement ID	Requirement	Compliance	Shown In

STK-OEM-01	The LLS system shall operate autonomously for 6 months.	YES	Chapter 6, Section 7.6.1, Section 8.6.1, Section 9.6.1, Section 10.6.1, Section 11.6.1, Section 12.6.1, Section 13.6.1, Section 14.4.1
STK-OEM-02	The LLS system shall enable the autonomous deployment of a soft kite AWE system to nominal operating conditions.	YES	Section 6.2
STK-OEM-03	The LLS System shall enable the autonomous retrieval of a soft kite AWE system from nominal operating conditions.	YES	Section 6.3
STK-OEM-04	The LLS System shall enable the autonomous storage of a soft kite AWE system.	YES	Section 6.4
STK-OEM-05	The LLS System shall be able to function within the operating window of the AWE system.	YES	Section 7.6.2, Section 8.6.2, Section 9.6.2, Section 10.6.2, Section 11.6.2, Section 12.6.2, Section 13.6.2, Section 14.4.2
STK-OEM-06	The LLS System shall not hinder the performance of the AWE system.	YES	Section 15.2.2
STK-OEM-07	The additional costs of the LLS System for the 100 kW variant shall be at maximum €40,000 per system.	YES	Section 15.3.1
STK-OEM-08	There shall be no financial impact of the LLS System on the other subsystems.	NO	Section 15.3.1
STK-OEM-09	The LLS System shall allow for the replacement of its individual components in case of failure.	YES	Section 7.6.3, Section 8.6.3, Section 9.6.3, Section 10.6.3, Section 11.6.3, Section 12.6.3, Section 13.6.3, Section 14.4.3
STK-OEM-10	The LLS System shall comply with the company sustainability goals.	YES	Chapter 19
STK-OEM-11	The LLS System shall be contained within a standard 20-foot shipping container.	YES	Section 12.3.8
STK-OEM-12	The LLS System shall not negatively affect the mobility of the AWE System	YES	Section 12.3.2
STK-OEM-13	The LLS System shall be able to sustain common transportation loads without damage	TBD	Section 12.3.8
STK-OEM-14	The LLS System shall be able to operate in harsh environments.	YES	Section 5.2
STK-OEM-15	The LLS System shall not lengthen the installation time of the AWE system over 24h.	YES	Section 18.3
STK-OEM-16	The LLS shall be able to operate on batteries when no energy is generated.	YES	Section 11.3

STK-OEM-17	The LLS shall be upgradeable to allow for the use of larger kite systems.	NO	Section 11.3
STK-PGO-01	The LLS System shall not cause damage to the power grid connected to the AWE system.	YES	Section 11.3
STK-PGO-02	The LLS System shall not hamper the interface with the power grid.	YES	Section 11.3
STK-GOV-01	The LLS System shall comply with the safety standards applicable to AWE systems.	YES	Section 7.6.4, Section 8.6.4, Section 9.6.4, Section 10.6.4, Section 11.6.4, Section 12.6.4, Section 13.6.4, Section 14.4.4
STK-DO-01	The design of the LLS System shall be completed in 10 weeks.	YES	Chapter 17
STK-DO-02	The LLS System shall be designed by 11 aerospace engineering students.	YES	Chapter 17
STK-DO-03	The LLS System design office shall have the freedom to redesign the other subsystems.	YES	Chapter 12, Chapter 13
STK-PVS-01	The LLS System shall keep noise generation within the bounds of the regulations applicable to the AWE system.	YES	Section 13.3.6
STK-PVS-02	The LLS System shall not produce toxic products harmful to the environment.	YES	Section 19.7

15.2.1. Non-compliance requirements

Some of the stakeholder requirements have not been met or have not been examined enough and this subsection will explain why these requirements have not been met.

STK-OEM-07 has not been met since the LLS design will introduce new costs to the existing subsystems. The ground station for example has been redesigned with new cutouts and the KCU has a new leading-edge retracting mechanism. Some other adjustments have been made but a financial impact on the original AWE system is present.

STK-OEM-17 has not been met since the LLS system is not upgradeable for larger kite systems. The Tower is currently 18.2 meters high which is proportional to the distance from the kite to the KCU and the kite's wingspan. If a larger kite is used the tower height would also increase and for considerably larger AWE systems the tower would become too large to fit into a 20-foot container. The storage is the only part of the design that would hinder the scalability so if a larger container can be used for a larger AWE system then the LLS would be upgradable.

It is unknown whether STK-OEM-13 is met or not. It is expected that the LLS system would be able to sustain the transportation loads since most components have been designed for higher load cases. However, the requirement is not fully met since in order to know whether the LLS system can bear transportation loads, validation has to be completed for which resources were limited.

15.2.2. Performance of the Final Design

The final design is a changed version of the existing AWE system of Kitepower. The performance is a measure of how much energy the kite will output when the kite is producing energy. The only component that changes the performance is the kite and KCU subsystem. Though,

as explained in Section 13.3.6, the change is minor. For this reason, it can be said that the performance does not change.

15.3. Resource Budget

The initial estimation for the pole's height is 15 metres, now the height is around 18.2m. At first, it was thought that the tower would be standing on top of the container but having analysed the structure it was more feasible to rotate the tower within the container. For this reason, now the tower has a slightly taller height. It is worth mentioning that this value will differ depending on the AWE system that is installed and the scale because the height depends on the size of the kite and the length of the bridle lines. If the span of the kite were to increase to 50 metres and the bridle lines are still 15 metres, the minimum required distance between the top of the tower and the main container would be 25 metres.

Regarding the winch's performance, it is the same as the estimated. The kite department calculated that at a certain tension of the tether 12 m/s reel-in speed would suffice to take-off. Dromec will be asked to manufacture such a machine that can perform in such a way and still have a 20% margin of maximum speed. This means that the machine will have to have a maximum reel-in speed of 14.5 m/s. By having this margin, a small safety factor is included if any unexpected disturbances may need additional speeds. In Chapter 6 it is explained how a minimum of 6 m/s apparent windspeed is needed. That is why when there is a 6m/s tailwind, the winch must be able to pull the kite at 12 m/s. For higher windspeed, a tower launch will be carried out.

The rough estimation of energy consumed to launch the system will be done by adding both the kinetic and potential energy of the kite in the first step. This is then multiplied by 3 because every step has similar heights achieved as well as the kite speed in that position is also similar. When landing, the kite is put in a parked position where it is static in the air and in equilibrium. Here only potential energy will be considered. Looking back at Chapter 7 the energy to fold and store the kite will be calculated using the rated power of the RSS and the time taken to carry out the procedure.

$$E_{total} = (E_P + E_K) \cdot 3 + E_{Pland} + E_{RSS} \quad (15.1)$$

$$E_{total} = (m \cdot g \cdot h_{step} + \frac{1}{2} \cdot m \cdot V^2) \cdot 3 + m \cdot g \cdot h_{max} + P_{RSS} \cdot t_{fold} \quad (15.2)$$

$$E_{total} = (185 \cdot 9.80665 \cdot 60 + \frac{1}{2} \cdot 185 \cdot 25^2) \cdot 3 + 186 \cdot 9.80665 \cdot 400 + 250 \cdot 100 \quad (15.3)$$

All these parameters have previously been specified in Chapter 6 and Chapter 7 and by substituting all of them it yields a total energy of $E_{total} = 0.34kWh$. This is about 63% of the initially estimated energy of 0.54 kWh. This allows for quite a large margin if more systems are to be involved.

For the time estimations to conduct the entire process a series of assumptions will be done. The total amount of time is directly related to the reeling speeds of the winch. The launching procedure consists of 3 step-tows. This means there will be 3 rises of the kite to achieve a higher altitude and 2 glides to reel out the tether. Each rise takes $\simeq 4 - 5$ seconds and each glide is $\simeq 60$ seconds. Landing will take place once the kite has been parked in the air, the winch will start reeling in the kite at 3 m/s. This speed is used since the assumed wind speed is 12 m/s and using the 1/4 reel-in factor from Chapter 6. Thus, the time taken to reach the ground from an altitude of 400 metres is $\simeq 134$ seconds. After the kite has been secured on the RSS, the rolling mechanism will be activated. For the entire kite to be folded it will take an estimated 50 seconds. Summing up all these times yields a total cycle time of $\simeq 6.5$ minutes. Additionally, in case of high winds, the launching period could be decreased since a tower launch would take place. The tower would take a certain amount of time to rotate and get aligned with the wind.

Then, the time taken to achieve the desired height will depend on the windspeed at that moment in time.

15.3.1. Cost Breakdown

With the cost breakdown, an overview of the costs that conform to the LLS will be displayed. Components for each subsystem will be quantified along with an estimated amount of money designated for research and development. The communications subsystem’s cost is considered negligible and for that reason, it has not been included in the table. Estimations for the maintenance and operations of the LLS have to be done. The requirement STK-OEM-07 does not take into account the costs related to the operations and maintenance of the AWE system and for that reason, they shall not be included within the breakdown. Table 15.2 shows the price for each subsystem’s components.

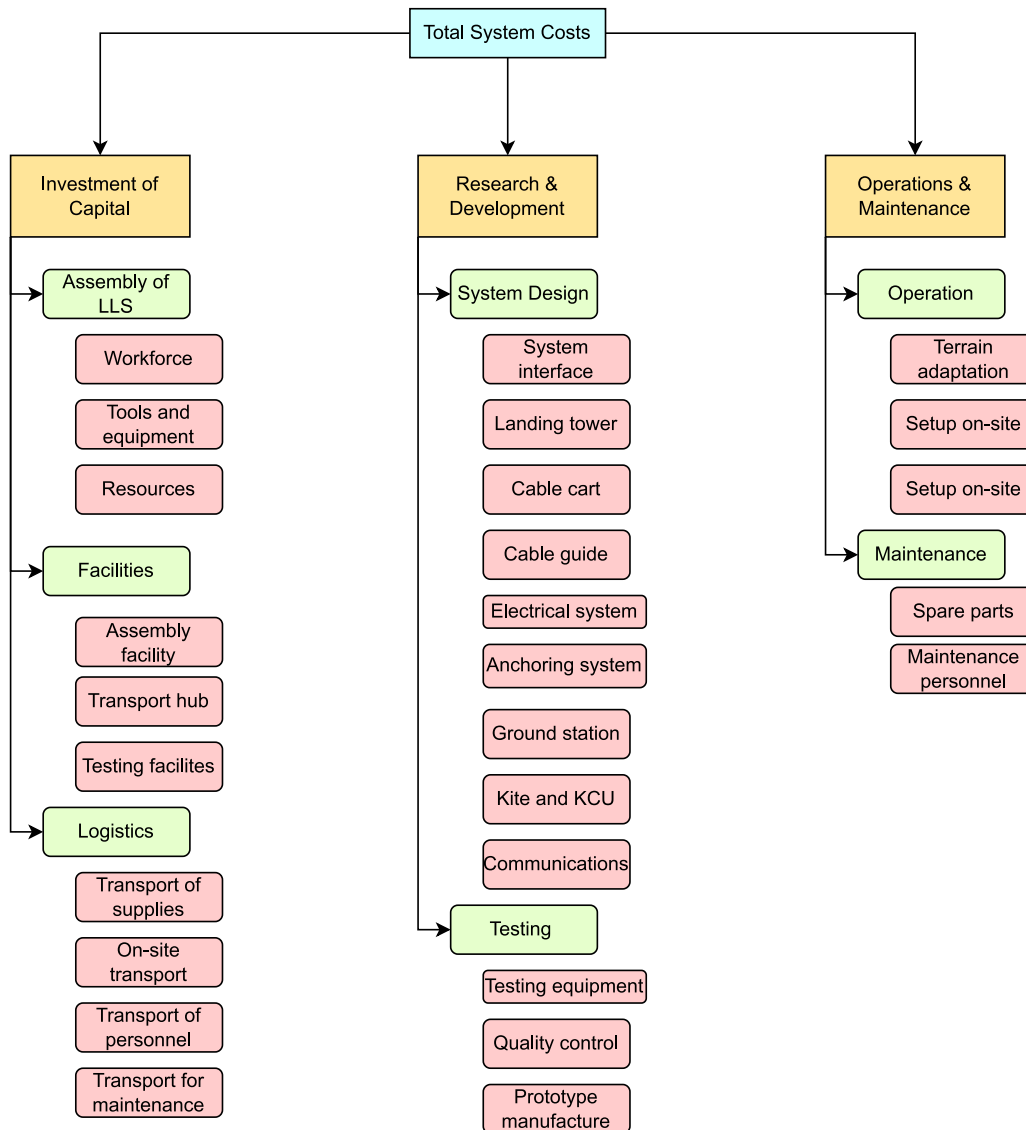


Figure 15.2: Cost Breakdown Structure

Table 15.2: Cost Component Breakdown

Subsystem	Parts	Cost per part[€]	Number of parts	Total cost[€]	cost percentages
Cable Cart	Pulley	10.3	3	30.9	
	Electric Motor	372	2	744	
	Wheel	6.41	8	51.28	
	Clamping	13.37	8	106.96	
	Brake System	40.88	4	163.52	
	Transmission Belt	66.76	4	267.04	
	Roller Upper Pulley	0.39	4	1.56	
	Upper Pulley Arms	18.12	1	18.12	
	Upper Pulley Beam	6	1	6	
	Lower Pulley Beam	6.84	4	27.36	
	Upper Wheel Shaft	0.84	4	3.36	
	Lower Wheel Shaft	0.52	4	2.08	
	Coupling Plates	30.3	2	60.6	
	Body	31.57	1	31.57	
	Motor Controller	130.69	2	261.38	
	Cart Wiring	47	1	47	
	Charging Inlet	94	1	94	
	Battery Cell	2.99	60	179.4	
	Battery Case and Case Wiring	90	1	90	
	Bolt	4.18	52	217.36	
Assembly	-	-	2000	11.2%	
Anchoring System	Ground Anchor	366	12	4392	
	Ratchet strap cable	10[€/m]	15[m]	150	
	Reinforcement bar	100	2	200	
	Attachment point	50	2	100	12.3%
Electrical System	Buck Converter	250	3	750	
	Internal wiring	6.65 [€/m]	31[m]	206.15	2.44%
Ground Station	Raw Metal	2.31[€/kg]	100[kg]	231	
	Assembly and welding	-	-	119	0.9%
Kite and KCU	Attachment ring + bridles+mid-strut	50.2	-	50.2	
	Leading Edge Tether	250	1	250	
	LET Retraction Mechanism	300	1	300	
	UV Coating	200	1	200	2.0%
Tower	Base Bearing	2983.23	1	2983.23	
	Base Motor	1850	1	1850	
	Main Structure	2481.3	1	2481.3	
	RSS Motor	1850	1	1850	
	RSS Bearing	500	1	500	
	TE Linear Actuator	592	1	592	
	Solenoid Locking	1023.1	1	1023.1	
	LE Winch	10000	1	10000	
	Hinge TE Clamp	7.58	1	7.58	
	Nuts and Bolts	0.8	18	14.4	
Assembly	-	-	2000	59.5%	
Guiding Cables	ulc Dyneema	4000	-	4000	
	Jack	500	1	500	
	Turnbuckle	40	1	40	
	Harp	94	1	94	11.8%
TOTAL		-	-	39287.45	100%

The RAMS of the final design is pretty much the result of integrating the RAMS of all subsystems and determining the most critical ones.

16.1. Reliability

The reliability of the complete LLS system is mostly affected by the electrical subsystem and the cable cart. All the other components are fairly stationary and reliable by design. To compensate for the unreliable parts of the electrical subsystem and the cable cart, redundant parts are added.

16.2. Availability

The autonomous nature of the LLS system, adds complexity to the current non-independent system in operation, with the addition of multiple parts and subsystems interconnected with each other. The awareness of this weak point of the system is reflected in over-design choices with the presence of extra components or high safety factors to increase its availability. Although this has a negative impact on the final weight of the system, it decreases downtime and boosts financial productivity.

16.3. Maintainability

The components of the LLS system most prone to failure or damage are the moving parts, namely the landing tower, the cart and the kite subsystems, due to their dynamic nature and interface with multiple components. In general, the system has been designed to not require any maintenance intervention for at least 6 months (STK-OEM-01). Every subsystem is efficiently accessible and the single components are easily replaceable, so to limit the downtime of the airborne system.

16.4. Safety

The LLS makes the AWE system autonomous which makes safety a less significant part of the RAMS. Though, when maintenance is performed people are in the so-called hazard zone. For the tower, it is important that no maintenance is performed in strong winds. Most significant is the guiding cable which has a very severe snapback when it breaks. For safety, the personnel should be informed and educated on this. Also, the electrical subsystem has high voltages. Therefore, fuses are implemented to cut the power if there is some form of electricity leakage. Lastly, the kite and KCU can pose a hazard. To mitigate this, the kite will be landed when any type of maintenance is required. Otherwise, during operation, no people are allowed in the ground buffer zone.

Design Development Overview

After 10 weeks, the 11-student team managed to come up with a complete design. However, this design is still far from being market ready, and the design would need to be further developed before it can be sold to the customers and deployed. In this chapter, the steps leading to a more refined design are outlined.

This process is shown in Figure 17.1: it starts from the design resulting in the DSE, and proceeds with the finalisation of the product until it can be implemented in the market. A Gantt Chart of the process is also included, to show the time-wise steps to follow to have a deployed design within two years.

One of the most important aspects of this process is using prototypes. The team expects that many prototypes (from low to high-fidelity) will need to be made, to validate the product. Once a small-scale prototype has been made and tested, the results will be presented to the customers, and their feedback will be implemented. Many iterations of this process will be necessary. Once the final product is completed, its financial, as well as, manufacturing, supply and logistics aspects will have to be arranged.

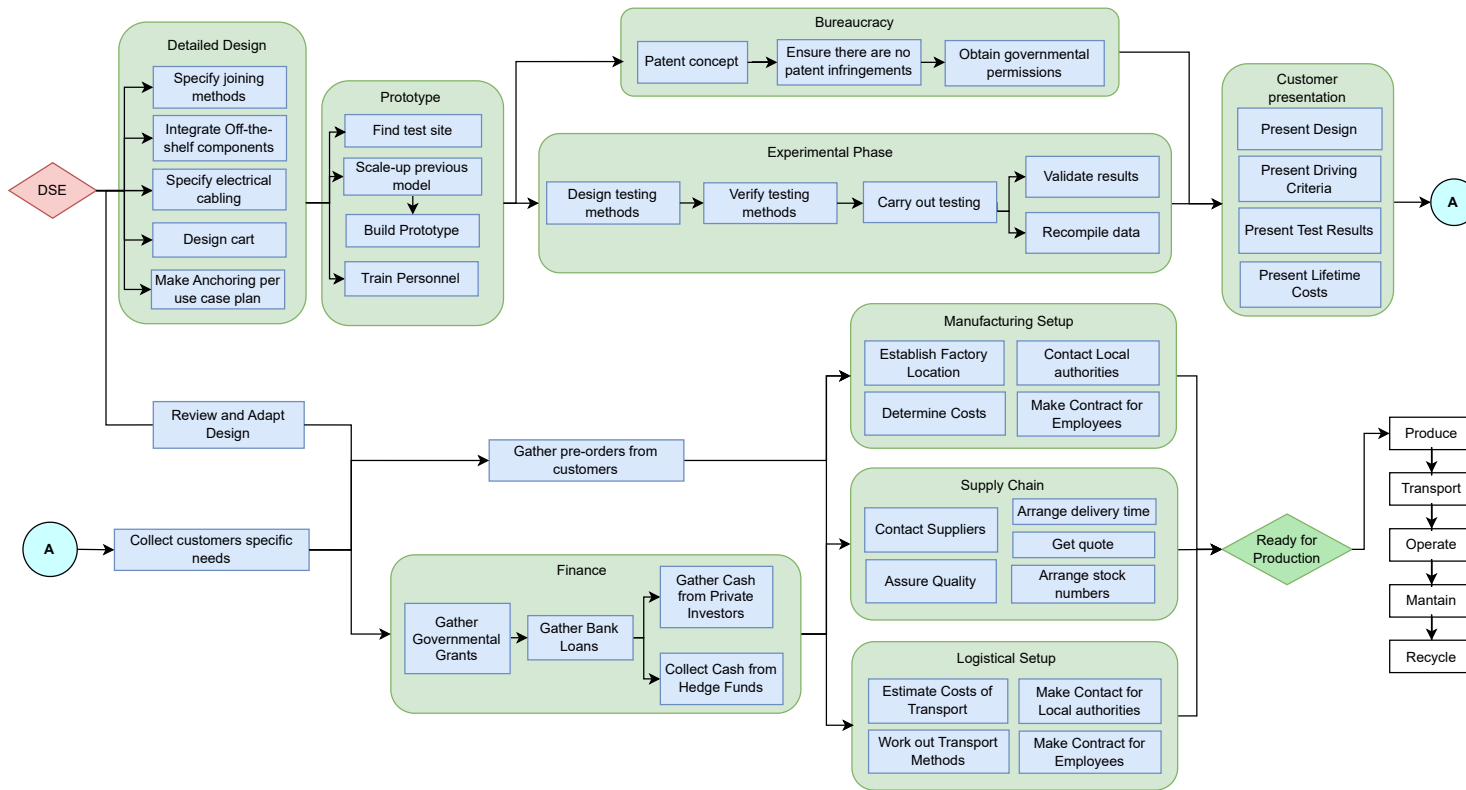
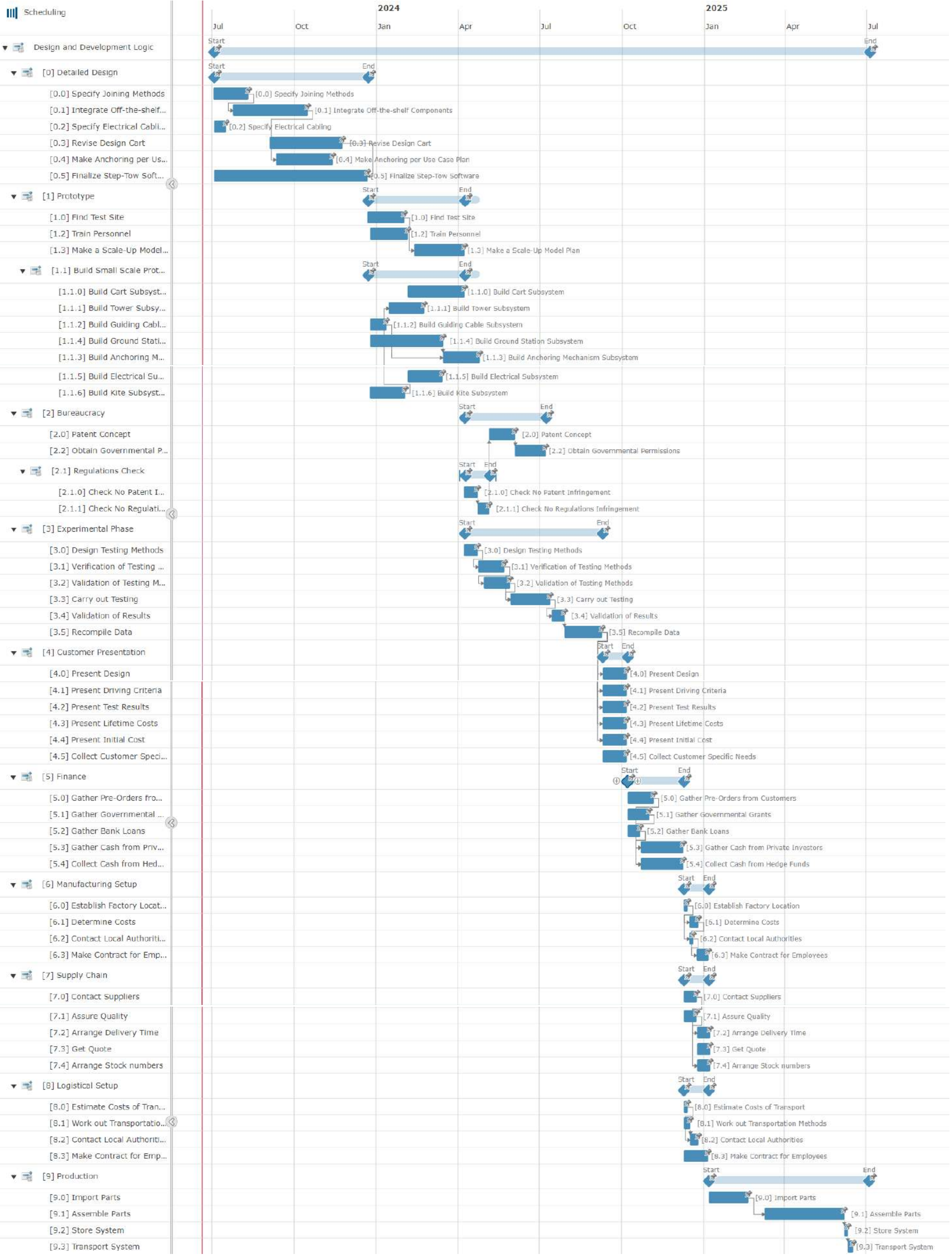


Figure 17.1: Project Design and Development Logic Diagram

Scheduling



Logistics is a vital part of supply chain management that deals with the movement of goods, services, or information from a point of origin to wherever said resources are needed. From the functional flow diagram shown in Chapter 3 the following functions are derived:

- FUN 0: Produce System
- FUN 1: Transport System
- FUN 2: Setup System
- FUN 9: Maintenance
- FUN 11: Execute End of Life

In this chapter, each of the functions will be investigated. Section 18.1 discusses production logistics, followed by the transportation of the system in Section 18.2 and the setup of the system in Section 18.3. Maintenance is discussed in Section 18.4, the end-of-life in Section 18.5, costs in Section 18.6 and sustainability considerations in Section 18.7.

18.1. Production Logistics

The location chosen to carry out the assembly of the LLS is Vilnius, Lithuania. This location has a series of benefits which make it attractive such as lower corporate taxes, direct access to the Baltic Sea, being the industrial pole of Lithuania a member of the EU and relatively low work wages.

By being within the EU and using the same currency, the euro, trading among countries of the EU reduces costs. This is partly due to the abolition of customs tariffs and the close cooperation with other countries. Most of the component suppliers are European, so the transport costs and carbon footprint due to emissions are as low as possible. Having access to the sea allows for the assembly plant to receive materials or parts via air, sea, and land.

Regarding the costs of labour, Lithuania has one of the lowest in the EU¹. The average labour cost in Lithuania within the construction and industry sector is roughly €12/hour, whereas in the Netherlands the average is €42.1/hour. Lithuania's standard corporate tax is of 15 %, if certain conditions are met it is possible for small companies to reduce this to a range of 0 % to 5 %. These benefits may very well improve the profitability of this project during its initial years².

Multiple companies are involved in the supply of different components since all the parts are outsourced from third parties. As a supplier for the aluminium parts, the Norwegian company Hydro will be contacted. They will supply aluminium tubes for the tower. The company was selected because they offer recycled aluminium, and they assure that the CO_2 emission will be cut down by 30 % by the year 2030³. As experts regarding anchoring mechanisms for structures, the British company Spirafix will supply the said mechanisms⁴. This company is selected since they appear to be the only company that produces the desired type of ground anchor. Austrian-based enterprise, Teufelberger, will supply the Dyneema® products needed

¹https://ec.europa.eu/eurostat/statistics-explained/index.php?title=Hourly_labour_costs, accessed 14-06-2023

²<https://taxsummaries.pwc.com/lithuania/corporate/taxes-on-corporate-income#:~:text=The%20standard%20CIT%20rate%20is,if%20certain%20conditions%20are%20met.>, accessed 14-06-2023

³<https://www.hydro.com/en/aluminium/products/all-products/>, accessed 14-06-2023

⁴<https://www.spirafix.com/>, accessed 15-06-2023

for both the guiding cables. Not only do they offer products of the highest quality, but they have multiple environmental goals that are in line with this project's⁵.

As a supplier for the cable cart, the Austrian company LCS Cable Cranes will be requested to manufacture this subsystem.⁶ This company is highly experienced in the construction of cable cart systems and thus has the necessary experience needed. Regarding the supplier for the motor used in the LLS system will be done by the German manufacturer Baumuller, whose main factories are located in southern Germany⁷. With a heritage of 90 years, Baumuller is one of the market leaders in electric motors, providing a wide variety of components used in the product. These motors will then move the cart along the guidelines and rotate the RSS.

Lastly, a large bearing is needed for rotating the landing tower. The provider will be SKF, they provided customisable slew bearings which is ideal for this case⁸. The battery, winch and jack screws used for the system have previously been specified and will be bought from the companies stated in their respective sections.

Most of these companies have specified and are working towards meeting their sustainability goals. For this reason, these companies were carefully selected, so the system may comply with the parent requirement CON-LLS-GEN-03. All these products will be shipped directly to the assembly factory, where the ground station frame is mounted into the container and the rest of the subsystems are loaded into the containers for transport.

The decision was taken in Chapter 2 to outsource the manufacturing of all the components. The logic behind this was to reduce initial development costs that would incur by implementing a custom production line. In consequence, only assembly processes, components, and integration tests would occur on site. As the production series are low (55-130 products per year), the most efficient option would be to assemble the products one by one using a trained workforce. It does not make much sense to use an automated line, as the cost incurred would be significant.

18.2. Transportation of System

The direct access to the sea makes it easier to transport the systems to customers around the globe. Maritime transport is selected over air and land for multiple reasons: very cost-effective for heavy and bulky transport, the carbon footprint left is smaller which helps comply with sustainability requirements in Chapter 4, and high reliability that the goods will reach their destination⁹. The delivery time is not that big of an issue because these systems are pre-ordered with a long waiting time in mind. Maritime transport shall always be used for very large distances to the country of destination. Barge or rail transport shall be prioritised when transporting within the country.

The components that will be provided by the companies stated in the previous section will be fully managed by those suppliers. For the LLS system, the team will only organise the transport of the system to the customer's desired location. The transport via trucks will be minimised as much as possible to lower the carbon footprint.

An estimate was calculated to transport 2x20ft containers from the port of Rotterdam (Netherlands) to the port of Bilbao (Spain). The price is €3530. This is including a number of charges from the freighting, destination and taxes. This yields a final cost of sea freight of $\simeq 2.02 \frac{N}{km}$ ¹⁰.

⁵<https://www.teufelberger.com/en/about-us/sustainability.html>, accessed 15-06-2023

⁶<https://www.lcs-cablecranes.com/en/company/about-us/>, accessed 15-06-2023

⁷<https://www.baumueller.com/en/products/motors>, accessed 15-06-2023

⁸<https://www.skf.com/group/products/slewing-bearings>, accessed 15-06-2023

⁹<https://www.seaspace-int.com/sea-vs-air-vs-land-freight-what-is-the-best-method-of-transport-for-you/>, accessed 14-06-2023

¹⁰<https://my.icontainers.com/quotes/2ed40dd0-2126-48c5-80b9-c77379c29398>, accessed 21-06-2023

In comparison, intra-continental transport by rail freight would cost around $2.38 \frac{N}{km}$ ¹¹.

18.3. Setup System

Before sending the system to the allocated place, a team of people will go study the site. Once the site has been approved as qualified for the setup of the system, some terrain modification may be done and the LLS will be shipped there. On-site, the system will be unloaded by mobile cranes. There are different options and types that will vary depending on the surface on which it has to go. Immediately after unloading all the containers (main, battery and off-set container), their anchoring system will be installed, so they may be securely fastened to the ground. The selected number of anchors is drilled into the ground. Using tension straps and a ratchet, the straps are tensioned until the desired tension is reached.

Then, all the other parts will be taken out from each container and installed. Where each part is stored had previously been described in Section 12.3.8. It is expected from the AWE company to hire qualified personnel with the necessary equipment to properly install the LLS system, the company will also be provided with detailed instructions on how to set up the system.

The guiding cables are guided through the cable cart, which is already fully assembled and stored in the correct location, and attached to the offset and main container. using the turnbuckles and jack screws, the guiding cables are brought to the correct tension. Finally, the tension of the cable cart springs must be adjusted to lock the cart on the guiding cable.

The tower assembly is the longest and heaviest component of the system. To start, the external tower segments are bolted together horizontally on the ground. The truck-mounted crane is used together with ropes to pivot the tower to an upright position, after which all bolts need to be tightened.

Additional crew specialised in the set-up and connection of the electrical system might be required. For example, an electrician will be tasked with connecting all the electrical components and making sure there is a secure connection between the AWE system and the microgrid. Once the set-up has been finalised, the AWE will be booted up and enter nominal operating conditions.

Once the system is fully assembled and connected to the grid, it is time to attach the kite. The easiest way to load the kite on the RSS is to do a manual launch and let the system store the kite itself. This can also function as a test of the system. The main tether is guided through the cable cart and connected to the KCU, and the secondary tether is attached to the leading edge. After a pre-flight check, the kite is launched once manually, after which autonomous operation can begin.

18.4. Maintenance

Different parts of the system will require different logistical tactics. If the kite were to fail, that kite would have to be replaced with a new one and the broken one would be analysed to see whether it could be repaired. Whenever the tether or cable guides are not up to standards for proper functioning, repairing would not be possible. A total replacement of the Dyneema® cables would be needed. In general, most electric failures would need a replacement of said part, since trying to fix them would be too costly. When possible, maintenance shall be done on-site to reduce the logistics necessary to take back some parts. Preferably, maintenance should be done as much as possible on-site in order to minimise the costs and time for transportation. Possible maintenance tasks that can occur during operation are:

¹¹<https://nl.dbcargo.com/resource/blob/6258240/09173779055894a91a4b7de4f2e4f0c7/7-example-download-with-picture-data.pdf>, accessed 21-06-2023

- **Replace cable guide:** The Dyneema® cable is removed and replaced with a new Dyneema® cable, this happens on-site.
- **Replace pulley or actuator:** The entire cable cart is replaced on-site, and the old one is transported to a workshop where it can be repaired.
- **Cleaning system:** The cable guide and RSS is cleaned on-site.
- **Monitoring state of tether cutter:** Routinely checks on the tether cutter, this happens on-site.

18.5. End of life

When the AWE has reached its end of life, the system will be dismantled and disassembled by the professional crew that had set it up. Once packed, a team back in the main assembly building in Lithuania will assess which components may be reused. To know more specifically which materials can be recycled, refer back to Section 19.4. This high recyclability capacity that there is makes it very attractive as a sustainable product.

18.6. Costs

The logistics for this project are really broad and for this reason, there are many factors which may influence the costs. The main contributor to the costs of the logistics is the international transport to the customer. All the outsourcing done is with European companies which leads to low transport fees, most of these components will also be transported in bulk. At this stage, the cost analysis will not be detailed further.

18.7. Sustainability

In order to calculate the emissions from transporting the system to and from the factory for assembly, it is assumed that first the AWE system has to be shipped to Lithuania, once there all the components of the LLS are assembled onto it, and finally, the entire the system is shipped back.

To account for a likely but also worst-case scenario regarding emissions, it is assumed that an AWE system deployed near Cape Town in South Africa is shipped to Vilnius, where the LLS is installed on it, and then it is sent back to Cape Town.

The journey from the main Lithuanian port, Klaipeda, to Cape Town is about 7031 nautical miles, or about 13 021 km. The emission intensity used is $5.3 \text{ g}_{\text{CO}_2\text{e}}/\text{tkm}$ for sea shipping between NW Europe and Africa, according to Table 19.7. For the mass, it is assumed for simplicity that the inbound system has the same mass as the fully assembled system minus the masses of the tower, guide cable, cable cart and anchor systems, which from Table 19.9 works out to be approximately 11 603 kg, while the mass of the outbound system is simply the full system's 12 240 kg. The shipping emissions are therefore about $801 \text{ kg}_{\text{CO}_2\text{e}}$ and $845 \text{ kg}_{\text{CO}_2\text{e}}$ for the inbound and outbound journeys by ship, respectively.

Land transport between Klaipeda and Vilnius can be done by train in a 400 km journey¹²¹³ which, assuming an intermodal diesel train, has an emissions intensity of $25 \text{ g}_{\text{CO}_2\text{e}}/\text{tkm}$, yielding emissions of about $116 \text{ kg}_{\text{CO}_2\text{e}}$ and $124 \text{ kg}_{\text{CO}_2\text{e}}$ for the inbound and outbound journeys, respectively, assuming the same masses used for the sea shipping calculations.

The total emissions for transport from Cape Town to Vilnius and back are, therefore, about $1886 \text{ kg}_{\text{CO}_2\text{e}}$ which, taking a capacity factor of 0.5 on a rated power of 100 kW with a grid carbon intensity of $523 \text{ g}_{\text{CO}_2\text{e}}/\text{kWh}$ as per Section 19.1, works out to a payback period of about 72 h.

¹²<http://www.intermodal.lt/en>, accessed on 21-06-2023

¹³<http://www.google.com/maps>, accessed on 21-06-2023

The sustainability of a project is a complex matter, involving carbon emissions as well as circular economy indicators, ethical considerations, ecosystem effects and numerous other pollutants that are of interest because of their impacts on human health, such as PM 2.5 fine particulate matter, bio-accumulative compounds and nitrogen dioxide emissions.

The current climate emergency dictates that the highest current priority lies on carbon emissions and circularity (for which recyclability is a good proxy), and due to the limited scope, resources and time available to develop the present report, only those two matters will be looked into regarding the project's sustainability. This requires a literature study as performed in the current chapter. Firstly, an overview of the calculation of greenhouse emissions payback period is displayed on Section 19.1, followed by data and observations of emissions from manufacturing in Section 19.2, transport in Section 19.3 and end-of-life in Section 19.4. Further on, the chapter will deal with organising and analysing the emissions payback period and recyclability obtained from the lifecycle assessment performed throughout the project in Section 19.5 and Section 19.6 respectively, and producing recommendations and observations that may be relevant beyond the current project's scope in Section 19.7 and Section 19.8 respectively.

19.1. Greenhouse Emissions Payback Period

The payback period for wind turbines in Northern Europe, in terms of greenhouse emissions, typically ranges from 1.8 to 22.5 months, with an average of 5.6 months [35]. AWE systems typically have a lower power rating but higher emissions due to battery usage, small-scale production, and regular transportation of the systems. Therefore, requirement CON-LLS-GEN-03-04 specifies that the payback period for the LLS system should be the upper limit mentioned earlier. On the other hand, requirement CON-LLS-GEN-03-01, stipulating that the system must be carbon neutral, is readily met as long as the system's lifetime is longer than the calculated emissions payback time.

For any payback period calculations within the present report, the electricity emissions intensity of Senegal will be used, as it serves as a representative value for disaster-struck areas where the AWE systems using the LLS system may be deployed. Said emissions intensity is of $523 \text{ g}_{\text{CO}_2\text{e}}/\text{kWh}^1$. Additionally, a capacity factor of the AWE system equal to 0.5 will be assumed, and the rated output used will be 100 kW.

To minimise emissions, it is essential to focus on manufacturing emissions, particularly material use, and on energy consumption during system operation. Since conducting a comprehensive lifecycle assessment is complex, the current report will only consider emissions related to material use during manufacturing and the transportation of the complete system from the production facility to the customer. Despite the project's limited duration, this approach allows for a sufficiently detailed overview of the emissions throughout the lifecycle of the LLS system.

19.2. Manufacturing

As with every physical product, a large part of the lifetime emissions of the LLS system will be its manufacture.

¹<https://ourworldindata.org/grapher/carbon-intensity-electricity?>, accessed on 12-06-2023

Battery

Requirement CON-LLS-GEN-03-08 constrains the system to use only the least polluting Li-Ion batteries, at less than $76 \text{ kg}_{\text{CO}_2\text{e}}/\text{kWh}$. From Table 19.1, it is evident that using SIB or Li-Air batteries when they become commercial would be highly desirable sustainability-wise. It is also important to note the ethical concerns surrounding the supply chain of cobalt used for many current generation lithium-ion batteries².

Table 19.1: LCA emissions of different types of high-energy-density modern batteries. Note that a large variability was observed for LFP and LMO batteries in the source material, and their emissions are thus reported as a range to accommodate for this. Also, note that Lithium Sulphate (LiS) batteries and Li-Air batteries are upcoming technologies and have not been demonstrated at a commercial scale. [36]

Batterytype	LCA modelling approach	GWP emissions ($\text{kg}_{\text{CO}_2\text{e}}/\text{kWh}$)
LiS	Cradle-to-Grave	67.94
SIB		64.35
Li-Air		10.15
LFP	Cradle-to-Gate	75.5-225
LMO		

Materials

The materials most likely to be used for the present project are hereby discussed.

Steel

As per Figure 19.1, European steel has, on average, equivalent emissions of $1.9 \frac{\text{t}_{\text{CO}_2}}{\text{t}_{\text{steel}}}$ [37], which complies with requirement CON-LLS-GEN-03-06 and will therefore be used. Emissions from Chinese steel are barely higher, but higher transport emissions for the raw material have to be factored in, too, despite not being included in the lifecycle assessment of the system.

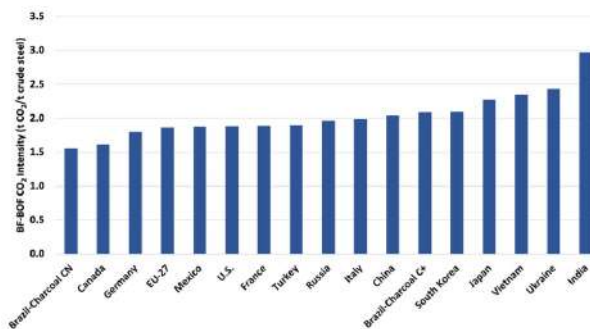


Figure 19.1: CO_2 equivalent intensity of steel production in various countries [37]

Aluminium

The emissions for the production of secondary, or recycled, aluminium in the EU are about $0.50 \frac{\text{t}_{\text{CO}_2}}{\text{t}_{\text{Al}}}$, which makes it compliant with requirement CON-LLS-GEN-03-05 and corresponds to less than 10 % of the emissions from producing primary aluminium, and around a quarter those of steel[38]. It is very important, however, to ensure that it is secondary aluminium and not primary that is being used, since primary aluminium would be far more polluting.

Copper

The emission intensity of copper corresponds to around 3.9 kg carbon equivalent per kg of refined copper [39]. Because of the nature of the supply chain of electrical components, it is

²<https://www.weforum.org/agenda/2020/01/how-to-secure-clean-cobalt/>, accessed on 20-06-2023

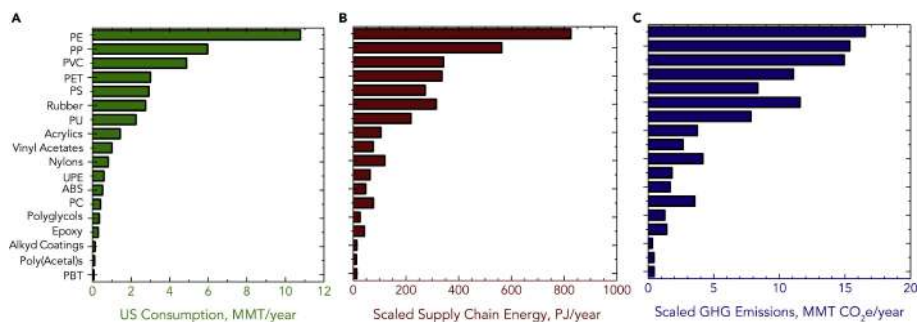
Table 19.2: Lifecycle emissions of the stages of secondary and semi-finished product production of aluminium in the EU [38]

Activity	Product vol.EU27 (Mt)		GHG emissions (Mt CO ₂ -eq.)
Secondary remelting	4.9	150 – 350	0.88
Secondary refining	3.0	250 – 390 ³	0.96
Rolling operations	4.8	20 – 235	0.35
Extrusion operations	3.3	50 – 250	0.30

difficult to pinpoint a specific origin for the refined copper used for wires and motors, and thus this general number will be used.

Polymers

The LLS system mostly uses High Molecular Weight Poly-Ethylene (HMWPE), also known by the trademark Dyneema®. In Figure 19.2, it can be observed that the US consumption of Poly-Ethylene (PE) is approximately 10.9 Mt per year, with the associated emissions being 16.5 Mt_{CO₂e} per year, yielding an equivalent emission ratio of about $1.5 \frac{t_{CO_2e}}{t_{PE}}$. The numbers for HMWPE specifically may be different, but due to a lack of data on the emissions associated to the production of HMWPE, the previously stated numbers will be used as a reference. Dyneema® also offers Bio-based Dyneema®, which is therefore suggested as a more sustainable alternative to fossil-based HMWPE, yielding requirement CON-LLS-GEN-03-07. A few other polymers used by the LLS or AWE systems are Nylon and Polyester (of which the most commonly used is Polyethylene Terephthalate (PET)), which can be found to produce about $5.1 \frac{t_{CO_2e}}{t_{Nylon}}$ and $3.7 \frac{t_{CO_2e}}{t_{PET}}$ respectively.

**Figure 19.2:** Consumption, energy consumption and CO₂ equivalent emissions of different polymer supply chains in the US [40]

19.3. Transport

Transportation represents a large contribution to emissions within any supply chain. For the LLS system, transportation impacts not only production and manufacturing emissions but also has a significant influence on operational emissions. This is particularly relevant because the LLS system is designed for soft-kite AWE systems, which are designed for highly mobile applications and therefore may be deployed on a site for a short or mid-term period and then transported for deployment elsewhere.

Given that the system is designed to be accommodated within two or more 20ft containers, only modes of transport relevant to container transport are taken into account during the analysis.

Rail

Among different modes of ground transport, rail transport stands out as the most efficient option, with emission levels varying depending on whether diesel or electric traction is utilised and how cargo logistics are managed. In scenarios involving the transport and delivery of multiple containers to a deployment location, the most efficient logistical strategy is to employ a locomotive that can move all the systems together as a block train, which simply means reserving an entire train. Conversely, transporting one or only a few systems via single wagon trains proves to be significantly less efficient. In such cases, it is preferable to opt for intermodal container trains, as indicated by the data presented in Table 19.3. While the availability of electric traction may be limited to certain areas or specific segments of a journey, it is advisable to prioritise the use of electric locomotives whenever feasible.

Table 19.3: Emissions of freight rail transport by modality (a Block train is a train entirely reserved by a single company for transporting its cargo) [41]

Transport Operation category	Empty running (% of distance)	Load factor (%)	Traction energy	GHG emission intensity value (gCO ₂ e/tkm)
Level 1: Overall sector average	33	40	Average	19
Level 2: Container train (intermodal)				
Diesel train	17	50	Diesel	25
Electric train	17	50	Electric	12
Level 2: Block train (RTC)				
Diesel train	50	100	Diesel	24
Electric train	50	100	Electric	12
Level 2 : Single Wagon train (RTC)				
Diesel train	50	100	Diesel	33
Electric train	50	100	Electric	16

Table 19.4: Emissions of inland-waterways freight shipping by modality [41]

Vesselcategory	Vessel weight (tonnes)	GHG emission intensity value (gCO ₂ e/tkm)
General cargo	0-4999	34.7
	5000-9999	26.1
	10000-19999	23.5
	20000+	12.4

Table 19.5: Emissions of freight road transport by modality [41]

Transport Operation category	Empty running (% of total distance)	Typical load (tonnes)	GHG emission intensity value (g CO ₂ e/tkm)
Container Truck	50	24	83

Table 19.6: Example calculations for shipping emissions per payload tonne for ports in the Caribbean (Central America), Asia and Africa, using the data from Table 19.7 and shipping distances from sea-distances.org³

Ports	Distance (nm)	Distance (km)	Emissions (gCO ₂ e/t)
Rotterdam - Port au Prince (Haiti)	4189	7758	45000
Rotterdam - Ho Chi Minh (Vietnam)	8934	16550	60000
Rotterdam - Djibouti (Djibouti)	4651	8614	75000

Table 19.7: Emissions of international freight shipping by modality [41]

Transport Category	Container Size (feet)	GHG emission intensity (gCO ₂ e/tkm)
Intra NW Europe	20'	7.4
	40'	12.0
NW Europe - Mediterranean	20'	5.2
	40'	8.5
NW Europe - Asia	20'	2.2
	40'	3.6
NW Europe - Africa	20'	5.3
	40'	8.7
NW Europe - South & Central America	20'	3.6
	40'	5.8
NW Europe - Middle East /India	20'	3.0
	40'	4.8
NW Europe - Oceania	20'	4.2
	40'	6.9

Sea shipping

In addition to being the primary mode of intercontinental freight transport, international freight shipping is also the most efficient means of long-distance transportation, with a maximum emission rate of only 12.0 gCO₂e/tkm for shipping between ports in Northwestern Europe, as illustrated in Table 19.7. Consequently, it is strongly recommended to make use of sea shipping whenever feasible for international transportation.

From Table 19.6, it becomes apparent that transport to East Africa has the highest emissions, despite not being the farthest destination from Northwestern Europe. (For shipping to Djibouti, the values for Africa were used instead of those for the Middle East).

Inland-waterway shipping

Inland-waterway ship transport can be a highly advantageous choice in specific scenarios. In situations where extensive waterways are accessible, but electrified rail systems are not in place, employing a barge exceeding 10,000 t proves to be more efficient than a diesel train. The emission levels for such barge transport range from 12.4 gCO₂e/tkm to 23.5 gCO₂e/tkm.

Furthermore, even when compared to road transport, barge transport remains more efficient regardless of the size of the barge. As a result, prioritising barge transport is recommended.

³<http://sea-distances.org/>, accessed on 09-06-2023

Road transport

Dedicated road transport (by container trucks) has, by far, the highest emissions of all considered modes of transport, at $83 \text{ g}_{\text{CO}_2\text{e}}/\text{tkm}$. It should therefore be exclusively reserved for last-mile transport whenever possible.

19.4. End-of-life

The End-of-life of the system should be as sustainable as possible. A relatively simple and robust way of ensuring this is to make it largely recyclable (at least 30 %), which yields requirement CON-LLS-GEN-03-02.

For the purposes of this report, any aluminium and steel used in the LLS system shall be considered fully recyclable, copper will also be considered 100 % recyclable, and any polymers (Dyneema[®], Nylon, Polyester) will be considered 0 % recyclable due to UV degradation.

19.5. Payback Period

Following the simplified LCA guidelines stipulated in Section 19.1 through Section 19.3, it can be seen in Table 19.8 that the total calculated emissions payback period of the system is 1754 h, or roughly 73 days of continuous operation, less than 2.5 months. This is well below the 22.5 months limit set by requirement CON-LLS-GEN-03-04. Even with all the additional emissions from kite and tether replacements and maintenance, it is very likely that the system's emissions payback period will still stay well clear of 22.5 months.

Table 19.8: Emissions and payback times per subsystem

Subsystem	Emissions [$\text{kg}_{\text{CO}_2\text{e}}$]	Payback Period [h]	Reference
Tower	137	5	Section 7.7
Guiding Cable	179	7	Section 8.7
Cable Cart	267	10	Section 9.7
Anchoring Mechanism	420	16	Section 10.7
Electrical System	37780	1445	Section 11.7
Ground Station	4560	174	Section 12.7
Kite & KCU	646	25	Section 13.7
Transport	1886	72	Section 18.7
Total	45876	1754	

19.6. Recyclability

Table 19.9: Mass of materials used per subsystem. Green is for recyclable materials, orange is for non-recyclable materials. *Note that the batteries' energy density is assumed to be 100 Wh/kg ⁴

Material Subsystem	Tower	Cable	Cart	Anchor	Elec. Sys.	Station	Kite & KCU	Total
Aluminium [kg]	274.4		48				63	385
Steel [kg]		69	88	221	4675	2400		7350
Copper [kg]			7.2		947		7	961
Nylon [kg]							100	100
Dyneema [®] [kg]		32					51.1	83
Polyester [kg]			0.76					0.76
Batteries* [kg]			4.2		3360			3364
Total	274	101	148	221	8982	2400	221	12240

⁴[https://www.cei.washington.edu/education/science-of-solar/battery-technology/#:~:text=Compared%20to%20the%20other%20high,%2D670%20Wh%2FL\).](https://www.cei.washington.edu/education/science-of-solar/battery-technology/#:~:text=Compared%20to%20the%20other%20high,%2D670%20Wh%2FL).) ., accessed on 19-06-2023

From Table 19.9 and according to the guidelines specified in Section 19.4, the total mass of recyclable materials in the system is about 8696 kg, or around 71% of the total mass of the system. This is well above the minimum of 30% set by requirement CON-LLS-GEN-03-02.

19.7. Observations

There are multiple possible points of concern regarding the sustainability of the system, some of the most important will be listed herein:

- Dyneema® cables may need frequent replacement due to damage from UV radiation and heat from friction from the cart wheels.
- While UV-radiation degradation products and microplastics/monomers from mechanical abrasion may be released into the environment by the Dyneema® in the system, the shed amounts of these contaminants are most likely negligible, and therefore the system can be considered to comply with requirement STK-PVS-02.
- Machining, surface treating and transport of finished individual pieces were not accounted for in the lifecycle assessment, while these processes may represent a significant source of emissions.
- There are uncertainties about the true emissions from each material and the batteries depending on the exact location of origin, processing and supply chain which cannot be captured in a report of the nature of the present report, and would have to be reviewed in order to get a more precise outlook on the project's emissions.

19.8. Recommendations

There are several recommendations which might be helpful for engineers wishing to further work on the design described in the present report.

- An environmental impact assessment regarding flora, fauna, soil and water quality should be conducted on different environments the system may operate in, in order to better understand its impact on the quality of the local ecosystem and resources.
- The use of Bio-based Dyneema® should be considered for Dyneema® DM20, as per requirement CON-LLS-GEN-03-07.
- Some sort of mantle to the Dyneema® cable could be considered. Otherwise, frequent reapplication of a strong UV treatment might help.
- The use of partially recycled Nylon for the kite could reduce the emissions from making it.
- A compromise between the use of aluminium and steel should be reached for a more detailed design. Aluminium is both less polluting (when secondary) and lighter, which means it leads to lower transport emissions, but it is also significantly more expensive than steel.
- Vilnius is a very convenient location because it is easily accessible by cargo ship and train. A similarly advantaged location should be considered should a different one be desired.
- Off-the-shelf mass-made parts are potentially less polluting than custom-made parts, and should therefore be used when possible.

The most important recommendation, of course, is that a truly in-depth lifecycle assessment of the entire system, both the LLS and AWE systems be performed, accounting for full supply chain emissions, assembly emissions, cumulative emissions from transport, maintenance and replacement throughout the system's lifetime, and so on. Only through such an in-depth assessment can the true impact of the project be understood.

Conclusion

The purpose of this report was to describe a design that fully automates the landing, storage and re-launching of an airborne wind energy system. This need has been tackled by considering four design concepts. From which the Offset Winch Launch (OWL) was chosen. In this concept, the kite takes off from a tower on top of the ground station. When enough wind is available the kite can lift off from the tower without winching. However, for wind speeds below 6.6 m s^{-1} , the kite will not naturally take off and is therefore winched up (pulled). Followed by a turn of the kite with the wind direction and a glide-down to increase the tether length. After this step, the kite is towed up again. This is called a Stepped Tow Launch (STL) and is repeated until the kite reaches enough altitude and can be parked.

The landing procedure consists of first descending the kite from operational to tower height by steering the kite to the edge of the power zone. The last part of the descent is performed with the kite at the azimuth, this allows for better control and a more beneficial position with respect to the tower.

For storage, the kite is rolled on top of the landing tower using the Rolling Storage System (RSS). This is done by connecting the kite to the tower with a connection eye at the leading edge and with a clamp at the trailing edge. Then the kite is deflated and rolled around the tower. During this procedure it is important to keep the bridles tensioned to prevent entanglement.

The operations of the OWL prescribe changes to the existing AWE system design. Therefore, 7 subsystems are designed. The tower is designed for structural integrity and storage capabilities. The guiding cable subsystem describes the structure of the cable that allows the cable cart to move between the main container and the offset point. The cable cart subsystem must drive along the guidance cable and guide the tether properly to the winch. The anchoring subsystem has the main purpose of keeping the station on the ground when the kite pulls on it. The electrical subsystem contains all electrical components inside the ground station, which itself is designed for structural, interface and storage purposes. Lastly, the kite and Kite Control Unit (KCU) are designed to make it compatible with the launch, landing and storage procedures. For this purpose, a connection eye, mid-strut, leading-edge tether and UV coating are added.

Although much effort has been put into the design, some parts turn out to be improvable. The following major recommendations for future OWL development are proposed:

- For a better financial overview more data on actual sales and failure are required to understand the total revenue and cost of the system.
- Improve on the understanding and modelling of the STL. This is a very important part of the functioning of the system. Although it is a proven method for paraglider take-off, at the moment the operation's dynamics are rather unknown.
- Make the tower more scalable by scaling the kite in the chordwise direction rather than the spanwise direction. This will limit the increase in kite-KCU distance when the kite is increased. The other option is designing an alternative for the tower itself.
- Replace the cable cart with a tether retraction link between the offset point and the main tether. This is very similar to the connection between the Leading Edge Tether (LET) and the KCU.
- Increase the electrical design detail by assessing the microgrids where the AWE system is operating and adapting the design based on this.

Bibliography

- [1] Salma, V., Friedl, F., and Schmehl, R., "Improving reliability and safety of airborne wind energy systems," *Wind Energy*, Vol. 23, 2020. <https://doi.org/10.1002/we.2433>.
- [2] Corporation, I. F., "The Dirty Footprint of the Broken Grid," , September 2019. <https://doi.org/10.13140/RG.2.2.25767.29602>.
- [3] Commission, E., for Research, D.-G., and Innovation, *Study on challenges in the commercialisation of airborne wind energy systems*, Publications Office, 2018. <https://doi.org/doi/10.2777/87591>.
- [4] Weber, J., Marquis, M., and et al., "Airborne Wind Energy," *Airborne Wind Energy*, 2021. URL <https://www.nrel.gov/docs/fy21osti/79992.pdf>.
- [5] IRENA, Jul 2022. URL http://www.irena.org/publications/2022/Jul/-/media/Files/IRENA/Agency/Publication/2022/Jul/IRENA_Power_Generation_Costs_2021_Summary.pdf?la=en&hash=C0C810E72185BB4132AC5EA07FA26C669D3AFBFC.
- [6] Watson et al., "Future emerging technologies in the wind power sector: A European perspective," *Renewable and Sustainable Energy Reviews*, Vol. 113, 2019, p. 109270. <https://doi.org/https://doi.org/10.1016/j.rser.2019.109270>, URL <https://www.sciencedirect.com/science/article/pii/S1364032119304782>.
- [7] Associates, B., "Getting airborne – the need to realise the benefits of airborne wind energy for net zero," , 2022. URL <https://airbornewindeurope.org/wp-content/uploads/2023/03/BVGA-Getting-Airborne-White-Paper-220929.pdf>.
- [8] "Our Vision for A Clean Planet for All: Industrial Transition," , Nov 2018.
- [9] "Offshore renewable energy," , 2023. URL https://energy.ec.europa.eu/topics/renewable-energy/offshore-renewable-energy_en.
- [10] Pietro Faggiani, R. S., "Design and Economics of a Pumping Kite Wind Park," , 2018. URL <https://www.awesco.eu/publication/faggiani-2018/faggiani-2018.pdf>.
- [11] IRENA, I., and Centre, T., *Off-grid Renewable Energy Systems: Status and Methodological Issues*, International Renewable Energy Systems, 2015. https://doi.org/https://www.irena.org/-/media/Files/IRENA/Agency/Publication/2015/IRENA_Off-grid_Renewable_Systems_WP_2015.pdf?rev=59541b40ebbb4acd9e9ce2bf8d52d075.
- [12] Viré, A., "Wind and Wave Resources," , 2022.
- [13] Schmehl, R., *Airborne Wind Energy: An overview of the technological approaches*, Springer, 2013.
- [14] Schmehl, R., "Project Guide Design Synthesis Exercise," , 2023.
- [15] Roling, P., "Course AE2230-1: Lecture Notes on Turning flight," , 2022.
- [16] Roling, P., "Course AE2230-1: Lecture Notes on Climb and descent," , 2022.
- [17] Ahmad, F., "Structural Optimization of Cantilever Beam in Conjunction with Dynamic Analysis," *Journal of Applied Mechanics and Materials*, 2011.

- [18] Morrison, S. C., *Damping Wind-Induced Vibrations on Low-Level Lighting Poles*, Publisher, 2017.
- [19] Briden, R., "A Guide to the Selection, Installation and Maintenance Including the Cause and Effects of Pole Vibration," , January 2016.
- [20] White, F. M., *Fluid Mechanics*, 4th ed., McGraw Hill, 1999.
- [21] T.Zhou, Razali, S., Hao, Z., and Cheng, L., "On the study of vortex-induced vibration of a cylinder with helical strakes," *Journal of Fluids and Structures*, Vol. 27, No. 7, 2011, pp. 903–917. <https://doi.org/https://doi.org/10.1016/j.jfluidstructs.2011.04.014>.
- [22] "Slewing Rings, technical handbook," , 2023. URL <http://www.balnex.pl/uploads/file/download/ksiazka-techniczna-lozyska-wiencowe.pdf>.
- [23] Buckham, B., Nahon, M., Seto, M., Zhao, X., and Lambert, C., "Dynamics and control of a towed underwater vehicle system, part I: model development," *Pergamon*, 2003.
- [24] FibrXL, "Dyneema® Product data sheet," , 2020. URL <https://fibrxl.com/wp-content/uploads/2020/07/FibrXL-PDS-performance-0720-DEF-Dyneema.pdf>.
- [25] Braids, E., "Dyneema® Max DM20," , 2020. URL https://www.moremarine.nl/pdf/dyneema_dm20_specs.pdf.
- [26] Back, J., "Lithium Battery Safety," *Environmental Health and Safety, University of Washington*, 2021.
- [27] Pedersen, N. L., "Stress concentration and optimal design of pinned connections," *The Journal of Strain Analysis for Engineering Design*, 2019. <https://doi.org/10.1177/0309324719842766>.
- [28] T.H.G, M., *Aircraft Structures for Engineering Students*, 6th ed., Todd Green, 2017.
- [29] DSE Group 20, "Design Synthesis Exercise: Baseline Report," Baseline Report, April 2023.
- [30] International Organization for Standardization, "ISO 668:2020," , 2020. URL <https://www.iso.org/standard/76572.html>, series 1 freight containers – Classification, dimensions and ratings.
- [31] Containerhandel, S., "Technical Specification for a typical 40'x 8'x 9'6" ISO Type Steel Dry Cargo Container "High Cube"," , 2012.
- [32] Zappalá, D., "Lecture 2 – Offshore Wind RAMS," , 2022.
- [33] Jehle, C., and Schmehl, R., "Applied Tracking Control for Kite Power Systems," *Journal of Guidance, Control, and Dynamics*, Vol. 37, No. 4, 2014, pp. 1211–1222. <https://doi.org/10.2514/1.62380>.
- [34] Aziz, E., Esche, S., and Chassapis, C., "Online Wind Tunnel Laboratory," *American Society for Engineering Education*, 2008. <https://doi.org/10.18260/1-2--3402>.
- [35] Dammeier, L., Loriaux, J., Steinmann, Z., Smits, D., Wijnant, I., Hurk, B., and Huijbregts, M., "Space, Time, and Size Dependencies of Greenhouse Gas Payback Times of Wind Turbines in Northwestern Europe," *Environmental Science & Technology*, Vol. 53, 2019. <https://doi.org/10.1021/acs.est.9b01030>.

- [36] Arshad, F., Lin, J., Manurkar, N., Fan, E., Ahmad, A., un Nisa Tariq, M., Wu, F., Chen, R., and Li, L., "Life Cycle Assessment of Lithium-ion Batteries: A Critical Review," *Coventry University*, 2022. <https://doi.org/https://doi.org/10.1016/j.resconrec.2022.106164>.
- [37] Hasanbeigi, A., "Part 1: Cleanest and Dirtiest Countries for Primary Steel Production," , 2020. URL <https://www.globalefficiencyintel.com/new-blog/2020/cleanest-dirtiest-countries-primary-steel-production-energy-co2-benchmarking>.
- [38] Ecofys, Fraunhofer Institute for Systems and Innovation Research, and Öko-Institut, "Methodology for the free allocation of emission allowances in the EU ETS post 2012: Sector report for the aluminium industry," , November 2009.
- [39] Lewis, A., "Energy-related CO₂ emissions intensity for an indicative refined copper production project under different energy consumption scenarios," , 2021. [Accessed 13-06-2023].
- [40] Nicholson, S. R., Rorrer, N. A., Carpenter, A. C., and Beckham, G. T., "Manufacturing energy and greenhouse gas emissions associated with plastics consumption," *Joule*, Vol. 5, No. 3, 2021, pp. 673–686. <https://doi.org/https://doi.org/10.1016/j.joule.2020.12.027>.
- [41] Smart Freight Centre, C., *Calculating GHG transport and logistics emissions for the European Chemical Industry*, 2021. URL <https://cefic.org/app/uploads/2021/09/Calculating-GHG-transport-and-logistics-emissions-for-the-European-Chemical-Industry-Guidance.pdf>.
- [42] Pietro, F., "Pumping Kites Wind Farm," Master's thesis, TU Delft, 2014.
- [43] Fingersh, L., Hand, M., , and Laxson, A., "Wind Turbine Design Cost and Scaling Model," Tech. rep., National Renewable Energy Laboratory, Midwest Research Institute, Battelle, dec 2006.

Risk Register

Table A.1: Technical risks of the landing tower subsystem

ID	Title	Category	Cause	Effect	Consequence	Initial Like- li- hood	Initial Im- pact	Initial risk	Risk Owner	Planned Response	New Like- li- hood	New Im- pact	New Risk
RSK-TCH-LT-01	Bearing failure	Technical	Wear on the bearing	Failure of bearings	Tower inoperable	3	4	12	CME	Use closed and dust-resistant bearings in addition to good lubrication	2	4	8
RSK-TCH-LT-02	Corrosion	Technical	Combination of water and metal	Corrosion on the metal structure	Tower structure is weaker than designed	4	2	8	CSM	Apply sufficient amounts of protective paint, especially in coastal regions. Identify critical areas and protect those more	1	2	2
RSK-TCH-LT-03	RSS motor failure	Technical	Motor components wear	RSS motor fails during operation	Tower inoperable	3	4	12	CE	Include a redundant motor	3	1	3
RSK-TCH-LT-04	Bridles entangled inside the RSS cylinder	Technical	Bridles lay at the RSS cylinder and can get rotated around the axle	Bridles get entangled around the axle	System inoperable	5	4	20	CSC	Use a guard to prevent the bridle lines from entangling in the RSS mechanism	2	4	8
RSK-TCH-LT-05	Kite clamping does not (sufficiently) close	Technical	Mechanism must interact with a highly dynamic kite	The clamping system cannot close around the attachment on the kite	The kite could fall off the tower and make the system inoperable.	3	4	12	CME	When this happens, the tether and the power tape are tensioned so the kite is pulled firmly on the RSS. Then there should be maintenance.	3	3	9
RSK-TCH-LT-06	Tower overload	Technical	High speed gust which is not expected	Stress in the tower can be higher than designed for	Tower might suffer plastic deformation	1	3	3	CSM	Include a fast response from the KCU to depower the kite to relief the tower from the loads	1	2	2
RSK-TCH-LT-07	Error in controlling the tower	Technical	System computer can encounter errors	The tower control is lost	System inoperable	3	3	9	CSS	Halt operation while the error is not solved. Make the system also manually operable	3	2	6
RSK-TCH-LT-08	RSS cylinder freezes	Technical	Low temperature environments	The RSS freezes	The kite cannot be stored due to limited rotation	1	3	3	CS	Make the system more resistant to the relevant environment by implementing heaters for moving parts of the system	1	1	1

Table A.2: Technical risks of the guidance cable subsystem

ID	Title	Category	Cause	Effect	Consequence	Initial Like-li-hood	Initial Im-pact	Initial risk	Risk Owner	Planned Response	New Like-li-hood	New Im-pact	New Risk
RSK-TCH-GC-01	Tensioning system failure	Technical	Continuous high loads	Tensioning system fails	Excessive cable sag	2	3	6	CME	Include health monitoring of the system	1	3	3
RSK-TCH-GC-02	Cable rupture	Technical	High loads with crack formation	Cable ruptures (during operation)	System becomes inoperable during low wind durations	1	4	4	CSM	Regularly inspect of the cable mantle. Do maintenance if damaged	1	4	4
RSK-TCH-GC-03	Cable unraveling	Technical	High loads with crack formation	Cable unravels	Cable cart cannot move over the cable	1	3	3	CSM	Regularly inspect of the cable mantle. Do maintenance if damaged	1	3	3

Table A.3: Technical risks of the cable cart subsystem

ID	Title	Category	Cause	Effect	Consequence	Initial Like-li-hood	Initial Im-pact	Initial risk	Risk Owner	Planned Response	New Like-li-hood	New Im-pact	New Risk
RSK-TCH-CC-01	Motor fails	Technical	Motor components wear	The cart motor fails during operation	Cart inoperable	3	3	9	CE	Include a redundant motor	3	1	3
RSK-TCH-CC-02	Wheel bearings fail	Technical	Wear on the bearing	Failure of bearings	Cart inoperable	3	3	9	CME	Use closed and dust-resistant bearings in addition to good lubrication	1	3	3
RSK-TCH-CC-03	Tether-pulley aligner fails	Technical	High lateral loads in the tether	The tether aligner cannot steer the tether	The tether will wear faster	2	2	4	CME	Include a failure check and fuse for when the aligner fails	2	1	2
RSK-TCH-CC-04	Pulley cannot rotate to align with the tether	Technical	Foreign objects can block the rotational joint	Excessive moments on the cart	Cart must stop operation for safety	2	3	6	CSM	Make the system IP4X rated or higher	1	3	3

Table A.4: Technical risks of the anchoring subsystem

ID	Title	Category	Cause	Effect	Consequence	Initial Like-li-hood	Initial Im-pact	Initial risk	Risk Owner	Planned Response	New Like-li-hood	New Im-pact	New Risk
RSK-TCH-ANC-01	Helix anchors lose grip	Technical	High repetitive loads can loosen the anchors	The anchors lose grip	The container be moved by the high loads	2	4	8	CSM	Study area beforehand and pick more/other anchors if normal ones don't hold soil	1	4	4
RSK-TCH-ANC-02	Helix anchors cannot penetrate the ground	Technical	Helix anchors are not suitable for hard soil types	The anchors cannot penetrate the ground	The container cannot operate in the terrain	3	4	12	CSM	Study area beforehand and pick other anchors if normal ones does not penetrate	1	4	4

Table A.5: Technical risks of the electrical subsystem

ID	Title	Category	Cause	Effect	Consequence	Initial Like-li-hood	Initial Im-pact	Initial risk	Risk Owner	Planned Response	New Like-li-hood	New Im-pact	New Risk
RSK-TCH-ES-01	Main electrical cable fails	Technical	Wear or damage to cable	Electrical cable fails	Energy cannot be transported between the main and battery container	3	4	12	CE	Have a backup battery in the groundstation to safely land the system etc	3	2	6
RSK-TCH-ES-02	System short cut	Technical	Wear or damage to the system	Short circuit	The system could catch fire	2	4	8	CE	Use fuses for all electric components	3	1	3
RSK-TCH-ES-03	Sudden loss of battery capacity	Technical	Water intrusion, series connection failure	Battery capacity becomes less	Less energy can be stored and used during operation	3	2	6	CE	Have a backup battery that can power critical systems and prevent further system failure	1	2	2
RSK-TCH-ES-04	Battery charge controller fails	Technical	Electrical components fail	Battery charge cannot be regulated	System must halt operations to prevent further damage	2	3	6	CE	Use a redundant battery charge controller	1	3	3
RSK-TCH-ES-05	Battery has no charge left	Technical	System uses electricity for launch, landing and storage	Battery could be completely empty	The system cannot finish a step launch, land or store the kite	2	3	6	CE	Use discharge protection so there will always be juice left to power the system, unstore and launch	1	3	3
RSK-TCH-ES-06	Generator fails	Technical	Electrical components fail	Generator fails	System inoperable	2	4	8	CE	Use higher specification parts for critical systems	1	4	4
RSK-TCH-ES-07	Generator overheated	Technical	High power and warm environment	Generator can over-heat	System inoperable	2	4	8	CE	Use a thermal control system	1	4	4

RSK-TCH-ES-08	Generator rectifier fails	Technical	Electrical components fail	Rectifier cannot transform the AC to DC	The system cannot use the energy that is produced	2	3	6	CE	Have a backup rectifier ready	1	3	3
RSK-TCH-ES-09	Anemometer failure	Technical	Sensors fail (impact, freezing, etc)	The anemometer fails	The exact wind speed and direction are unknown	2	1	2	CE	Use two anemometers	1	1	1

Table A.6: Technical risks of the ground station subsystem

ID	Title	Category	Cause	Effect	Consequence	Initial Like-li-hood	Initial Im-pact	Initial risk	Risk Owner	Planned Response	New Like-li-hood	New Im-pact	New Risk
RSK-TCH-MC-01	Winch motor fails	Technical	Motor components wear	The winch motor fails during operation	The system is inoperable	3	4	12	CE	Include a redundant motor	3	1	3
RSK-TCH-MC-02	Tether-drum aligner fails	Technical	High lateral loads in the tether	The tether aligner cannot steer the tether	The tether can cut into itself or the drum can be damaged	2	3	6	CME	Include a failure check and fuse for when the aligner fails	2	1	2
RSK-TCH-MC-03	Winch support structure overload	Technical	High gust loads	The winch support structure can be overloaded	The system gets damaged	1	3	3	CSM	Include a fast response from the KCU to depower the kite to relief the tower from the loads	1	2	2
RSK-TCH-MC-04	Increase in signal noise	Technical	Higher temperatures, more signal from neighboring systems	The signal noise increases	Communication could fail	2	3	6	CS	Overdesign the communication link	2	1	2
RSK-TCH-MC-05	Antenna failure	Technical	Components fail	Antenna fails	System inoperable	2	4	8	CE	Add redundant antenna	2	1	2
RSK-TCH-MC-06	Receiver failure	Technical	Components fail	Receiver fails	System inoperable	2	4	8	CE	Add redundant receiver	2	1	2
RSK-TCH-MC-07	Transmitter failure	Technical	Components fail	Transmitter fails	System inoperable	2	4	8	CE	Add redundant transmitter	2	1	2

RSK-TCH-MC-08	Water leak	Technical	Wear of the container, insufficiently closed cable cart opening	Water leak in the main container	Water damage inside the container	1	1	1	CE	Make the system water resistant to IPx6 or higher. Keep electrical and other water or moisture-sensitive components above the container floor.	1	1	1
---------------	------------	-----------	---	----------------------------------	-----------------------------------	---	---	---	----	--	---	---	---

Table A.7: Technical risks of the kite subsystem

ID	Title	Category	Cause	Effect	Consequence	Initial Like-li-hood	Initial Im-pact	Initial risk	Risk Owner	Planned Response	New Like-li-hood	New Im-pact	New Risk
RSK-TCH-KT-01	Bridles get entangled during launch	Technical	Relative motion between ground station components and bridles	The bridles might get entangled	The kite cannot take-off	5	4	20	CSC	Put bridles under some tension when unstoring and landing	3	4	12
RSK-TCH-KT-02	Reattachment mechanism from KCU to LE tether fails	Technical	The attachment must sustain high tension when reattaching	The LE tether cannot reach the KCU	The LE tether will entangle with the bridles during landing	3	3	9	CSC	Make sure the kite is still able to land without this	3	2	6
RSK-TCH-KT-03	LE bridle tension control fails	Technical	The tension sensor fails	LE bridle tension cannot be measured	Control of the kite deteriorates	2	3	6	CE	Automatic release of LE tether	2	2	4
RSK-TCH-KT-04	Tether fails in flight	Technical	Lightning impact or an extreme gust	Tether gets burnt and snaps	Tether flies away and can hit buildings or people	2	5	10	CME	Depower the kite when tether snaps by sensing 0 N tension in the tether. Include control program which steers the kite towards a safe area on the ground	2	3	6
RSK-TCH-CDH-01	Main communication link between KCU and GCU fails	Technical	Electrical malfunction	Communication link becomes inoperable	No communication possible between KCU and GCU	2	4	8	CE	Implement a second and third communication link as redundancies	1	4	4
RSK-TCH-CDH-02	Communication link between GCU and cart fails	Technical	Electrical malfunction	Communication link becomes inoperable	No communication possible between GCU and cart	2	3	6	CE	Implement a second communication link as a redundancy	1	3	3
RSK-TCH-CDH-03	Communication link between GCU and external control centre fail	Technical	Electrical malfunction	Communication link becomes inoperable	No communication possible between GCU and external control centre	2	2	4	CE	Implement a second communication link as a redundancy, land and stay grounded until repaired	1	1	1

Financial Overview Model

This chapter discusses the model developed to conduct the financial analysis and produce the financial overview of the project discussed in Chapter 2. Section B.3 introduces the equations used in constructing the model. This is followed by the glossary for the parameters used in the analytical model at Section B.4.

B.1. Access to the Model

The financial model allows the user to vary multiple parameters with high levels of freedom and observe the change in the financial impact of the AWE+LLS project. It is possible to access the model using the link provided:

<https://docs.google.com/spreadsheets/d/1f99PhzI6HfeuH-mXRMHXrph3RMiWAB67/>

B.2. Model Interface

The financial overview has been developed in Excel and utilises the inter-dependency between parameters, which are provided in Section B.4. This section has been divided into two parts with Section B.2.1 explaining the inputs of the model and Section B.2.2 the outputs.

B.2.1. Input

The model takes the market scaling and learning parameters in order to simulate the growth in demand for the product. The learning rate is used to simulate the decrease in cost of manufacturing over the years, which is dependent on the number of units produced. This part of the interface is shown in Figure B.1. These inputs are used with the pricing parameters, shown in Figure B.2, which in turn generate the annual cash flows as shown in Figure B.5.

Market and Tech. Scale Parameters		
Target Market Size [units]		5,00E+06
First Year Sales [#]		40
Target Market Growth [%]		9%
Initial Market Share Growth [%]		30%
Learning Rate [%]		8%
Discount Rate [%]		6,73%
Corporate Income Tax [%]		22%
Dollar to Euro exchange rate [-]		0,93

Figure B.1: Market and technology scale input parameters

Pricing		
Selling Price		€ 812.369,10
Downpayment [€]		€ 300.576,57
Downpayment fraction [%]		37%
Downpayment premium [%]		0%
Annual Installment [€]		€ 25.589,63
Initial Manufacturing Cost [€]	\unit	€ 175.000,00
Initial O&M Cost [€]	\unit\yr	€ 25.275,00
Initial Logistical Cost [€]	\unit	€ 8.920,00
R&D Investment TOTAL - TRLS [ME]		€ 40.000.000,00
R&D Investment KITEPOWER - TRLS [ME]		€ 30.000.000,00
R&D Investment LLS - TRLS [ME]		€ 15.000.000,00
R&D Grants		€ 5.000.000,00
Cost of Decom. /unit [€]	\unit	€ 4.920,00

Figure B.2: Pricing input interface

Note that the cells highlighted in yellow indicate an input cell, while white cells that are not highlighted are automatically calculated based on the input cells.

The freedom to also modify the individual cost components is also present in the model. The cost breakdown section is used for this purpose alone, which is shown in Figure B.3. The values as seen in Figure B.3 are taken from [42] where a statistical approach based on the rated power of an AWE system was conducted to estimate some of the cost components.

Cost Breakdown		
Operation and Maintenance		
Consumables	\unit\yr	€ 17.000,00
O&M	\unit\yr	€ 6.525,00
Insurance	\unit\yr	€ 1.750,00
Installation and Decommissioning - Logistics		
Transport and Installation	\unit	€ 4.000,00
Civil Works	\unit	€ 4.920,00
Cables Installation	\unit	€ -
Units Removal	\unit	€ 4.920,00
Cables Removal	\unit	€ -

Figure B.3: Cost breakdown interface

B.2.2. Output

The annual sales, market growth, change in market share and size can be seen in the top part of the sheet. This part, with a snippet shown in Figure B.4, extends to cover the entirety of the project's lifetime of 30 years. An additional note to make at this point is that all values seen in this section are not final and are provided as an example.

Year [-]	1	2	3
Sales Growth [%]	42%	42%	42%
Cum. Demand Growth [%]	42%	60%	85%
Market Share Growth Slowdown [%]	0%	0%	0%
Sold Units (per Year)	40	57	81
Sold Units (cum)	40	97	178
Market Size (units)	5,00E+06	5,47E+06	5,98E+06
Market Share [%]	0,0008%	0,0018%	0,0030%

Figure B.4: Market simulation interface

The variables in Figure B.4 are explained in further detail in Table B.1. This section only involves the simulation of the market in terms of sales. A number of sales are used to generate the annual revenue and expenses, which in turn give the annual cash flow. All financial values on a yearly basis are shown in Figure B.5. Following the annual values, parameters that indicate that the project is worth investing in (or not) are provided in the interface shown in Figure B.6.

Year [-]	1
Revenue Streams	
Sales Revenue	€ 12.023.062,64 €
Installment Revenue	€ 1.023.585,06 €
Expenses	
Manufacture Cost /unit	€ 175.000,00 €
Annual Manufacture Costs	€ 7.000.000,00 €
O&M Costs / time	€ 25.275,00 €
Annual O&M Costs	€ 1.011.000,00 €
Logistical Costs / time	€ 8.920,00 €
Annual Logistical Costs	€ 356.800,00 €
Cost of Decommissioning	€ - €
Taxes	€ 2.805.029,26 €
Cash Flow	
Net Cash Flow	€ 1.873.818,45 €
NPV	€ 41.740.110,75 €

Figure B.5: Annual cash flow interface

Finances - Investment	
Net Revenue (30 yrs) [€]	€ 0,00
Net Present Value (NPV) (TODAY)	€ 59.155.274,21
Internal Rate of Return (IRR)	30,24%
Return of Investment (ROI)	0%
Payback Period (PBP)	5 years
Capital Recovery Factor (CRF)	9%
Fixed Charge Rate (FCR)	14%
LCOE - Customer [€/kWh]	€ 0,116
LCOE - Manufacturer [€/kWh]	€ 0,087

Figure B.6: Investor's interface

The green and red symbols next to some entries provided in Figure B.5 and Figure B.6 indicate that the parameter is above or below a certain threshold. In short, green indicates an acceptable value while red means an unwanted value, thus requiring the user to apply changes to the input parameters. The aforementioned "thresholds" or conditional arguments for these parameters can be summarised as follows (if the condition holds, the value is acceptable):

- $Net\ Revenue > 0$
- $NPV > 0$ ¹
- $IRR > r$ ²
- $ROI - N/A$
- $PBP - N/A$
- $CRF - N/A$
- $FCR - N/A$
- $LCOE_{AWE} < LCOE_{diesel}$

Parameters that have N/A as their condition, will need to be assessed by the investor to confirm if the project generates the required amount of revenue or value in a predefined time frame.

¹<https://www.theforage.com/blog/skills/npv>, accessed 14-06-2023

²<https://www.investopedia.com/terms/i/irr.asp>, accessed 14-06-2023

B.3. Analytical Approach

The equations are introduced in a logical order, where the information from each step is carried to the next, but all calculations are done instantaneously. In this section, the equations used to describe the different parts of the model are presented in groups. All symbols and their meanings are explained in the glossary provided in Section B.4.

B.3.1. Yearly Values

The year-specific calculations describe the market behaviour over the years. This relates to the number of units sold each year and the increase in the market share. All equations are formulated by the team, and the results were discussed with experts in the field from Kitepower³ to validate the accuracy of the market simulation.

$$fSG_i = [(1+fMI) \cdot (1+fMSG) - 1] - fMSS_i \quad (\text{B.1}) \quad fSG_{cum_i} = fSG_{cum_{i-1}} \cdot fSG_i \quad (\text{B.2})$$

$$N_{units_i} = N_{units_{i-1}} \cdot fSG_{i-1} \quad (\text{B.3})$$

The revenue and expenditure from all streams of cash flow are calculated based on the units sold during each year as calculated with Equation B.3. It should be noted that the iteration through years occurs based on the year index and not the number of units produced. For example, the learning rate equation does take into account the cumulative number of units produced up until the end of year i , but the cost of manufacturing only updates at the start of each year. This is a rather simplified approach but is considered to be accurate enough given the lack of real-world data.

$$R_{sales_i} = N_{units_i} \cdot C_{selling\ price} \quad (\text{B.4}) \quad E_{O\&M_i} = \sum_{i=1}^I N_{units_i} \cdot C_{O\&M} \quad (\text{B.8})$$

$$R_{inst_i} = \sum_{i=1}^I N_{units_i} \cdot C_{inst} \quad (\text{B.5}) \quad E_{log_i} = N_{units_i} \cdot C_{log} \quad (\text{B.9})$$

$$C_{manu_i} = C_{manu_0} \cdot N_{units_i}^{-\lambda} \quad (\text{B.6}) \quad E_{decom_t} = N_{units_{(t-20)}} \cdot C_{decom} \quad (\text{B.10})$$

$$E_{manu_i} = C_{manu_i} \cdot N_{units_i} \quad (\text{B.7}) \quad E_{tax_i} = (R_{sales_i} + R_{inst_i}) \cdot f_{tax} \quad (\text{B.11})$$

$$R_{net_i} = [R_{sales_i} + R_{inst_i}] - [E_{manu_i} + E_{O\&M_i} + E_{log_i} + E_{tax_i}] \quad (\text{B.12})$$

B.3.2. Investment values

The model uses a Discounted Cash Flow (DCF)⁴ method to provide a present value of the project by predicting the time value of future cash flows. Many methods of project/company valuation exist, but DCF analysis is a common approach in many industries and is applicable to this project. Note that an investor may choose not to invest in the project even if the condition for a parameter is positive. However, the methodology for the valuation of the project at its current preliminary stage is valid.

³<https://thekitepower.com>

⁴<https://www.investopedia.com/terms/d/dcf.asp>

$$NPV = \sum_{t=1}^T \frac{R_{net_t}}{(1+r)^t} \quad (\text{B.13})$$

$$LCOE_{customer} = \frac{NPV_{sell\ price}}{NPV_{total\ electricity}} \quad (\text{B.16})$$

$$PBP = \min(E_{total_t} - R_{net_t} < 0, t) \quad (\text{B.14})$$

$$ROI = \sum_{i=t}^T \frac{R_{net_t}}{E_{R\&D}} \quad (\text{B.15})$$

$$LCOE_{manufacture} = \frac{NPV_{total\ costs}}{NPV_{total\ electricity}} \quad (\text{B.17})$$

B.3.3. Operations & Maintenance Cost Breakdown

The individual costs for operations & maintenance-related expenses are taken from [42]. One leading assumption is that the cost of service scale up almost linearly with the rated power of the AWE system. This goes against the exponential relationship between the two parameters as seen in existing wind turbines [43], but the linear relationship has been implemented to the model as can be seen in Equation B.18.

$$C_{service} = 4500 + 4.5 \cdot P_{output} \quad (\text{B.18})$$

$$C_{insurance} = 0.01 \cdot C_{manufacturing} \quad (\text{B.19})$$

$$C_{O\&M} = C_{consumables} + C_{service} + C_{insurance} \quad (\text{B.20})$$

B.3.4. Installation and Decommissioning Logistics Cost Breakdown

Equations are taken from [43].

$$C_{installation} = C_{transport\ installation} + C_{civil\ works} + C_{cables\ installation} \quad (\text{B.21})$$

$$C_{decommissioning} = C_{units\ removal} + C_{cables\ removal} \quad (\text{B.22})$$

B.4. Glossary for Financial Overview Model

Table B.1 to Table B.3 show the list of symbols used in the financial overview model.

Table B.1: Market simulation parameters.

Symbol	Definition	Unit	Remark
f_{MI}	Target Market Growth	[%]	Parameter for sales forecast. Expected growth of the target market.
f_{MSG}	Market AWE Share Growth	[%]	Parameter for sales forecast. Expected growth of the share of AWE systems within the target market.
f_{MSS}	Market Share Growth Slowdown	[%]	Parameter for sales forecast. Slowdown in growth of AWE systems share in the target market.
f_{SG}	Sales Growth Rate	[%]	Parameter for sales forecast. Simulated growth of sales over the first 10 financial years.
f_{SGcum}	Cumulative Sales Growth	[%]	Parameter for sales forecast. Yearly sales growth multiplied by the sales growth rate.
N_{units}	Number of Units Sold per Year	[/yr]	Expected number of sales for the first 10 financial years based on the simulated growth in demand.

Table B.2: Annual cashflow parameters.

Symbol	Definition	Unit	Remark
$C_{selling\ price}$	AWE + LLS Selling Price	[€]	Selling price of the whole system (AWE + LLS).
R_{sales}	Annual Sales Revenue	[€]	Annual revenue from sales of new units alone.
C_{inst}	AWE + LLS Annual Installment Fee	[€]	Annual instalment fee of an individual unit - instalment paid over 20 years.
R_{inst}	Annual Installments Revenue	[€]	Annual revenue from installment fees of all units.
C_{manu}	Cost of Manufacturing of One Unit	[€]	Cost of manufacturing one unit of AWE + LLS system.
λ	Learning Rate	[%]	Learning rate for reduction in cost of manufacturing as more units are produced/sold.
E_{manu}	Total Annual Manufacturing Expenses	[€]	Total annual expenditure on manufacturing. Scales linearly with number of units sold at that year.
$C_{O\&M}$	Cost of Operation & Maintenance of One Unit	[€/yr]	The annual cost of operating and maintaining one unit.

$E_{O\&M}$	Total Annual Operation & Maintenance Expenses	[€]	Total annual expenditure on operation & maintenance. Scales linearly with total number of units sold until and including that year.
C_{log}	Logistical Costs of One Unit	[€]	Cost of transporting and setting up one unit of AWE + LLS system at the customer destination.
E_{log}	Total Annual Logistical Expenses	[€]	Total annual expenditure on logistics. Scales linearly with total number of units sold until and including that year.
C_{decom}	Cost of Decommissioning of One Unit	[€]	Cost of decommissioning one unit of AWE+LLS system.
E_{decom}	Total Annual Cost of Decommissioning	[€]	Total cost of decommissioning all units that have reached their end-of-life.
f_{tax}	Corporate Income Tax	[%]	Average corporate income tax for the EU.
E_{tax}	Expenses due to Income Tax	[€]	Total cash inflow multiplied by the corporate income tax rate.

Table B.3: Glossary for parameters used in the financial analysis

Symbol	Definition	Unit	Remark
r	Discount rate	[%]	Interest rate used to determine the value of a project with a discounted cash-flow.
NPV	Net Present Value	[€]	The current value of a future stream of payments. Higher value makes the investment more lucrative.
IRR	Internal Rate of Return	[%]	Discount rate at which the NPV becomes zero. Higher value makes the investment more lucrative.
PBP	Payback Period	[€]	Time taken to recover the cost of investment. Calculated using subtraction method. Lower value makes the investment more lucrative.
$E_{R\&D}$	R&D Investment Costs	[€]	Total cost of investment to develop AWE+LLS system to TRL9. Lower value makes the investment more lucrative.
ROI	Return of Investment	[%]	Percentage gain from the initial investment. Higher value makes the investment more lucrative.
$LCOE$	Levelized Cost of Energy	[€/kWh]	The cost of producing one unit of energy. Lower value makes the investment more lucrative.